Applied Mathematical Modelling 151 (2026) 116531

Contents lists available at ScienceDirect

Applied Mathematical Modelling

journal homepage: www.elsevier.com/locate/apm

Green's functions for the static curvature and deflection of two-phase peridynamic elastic Euler-Bernoulli beams with exponential kernels

Ahmad Aftabi-Sani [a], Noël Challamel [b,*]

[a] Department of Civil Engineering, Faculty of Engineering, Ferdowsi University of Mashhad, Iran
[b] Université de Bretagne Sud, IRDL (CNRS UMR 6027), Centre de Recherche, Rue de Saint Maudé – BP 92116, 56321 Lorient cedex, France

ARTICLE INFO

Keywords:
Two-phase peridynamic model
Nonlocal theory
Euler-Bernoulli beam
Green's function
Concentrated load
FDM's order of convergence

ABSTRACT

The aim of this paper is to analyze the static response of two-phase peridynamic Euler-Bernoulli beams under different loading conditions, using the Green's function method. The methodology is applied to both statically determinate and indeterminate peridynamic elastic beams. For normalized exponential kernel, the integro-differential deflection equation of the two-phase peridynamic Euler-Bernoulli beam problem can be reformulated in a higher-order differential form. Three different types of Green's functions are extracted according to the beams' determinacy and loading type. The first kind of Green's function is introduced for static analysis of determinate beams under distributed loading and in absence of concentrated load. In this case, the bending moment function of the beam is known, and the first derivative of the curvature is continuous. The Green's function is straightforwardly obtained by solving a second-order differential equation together with the associated two boundary conditions. The second kind of Green's function valid for two-phase peridynamic Euler-Bernoulli beams under distributed loading and for general boundary conditions depends on a sixth-order differential equation together with six boundary conditions. The third kind of Green's function which could be used for the both determinate and indeterminate beams, is obtained in presence of concentrated load, using two segmented peridynamic beams. In this case, the Green's function is obtained by solving two sixth-order differential equations together with twelve boundary conditions. The above-mentioned three kinds of Green's functions are thoroughly illustrated in the paper for two determinate beams (clamped-free CF and simply supported SS boundary conditions), and two indeterminate beams (clamped-hinge CS and clamped-clamped CC boundary conditions). For all peridynamic beams, the closed-form expressions are obtained for the curvature and the deflection functions. Moreover, a series solution is also presented, as a complementary solution, for simply supported two-phase peridynamic beam under both distributed and concentrated loading. The analytical static deflection of the two-phase peridynamic beam under general boundary conditions is numerically corroborated using the finite difference method (FDM). The experimental order of convergence for the proposed FDM formulation of the two-phase peridynamic deflection is shown to be equal to 2, whatever the boundary conditions. The two-phase peridynamic beam theory presents a softening scale effect, compared to the classical Euler-Bernoulli beam, a phenomenon controlled by the peridynamic phase and length scale parameters.

* Corresponding author.
E-mail addresses: aftabi@ferdowsi.um.ac.ir (A. Aftabi-Sani), noel.challamel@univ-ubs.fr (N. Challamel).

https://doi.org/10.1016/j.apm.2025.116531
Received 16 June 2025; Received in revised form 21 September 2025; Accepted 24 October 2025
Available online 30 October 2025

1. Introduction

From etymological point of view, the term “peridynamic”, as an adjective, comes from the prefix “peri-“, which means “near, all around, or surrounding”; and the root “dyna”, which means “force or power”. Also, the term “peridynamics”, as a noun, is a shortened form of the phrase “peridynamic model of solid mechanics” [1]. From physical point of view, “peridynamics” is a non-local formulation of continuum mechanics that is oriented toward deformations with discontinuities, including fracture problems. In fact, the characteristic feature of peridynamics, which makes it different from classical local mechanics, is the presence of finite-range bonds between any two points of the material body. Moreover, the peridynamic equations do not usually contain any spatial derivatives of the displacement components. Therefore, their solution could be easily performed in the presence of any discontinuities. Generally, the peridynamic model does not involve the theoretical and computational complexities of the molecular dynamics. Therefore, peridynamics can fill the gap between molecular dynamics and the classical local continuum mechanics. Up to now, its capabilities have been proven in several applications, including fracture and failure of composites, nanofiber networks, polycrystal fracture, and the micro-scale phenomena, such as crack formation and propagation, wave dispersion, and intra-granular fracture. All of these recommend peridynamics as a practical multiscale material model for length scales ranging from molecular dynamics to those of classical elasticity.

Silling [1] introduced a general peridynamic continuum mechanics theory, as an alternative nonlocal model, which avoids the displacement differentiability. The peridynamic theory has been successfully applied to some static (mode III fracture problem) and dynamic (wave dispersion analysis in peridynamic media) problems. Since the paper of Silling [1], the peridynamic theory has been applied to many static and dynamic 3D peridynamic media, and also to peridynamic structural members such as peridynamic beams or plates (the reader can read the extensive presentation of peridynamic models in the “Handbook of Peridynamic Modeling”, co-edited by Bobaru, Foster, Geubelle and Silling [2]. The peridynamic model proposed in [1] was numerically investigated from an adaptive refinement algorithm by Bobaru and his co-researchers in [3]. In that study, they used scaling of the micromodulus and discussed the adaptivity in peridynamics. Moreover, three types of different numerical convergence were investigated for peridynamics, and uniform convergence to the classical solutions of one-dimensional elasticity problems was obtained.

The constitutive correspondence framework of peridynamics was introduced in [4] to address unphysical deformation modes represented in the original constitutive peridynamic model. For this reason, the generalized nonlocal peridynamic strain tensors based on corresponding bond-level Seth–Hill strain measures were utilized to avoid the violations of the matter interpenetration constraint. This modified theory avoids issues of matter interpenetration as presented by the original peridynamic theory, and this improvement was shown by several analytic examples in [4]. On the other hand, some researchers work on some alternative approaches to derive peridynamic equations of motion, using peridynamic differential operators [5]. Madenci et al. [5] transformed the Navier’s displacement equilibrium equations into their nonlocal form by introducing the peridynamic differential operator. This operator also allows the use of nonlocal expressions to find the stress and strain components. Moreover, Kilic and E Madenci [6] proposed an alternative method to find the steady-state solutions of nonlinear peridynamic equations by the well-known dynamic relaxation method.

Along with the development of 3D peridynamic models, the use of this model in beam analysis has also attracted the attention of some researchers [7,8]. For instance, O’Grady and Foster [9] proposed a new peridynamic state based model for the static bending of a peridynamic Euler–Bernoulli beam. Their model utilized the concept of a rotational spring between bonds. The asymptotic equivalence between this model and the well-known Eringen’s nonlocal elasticity was also shown in [9]. After that, a higher-order peridynamic beam formulation was presented by Yang et al. [10]. They used the Euler-Lagrange equations and the Taylor’s expansion to derive their formulation. Yang et al. also implemented the finite element method to find the transverse displacements and compared them with those obtained by peridynamics (for both peridynamic beams and peridynamic plates) [11].

Since the peridynamic equations are usually derived in the form of integro-differential equations and only few analytical solutions to these equations are reported in the literature, Yang et al. have tried to present some analytical solutions to peridynamic beam equations in [12] (static and free vibration peridynamic beam problems). They found some general solutions for the deflection functions of the beams by using trigonometric series. For instance, in the static case, they presented some closed-form expressions for the series’ coefficients. Moreover, in the dynamic case, they derived the solution for a simply supported beam utilizing the well-known method of the separation of variables. It is worth to mentioning that the similar work was performed for the beam buckling analysis in [13]. In this article, some explicit expressions for the buckling loads of three types of boundary conditions were reported. The peridynamic results were also compared with the classical results for buckling loads. During this comparison, an adequate agreement was observed between the non-local and the classical theories when the small length sizes are utilized.

In recent years, there are several studies focusing on the strongly nonlocal mechanics, especially strongly nonlocal beam mechanics. Among them, one of the models that have been welcomed by many researchers is the relative rotation-based integral nonlocal beam model, or “peridynamic” nonlocal beam model. In general, relative displacement-based integral models, also called peridynamic models, have been introduced by Silling for 3D solids [1]. Strain-driven nonlocal models relate the stress to the strain through an integral operator valid in the whole range of the solid, whereas relative-based displacement models express the balance equation through an integral operator of the displacement difference, which avoids the calculation of the strain through a gradient operator [14].

Recently, the Cosserat theory has also been used to explain complex material behavior by generalized continua models, along with the peridynamic theory. The main idea of Cosserat theory is based on the premise that translations are independent of rotations, and similarly, the forces are independent of moments. This model can explain some additional effects in continuum mechanics in a more satisfying way. The Cosserat-type theories of plates and shells are reviewed as a special application of the Cosserat theory by Altenbach

et al. [15]. As an example, a prismatic cylinder which is filled with a thermo-elastic material was studied by the Cosserat theory in [16]. This theory is defined as a framework that includes small perturbations to describe the dynamic behavior of materials, utilizing several concepts such as micro-rotations and associated deformation tensors to establish a relationship between the current states of material points to their initial configuration. It should also be noted that both peridynamic and Cosserat theories may be used to analyze nanostructures. Meanwhile, the analysis of nano-coatings has also attracted the attention of researchers in recent years [17].

In parallel with the development of peridynamic nonlocal models, research has also been conducted on the combination of local and nonlocal models. Generally, the combination of the local and nonlocal peridynamic approach which could be named as the two-phase peridynamic model has been developed by Di Paola and his colleagues in 2009 [18]. The two-phase peridynamic theory has been applied to peridynamic rod problems [18], peridynamic Timoshenko beam problems [19,20] and peridynamic Euler-Bernoulli beams [21]. Di Paola et al. [21] presented numerical results for the static response and the free vibration of two-phase peridynamic Euler-Bernoulli beam with an exponential attenuation function. More recently, Challamel and Zingales investigated the static, dynamic and buckling behavior of two-phase peridynamic Euler-Bernoulli beams [22]. For this purpose, they introduced an exponential kernel normalized along the finite length of the structural member. For such normalized exponential kernel, they converted the integro-differential problem into a differential problem with consistent peridynamic boundary conditions (also called peridynamic constitutive boundary conditions). These peridynamic boundary conditions coincide with the ones derived by di Paola and collaborators cited earlier for the two-phase peridynamic beam model (or mixed local/nonlocal peridynamic model), which preserve locality at the boundaries.

On the other hand, the Green's function method has recently been used for nano-structural analysis. As a frontiers series of researches, we can allude to the works performed by Hozhabrossadati et al. [23], Behnam-Rasouli et al. [24], and Challamel and Aftabi-Sani [25]. In the last-mentioned study, the exact solution for Timoshenko nano-beams is obtained by the help of Green's function method. In this work, the authors extracted the Green's function for three different models of Timoshenko nano-beam: (1) stress-driven nonlocal integral model, (2) strain gradient elastic model without transversal strain gradient effect, and (3) strain gradient model with transversal strain gradient effect. For this reason, they firstly constructed the boundary value problem (BVP) for this nano-structural problem, which consisted of one or two six-order differential equations (DEs) and six or twelve boundary conditions (BCs), depending on the type of model.

Continuing previous researches, in this article, the static analysis of two-phase peridynamic Euler-Bernoulli beams, under general concentrated and distributed loading, is thoroughly investigated, by the help of the Green's function method. For this purpose, three different types of Green's function will be obtained for four different beams (clamped-free, simple-simple, simple-clamped, and clamped-clamped). These three types of Green's functions are introduced in the article, respectively, as the following order:

1- The Green's function corresponds to the second-order differential equation governs on the curvature: This Green's function is utilized for determinate beams under distributed loading. It should be noted that for this kind of loading, the first derivative of curvature is continuous for two-phase peridynamic Euler-Bernoulli beam.
2- The Green's function corresponds to the sixth-order differential equation governs on the deflection: This Green's function is used for the both determinate and indeterminate beams under distributed loading. Similar to the previous type of Green's function, the first derivative of curvature is continuous for this kind of loading, due to the absence of concentrated external load.
3- The piecewise Green's function corresponds to the sixth-order differential equation governs on the deflection: This Green's function could be utilized for the both determinate and indeterminate beams under general concentrated load. On the contrary of the two previous types of Green's function, the first derivative of curvature is discontinuous for this kind of loading, due to the presence of concentrated external load.

In the current article, all three types of the above-mentioned Green's function are extracted for different determinate and indeterminate beams. The closed-from expressions are obtained for the deflection and curvature functions of the "clamped-free, simply supported, hinge-clamped, and clamped-clamped" beams under concentrated, uniformly distributed, and sinusoidal distributed loadings. Also, for verification purposes, a Navier-type series solution is built for the simply supported two-phase peridynamic beam. Fortunately, the series solution coincides with the closed-form one.

Furtheremore, the closed-form results obtained by the Green's functions for all four beams examined in the paper, i.e., SS, CS, CC and CF beams, are also verified by the help of numerical results obtained by FDM. The methodology of FDM utilized in the article is briefly presented in Section 7, and the deflection curves obtained by the both analytical and numerical methods are also shown in that section. The experimental order of convergence for the proposed FDM scheme is shown to be equal to 2, whatever the boundary conditions. The paper concludes with a discussion of the pure bending case, which could be interesting as well to show the possible ill-posedness of the pure peridynamic problem.

2. Two-phase peridynamic beam model

As shown in Appendix A, the two-phase peridynamic Euler-Bernoulli beam is governed by an integro-differential equation of the beam deflection. For a normalized exponential kernel, this integro-differential equation can be reformulated as a higher-order differential problem (as shown by Challamel and Zingales, 2025) [22]. This peridynamic Euler-Bernoulli beam model can be reduced to the following differential form coupled to the constitutive boundary conditions:

$$M - l_c^2 \frac{d^2M}{dx^2} = EI\left(\kappa - \xi_1 l_c^2 \frac{d^2\kappa}{dx^2}\right) \text{ with } M(0) = EI\xi_1\kappa(0) \text{ and } M(\mathrm{L}) = EI\xi_1\kappa(\mathrm{L}) \tag{1}$$

where we have used the curvature $\kappa = d^2w/dx^2$, and $w(x)$ denotes the deflection displacement field. Herein, ξ_1 is the local phase parameter; $0 < \xi_1 \leq 1$ which can be also understood as a regularization parameter. For ξ_1=*0*, the two-phase peridynamic model can be considered as a pure peridynamic beam. For ξ_1=*1*, the two-phase peridynamic model coincides with the local Euler-Bernoulli beam. The phase parameter controls the combination between the local elasticity and the pure peridynamic elasticity. It can be shown that this phase parameter can play a regularization parameter, as the pure peridynamic beam problem may be ill-posed (as for instance for a pure peridynamic beam under uniform bending moment). Also, l_c is a characteristic length, E is the Young modulus, I the moment of inertia and EI the elastic bending rigidity.

This gives a sixth-order differential equation of the deflection, for a beam loaded by a distributed loading $p(x)$:

$$EI\left[w^{(4)}(x) - \xi_1 l_c^2 w^{(6)}(x)\right] = p - l_c^2 p^{(2)} \tag{2}$$

coupled with the 6 boundary conditions (four classical and the two additional boundary conditions given by Eq. (1)).

The four classical boundary conditions can be also obtained from the principle of virtual work, applied to the static behavior of the uniform beam of length L under distributed lateral load $p(x)$ and concentrated end load P, may be equivalently expressed from the principle of virtual work:

$$\int_0^{\mathrm{L}} [M\,\delta w'' - p\,\delta w]\,dx - P\,\delta w(\mathrm{L}) = 0 \tag{3}$$

which means after two integration by parts, that:

$$\int_0^{\mathrm{L}} [M'' - p]\,\delta w\,dx + [M\,\delta w']_0^{\mathrm{L}} - [M'\,\delta w]_0^{\mathrm{L}} - P\,\delta w(\mathrm{L}) = 0 \tag{4}$$

In the next sections, based on the above-mentioned model, we thoroughly investigate several beams in two general categories, i.e., (1) statically determinate beams, and (2) statically indeterminate beams, by using the Green's function method. The analyzed beams are clamped-free, simple-simple, simple-clamped, and clamped-clamped. For determinate beams, the moment function is known, and then, we can solve Eq. (1). However, for indeterminate beams, we have to solve Eq. (2) together with six boundary conditions. The two-phase peridynamic model formulated in its integral form is presented in Appendix

3. Clamped-free two-phase peridynamic beam model

In this section, we focus on some statically determinate beams. For this kind of beams, the moment function is known, and then, we can directly solve Eq. (1). To show the solving process, firstly, the cantilever beam under end tip load is analyzed. It should be mentioned that this example has already been solved in [22].

3.1. End tip load (second-order DE)

The first example is as shown in Fig. 1.

The moment function for this beam is:

$$M(x) = P(\mathrm{L} - x) \tag{5}$$

The second derivative of the moment function is equal to zero. Therefore, Eq. (1) becomes:

$$\kappa(x) - \xi_1 l_c^2 \frac{d^2\kappa}{dx^2} = \frac{P(\mathrm{L} - x)}{EI} \tag{6}$$

with two following boundary conditions (Eq. (27) in [22]):

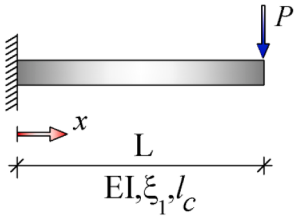

Fig. 1. Two-phase peridynamic clamped-free beam under end tip Load.

$$\begin{cases} \xi_2\kappa(0) - \xi_1 l_c^2 \kappa^{(2)}(0) = 0 \\ \xi_2\kappa(\mathrm{L}) - \xi_1 l_c^2 \kappa^{(2)}(\mathrm{L}) = 0 \end{cases} \tag{7}$$

To solve this differential equation by the help of Green's function, firstly, both sides of the differential Eq. (6) are multiplied by the Green's function, which will be found in the next steps. Also, the independent variable is changed form x to ξ:

$$G(\xi;x)\left(\kappa(\xi) - \xi_1 l_c^2 \frac{d^2\kappa}{d\xi^2}\right) = G(\xi;x)\frac{P(\mathrm{L}-\xi)}{EI} \tag{8}$$

Assuming that the Green's function is known, the right-hand side of the above equation is known. For the left-hand side, using the well-known "integration by parts" technique, we have:

$$\int_0^{\mathrm{L}} G\left(\kappa - \xi_1 l_c^2 \frac{d^2\kappa}{d\xi^2}\right)d\xi = -\xi_1 l_c^2\left[G\frac{d\kappa}{d\xi} - \kappa\frac{dG}{d\xi}\right]_0^{\mathrm{L}} + \int_0^{\mathrm{L}} \kappa(\xi)\underbrace{\left(G - \xi_1 l_c^2 \frac{d^2G}{d\xi^2}\right)}_{\delta(\xi-x)}d\xi \tag{9}$$

The left-hand side of Eq. (9) is known, based on Eq. (7). Moreover, we have:

$$\int_0^{\mathrm{L}} \kappa(\xi)\,\delta(\xi-x)d\xi = \kappa(x) \tag{10}$$

Therefore, by substituting Eqs. (6) and (10) into Eq. (9), the unknown function is obtained as:

$$\kappa(x) = \int_0^{\mathrm{L}} G(\xi;x)\frac{P(\mathrm{L}-\xi)}{EI}d\xi + \xi_1 l_c^2\left[G\frac{d\kappa}{d\xi} - \kappa\frac{dG}{d\xi}\right]_0^{\mathrm{L}} \tag{11}$$

As it is cleared, the bracket in Eq. (11) depends on the boundary values of unknown function κ and its "first" derivative, i.e., $\kappa^{(1)}$, at both ends of the beam; and this is while in the boundary conditions (7), the "second" derivative of the unknown function is given.

To remedy this problem, we straightforwardly use the differential equation twice: firstly at $x = 0$, and secondly at $x = \mathrm{L}$. Also, each time, we solve a linear system of equations, including a boundary condition along with a new equation generated using the differential equation, as follows:

$$\begin{cases} \kappa(0) - \xi_1 l_c^2 \kappa^{(2)}(0) = \dfrac{P\mathrm{L}}{EI} \\ \xi_2\kappa(0) - \xi_1 l_c^2 \kappa^{(2)}(0) = 0 \end{cases} \Rightarrow (1-\xi_2)\kappa(0) = \frac{P\mathrm{L}}{EI} \tag{12}$$

or:

$$\kappa(0) = \frac{1}{1-\xi_2}\frac{P\mathrm{L}}{EI} \tag{13}$$

and, similarly:

$$\begin{cases} \kappa(\mathrm{L}) - \xi_1 l_c^2 \kappa^{(2)}(\mathrm{L}) = 0 \\ \xi_2\kappa(\mathrm{L}) - \xi_1 l_c^2 \kappa^{(2)}(\mathrm{L}) = 0 \end{cases} \Rightarrow \kappa(\mathrm{L}) = 0 \tag{14}$$

Eqs. (13) and (14) are our new boundary conditions with order "zero". Now, we can easily apply them into bracket (11). This bracket is expanded as:

$$\left[G\frac{d\kappa}{d\xi} - \kappa\frac{dG}{d\xi}\right]_0^{\mathrm{L}} = G(\mathrm{L};x)\,\kappa^{(1)}(\mathrm{L}) - G^{(1)}(\mathrm{L};x)\,\kappa(\mathrm{L}) - G(0;x)\,\kappa^{(1)}(0) + G^{(1)}(0;x)\,\kappa(0) \tag{15}$$

By substituting Eqs. (13) and (14) into Eq. (15), we have:

$$\left[G\frac{d\kappa}{d\xi} - \kappa\frac{dG}{d\xi}\right]_0^{\mathrm{L}} = G(\mathrm{L};x)\,\kappa^{(1)}(\mathrm{L}) - G(0;x)\,\kappa^{(1)}(0) + G^{(1)}(0;x)\left(\frac{1}{1-\xi_2}\frac{P\mathrm{L}}{EI}\right) \tag{16}$$

Since $\kappa^{(1)}(0)$ and $\kappa^{(1)}(\mathrm{L})$ are unknowns, we set their coefficients to zero in Eq. (16). Thus:

$$\begin{cases} G(0;x) = 0 \\ G(\mathrm{L};x) = 0 \end{cases} \tag{17}$$

Eq. (17) shows the boundary conditions of the Green's function. Based on Eq. (9), the governing differential equation for the of Green's function is:

$$G(\xi;x) - \xi_1 l_c^2 \frac{d^2 G(\xi;x)}{d\xi^2} = \delta(\xi - x) \tag{18}$$

Eq. (18) has a complementary solution, named G_c, and a particular solution, named G_p, which $G = G_c + G_p$. Obviously, G_c should satisfy the homogenous version of Eq. (18). It could be easily found as the below:

$$G_c = c_1(x)\sinh\left(\frac{\xi}{\sqrt{\xi_1} l_c}\right) + c_2(x)\cosh\left(\frac{\xi}{\sqrt{\xi_1} l_c}\right) \tag{19}$$

The particular solution is assumed as the following form:

$$G_p = f(\xi)\,\widehat{H}(\xi - x) \tag{20}$$

where $\widehat{H}$ is Heaviside function, and defined as:

$$\widehat{H}(\xi - x) = \begin{cases} 1 & \xi > x \\ 0 & \xi < x \end{cases} \tag{21}$$

Obviously, we have from Eq. (20):

$$\frac{\partial^2 G_p}{\partial \xi^2} = f^{(2)}(\xi)\,\widehat{H}(\xi - x) \tag{22}$$

By substituting Eqs. (20) and (22) into Eq. (18), it yields:

$$\left(f(\xi) - \xi_1 l_c^2 f^{(2)}(\xi)\right)\widehat{H}(\xi - x) = \delta(\xi - x) \tag{23}$$

For any $\xi > x$, the right-hand side of Eq. (23) becomes zero, and $\widehat{H}(\xi - x) = 1$. Therefore, the parenthesis behind $\widehat{H}(\xi - x)$ should be equal to zero. Then:

$$f(\xi) - \xi_1 l_c^2 f^{(2)}(\xi) = 0 \tag{24}$$

The solution of Eq. (24) is:

$$f(\xi) = A\sinh\left(\frac{\xi}{\sqrt{\xi_1} l_c}\right) + B\cosh\left(\frac{\xi}{\sqrt{\xi_1} l_c}\right) \tag{25}$$

In the following, we integrate from the both sides of Eq. (23) over ξ, from x^- through x^+. Herein, each term will be computed separately. The function $f(\xi)$ is considered as a continuous function. For any continuous function, we have:

$$\int_{x^-}^{x^+} f(\xi)\widehat{H}(\xi - x)d\xi = 0 \tag{26}$$

For the second term, we have:

$$\int_{x^-}^{x^+} f^{(2)}(\xi)\widehat{H}(\xi - x)d\xi = f^{(1)}(x^+)\underbrace{\widehat{H}(x^+ - x)}_{1} - f^{(1)}(x^-)\underbrace{\widehat{H}(x^- - x)}_{0} = f^{(1)}(x^+) \tag{27}$$

Similar to the function $f(\xi)$, its first derivative is also assumed as a continuous function. Therefore:

$$f^{(1)}(x^+) = f^{(1)}(x) \tag{28}$$

and finally, the integration of the right-hand side of Eq. (23) is:

$$\int_{x^-}^{x^+} \delta(\xi - x)d\xi = 1 \tag{29}$$

By using Eqs. (26–29), we have:

$$0 - \xi_1 l_c^2 f^{(1)}(x) = 1 \Rightarrow f^{(1)}(x) = -\frac{1}{\xi_1 l_c^2} \tag{30}$$

Eq. (30) is the first boundary condition of the differential Eq. (24) which helps us to find the two unknown constants of solution (25).

On the other hand, since the Heaviside function $\widehat{H}$ is discontinuous at $\xi = x$, however, the particular solution H_p is continuous at $\xi = x$, therefore $f(\xi)$ must be equal to zero at $\xi = x$ so that the discontinuity of Heaviside function $\widehat{H}$ does not cause the particular solution G_p to become discontinuous. Then:

$$f(x) = 0 \tag{31}$$

Eq. (31) is the second boundary condition of the differential Eq. (24) which helps us to find the two unknown constants of solution (25). Thus, the complete boundary value problem (BVP) related to $f(\xi)$ is introduced as:

$$\begin{cases} \text{D.E. }: f(\xi) - \xi_1 l_c^2 f^{(2)}(\xi) = 0 \\ \text{B.C. }: \begin{cases} f(x) = 0 \\ f^{(1)}(x) = -\dfrac{1}{\xi_1 l_c^2} \end{cases} \end{cases} \tag{32}$$

By the help of Eqs. (25) and (32), we can find constants A and B as:

$$\begin{cases} A = -\dfrac{1}{\sqrt{\xi_1} l_c} \cosh\left(\dfrac{x}{\sqrt{\xi_1} l_c}\right) \\ B = \dfrac{1}{\sqrt{\xi_1} l_c} \sinh\left(\dfrac{x}{\sqrt{\xi_1} l_c}\right) \end{cases} \tag{33}$$

By substituting Eq. (33) into Eq. (25), we can find the function f as the following:

$$f(\xi) = \frac{1}{\sqrt{\xi_1} l_c} \sinh\left(\frac{x - \xi}{\sqrt{\xi_1} l_c}\right) \tag{34}$$

Putting Eq. (34) into Eq. (20) gives us the particular solution G_p. By adding the obtained particular solution and the complementary solution G_c which was expressed as Eq. (19), we can introduce the Green's function G as below:

$$G(\xi; x) = c_1(x) \sinh\left(\frac{\xi}{\sqrt{\xi_1} l_c}\right) + c_2(x) \cosh\left(\frac{\xi}{\sqrt{\xi_1} l_c}\right) + \frac{1}{\sqrt{\xi_1} l_c} \sinh\left(\frac{x - \xi}{\sqrt{\xi_1} l_c}\right) \widehat{H}(\xi - x) \tag{35}$$

The remaining two unknown constants $c_1(x)$ and $c_2(x)$ are obtained using the boundary conditions (17). It is noticeable that for $\xi = 0$ we have $\widehat{H}(\xi - x) = 0$, and for $\xi = \mathrm{L}$ we have $\widehat{H}(\xi - x) = 1$. Therefore, by using Eq. (35), Eq. (17) becomes:

$$\begin{cases} G(0; x) = c_2(x) = 0 \\ G(\mathrm{L}; x) = c_1(x) \sinh\left(\dfrac{\mathrm{L}}{\sqrt{\xi_1} l_c}\right) + \dfrac{1}{\sqrt{\xi_1} l_c} \sinh\left(\dfrac{x - \mathrm{L}}{\sqrt{\xi_1} l_c}\right) = 0 \end{cases} \tag{36}$$

Therefore:

$$c_1(x) = \frac{1}{\sqrt{\xi_1} l_c} \operatorname{csch}\left(\frac{\mathrm{L}}{\sqrt{\xi_1} l_c}\right) \sinh\left(\frac{\mathrm{L} - x}{\sqrt{\xi_1} l_c}\right) \tag{37}$$

Thus:

$$G(\xi; x) = \frac{1}{\sqrt{\xi_1} l_c} \operatorname{csch}\left(\frac{\mathrm{L}}{\sqrt{\xi_1} l_c}\right) \sinh\left(\frac{\mathrm{L} - x}{\sqrt{\xi_1} l_c}\right) \sinh\left(\frac{\xi}{\sqrt{\xi_1} l_c}\right) + \frac{1}{\sqrt{\xi_1} l_c} \sinh\left(\frac{x - \xi}{\sqrt{\xi_1} l_c}\right) \widehat{H}(\xi - x) \tag{38}$$

By substituting the Green's function (38) and its first derivative into Eqs. (11) and (16), and by attention to Eq. (17), we can find the unknown function by the following equation:

$$\begin{aligned} \kappa(x) &= \int_0^{\mathrm{L}} G(\xi; x) \frac{P(\mathrm{L} - \xi)}{EI} d\xi + \xi_1 l_c^2 G'(0; x) \left(\frac{1}{1 - \xi_2} \frac{P\mathrm{L}}{EI}\right) \\ &= \frac{P(\mathrm{L} - x)}{EI} + \frac{\xi_2}{\xi_1} \frac{P\mathrm{L}}{EI} \cosh\left(\frac{x}{l_c \sqrt{\xi_1}}\right) - \frac{\xi_2}{\xi_1} \frac{P\mathrm{L}}{EI} \left(\frac{\cosh\left(\dfrac{\mathrm{L}}{l_c \sqrt{\xi_1}}\right)}{\sinh\left(\dfrac{\mathrm{L}}{l_c \sqrt{\xi_1}}\right)}\right) \sinh\left(\frac{x}{l_c \sqrt{\xi_1}}\right) \end{aligned} \tag{39}$$

which is exactly the same as the solution presented as Eq. (28) in [22]. Also, by setting $\xi_1 = 1$, ξ_2 becomes zero ($\xi_2 = 1 - \xi_1$), and Eq. (39) agrees with the curvature of CF beam in local elasticity.

3.2. Uniformly distributed loading (second-order DE)

As a next example, we change the type of loading for clamped-free beam, as it is shown in Fig. 2. The right-hand side of Eq. (6) is the

moment function devided by bending rigidity. For clamped-free beam under uniformly distributed load, we have:

$$M(x) = -\frac{qx^2}{2} + qLx - \frac{qL^2}{2} \tag{40}$$

The second derivative of the moment function in this case is not equal to zero:

$$\frac{d^2M}{dx^2} = -q \tag{41}$$

Therefore, Eq. (1) becomes:

$$\kappa(x) - \xi_1 l_c^2 \frac{d^2\kappa}{dx^2} = \frac{1}{EI}\left(-\frac{qx^2}{2} + qLx - \frac{qL^2}{2} + ql_c^2 \right) \tag{42}$$

Compared to Eq. (6), which was the governing equation for the curvature of the same clamped-free cantilever beam, but under concentrated end load, we find that under distributed loading, the right-hand side of the differential equation depends on l_c. In fact, the effect of non-locality which manifests itself partially in l_c, enters both sides of the differential equation. Besides, the order of the differential Eq. (42), similar to Eq. (6) is still equal to two, due to the fact that the both differential equations govern the curvature.

Also, two constitutive boundary conditions change slightly, due to $M^{(2)}(0)$ and $M^{(2)}(L)$ are not equal to zero. Based on Eq. (19) in [22], we have:

$$\begin{cases} -q - EI\xi_1\kappa^{(2)}(0) + \dfrac{EI}{l_c^2}\xi_2\kappa(0) = 0 \\ -q - EI\xi_1\kappa^{(2)}(L) + \dfrac{EI}{l_c^2}\xi_2\kappa(L) = 0 \end{cases} \tag{43}$$

or:

$$\begin{cases} \xi_2\kappa(0) - \xi_1 l_c^2\kappa^{(2)}(0) = \dfrac{ql_c^2}{EI} \\ \xi_2\kappa(L) - \xi_1 l_c^2\kappa^{(2)}(L) = \dfrac{ql_c^2}{EI} \end{cases} \tag{44}$$

To solve Eq. (42) using Green's function, both sides of the inhomogeneous differential Eq. (42) are multiplied by the Green's function. Moreover, the independent variable is changed form x to ξ:

$$G(\xi;x)\left(\kappa(\xi) - \xi_1 l_c^2 \frac{d^2\kappa}{d\xi^2}\right) = G(\xi;x)\frac{1}{EI}\left(-\frac{q\xi^2}{2} + qL\xi - \frac{qL^2}{2} + ql_c^2 \right) \tag{45}$$

Exactly similar to the first example, the unknown function is obtained after two integration by parts as:

$$\kappa(x) = \int_0^L G(\xi;x)\frac{1}{EI}\left(-\frac{q\xi^2}{2} + qL\xi - \frac{qL^2}{2} + ql_c^2 \right)d\xi + \xi_1 l_c^2\left[G\frac{d\kappa}{d\xi} - \kappa\frac{dG}{d\xi} \right]_0^L \tag{46}$$

To obtain the "first" derivative of unknown function, i.e., $\kappa^{(1)}$, at both ends of the beam; we straightforwardly use the differential Eq. (42) twice: firstly at $x = 0$, and secondly at $x = L$. Also, each time, we solve a linear system of equations, including a boundary condition (44) along with a new equation generated using the differential equation, as follows:

$$\begin{cases} \kappa(0) - \xi_1 l_c^2\kappa^{(2)}(0) = \dfrac{q}{EI}\left(l_c^2 - \dfrac{L^2}{2} \right) \\ \xi_2\kappa(0) - \xi_1 l_c^2\kappa^{(2)}(0) = \dfrac{ql_c^2}{EI} \end{cases} \quad \Rightarrow \kappa(0) = \frac{1}{1-\xi_2}\left(-\frac{qL^2}{2EI} \right) = -\frac{qL^2}{2\xi_1 EI} \tag{47}$$

and, similarly:

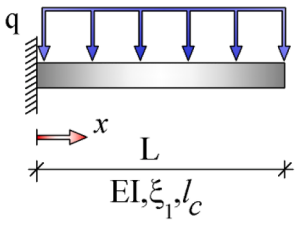

Fig. 2. Two-phase peridynamic clamped-free beam under uniformly distributed loading.

$$\begin{cases} \kappa(\mathrm{L}) - \xi_1 l_c^2 \kappa^{(2)}(\mathrm{L}) = \dfrac{q l_c^2}{EI} \\ \xi_2 \kappa(\mathrm{L}) - \xi_1 l_c^2 \kappa^{(2)}(\mathrm{L}) = \dfrac{q l_c^2}{EI} \end{cases} \Rightarrow \kappa(\mathrm{L}) = 0 \tag{48}$$

Interestingly, both boundary conditions obtained above are consistent with the two constitutive boundary conditions coupled with Eq. (1). At the end point with $x = \mathrm{L}$, the moment is zero, and consequently, the curvature will also be zero. Also, at $x = 0$, both the moment and the curvature are non-zero.

Eqs. (47) and (48) are our new boundary conditions with order "zero". Now, we can easily apply them into bracket (15). This bracket is now expanded as:

$$\left[G \frac{d\kappa}{d\xi} - \kappa \frac{dG}{d\xi} \right]_0^{\mathrm{L}} = G(\mathrm{L}; x)\, \kappa^{(1)}(\mathrm{L}) - G(0; x)\, \kappa^{(1)}(0) + G^{(1)}(0; x) \left(- \frac{q \mathrm{L}^2}{2 \xi_1 EI} \right) \tag{49}$$

By substituting the boundary condition of Green's function, i.e., Eq. (17), into Eq. (49), we have:

$$\left[G \frac{d\kappa}{d\xi} - \kappa \frac{dG}{d\xi} \right]_0^{\mathrm{L}} = G^{(1)}(0; x) \left(- \frac{q \mathrm{L}^2}{2 \xi_1 EI} \right) \tag{50}$$

By substituting the Green's function (38) and its first derivative into Eqs. (46) and (50), the unknown curvature function is attained by the following equation:

$$\begin{aligned} \kappa(x) &= \int_0^{\mathrm{L}} G(\xi; x) \frac{1}{EI} \left(- \frac{q\xi^2}{2} + q\mathrm{L}\xi - \frac{q\mathrm{L}^2}{2} + q l_c^2 \right) d\xi - G^{(1)}(0; x) \left(\frac{q l_c^2 \mathrm{L}^2}{2EI} \right) \\ &= \frac{q}{2\xi_1 EI} \Big[- \xi_1 \left(\mathrm{L}^2 - 2\xi_2 l_c^2 - 2\mathrm{L}x + x^2 \right) - \xi_2 \Big(\left(\mathrm{L}^2 + 2\xi_1 l_c^2 \right) \cosh \left(\frac{x}{\sqrt{\xi_1} l_c} \right) \\ &\quad - \left(\left(\mathrm{L}^2 + 2\xi_1 l_c^2 \right) \coth \left(\frac{\mathrm{L}}{\sqrt{\xi_1} l_c} \right) - 2\xi_1 l_c^2 \operatorname{csch} \left(\frac{\mathrm{L}}{\sqrt{\xi_1} l_c} \right) \right) \sinh \left(\frac{x}{\sqrt{\xi_1} l_c} \right) \Big) \Big] \end{aligned} \tag{51}$$

Based on Eq. (29) in [22], the following dimensionless variables can be introduced:

$$\kappa^* = \frac{EI\kappa}{q\mathrm{L}^2}; \quad x^* = \frac{x}{\mathrm{L}}; \quad l_c^* = \frac{l_c}{\mathrm{L}} \tag{52}$$

The dimensionless curvature can then be re-expressed by:

$$\begin{aligned} \kappa^*(x^*) &= \frac{1}{2\xi_1} \Big(- \xi_1 \left(1 - 2\xi_2 \left(l_c^* \right)^2 - 2x^* + (x^*)^2 \right) - \xi_2 \Big[\left(1 + 2\xi_1 \left(l_c^* \right)^2 \right) \cosh \left(\frac{x^*}{\sqrt{\xi_1} l_c^*} \right) \\ &\quad - \left(\left(1 + 2\xi_1 \left(l_c^* \right)^2 \right) \coth \left(\frac{1}{\sqrt{\xi_1} l_c^*} \right) - 2\xi_1 \left(l_c^* \right)^2 \operatorname{csch} \left(\frac{1}{\sqrt{\xi_1} l_c^*} \right) \right) \sinh \left(\frac{x^*}{\sqrt{\xi_1} l_c^*} \right) \Big] \Big) \end{aligned} \tag{53}$$

In the next sub-section, the same problem, i.e., the clamped-free beam under uniformly distributed loading will be solved by another Green's function. Up to now, So far, we have only used the Green's function of curvature, which corresponds to the second-order differential Eq. (1). However, in the next section, the Green's function of deflection will be obtained by solving the six-order differential Eq. (2).

3.3. Uniformly distributed loading (sixth-order DE)

In previous section, we solve this problem by using $M(x)$ which is known for this determinate beam. However, we want to solve the six-order differential Eq. (2) which becomes as the following for this example:

$$w^{(4)}(x) - \xi_1 l_c^2 w^{(6)}(x) = \frac{1}{EI} \left(p - l_c^2 p'' \right) = - \frac{q}{EI} \tag{54}$$

It should be mentioned that the uniformly distributed loading is downward and therefore negative. Also, its second derivative is equal to zero, because it is constant. Besides, the order of the differential Eq. (54) is equal to six, unlike Eqs. (6) and (42), due to the fact that Eq. (54) governs the deflection, on the contrary to Eqs. (6) and (42) which govern the curvature.

The differential Eq. (54) needs six boundary conditions. To find these boundary conditions, we start by the moment function as the following:

$$M - l_c^2 M^{(2)} = EI \left(w^{(2)} - \xi_1 l_c^2 w^{(4)} \right) \tag{rep.1}$$

We know $M''(x) = -q$. Therefore:

$$M = EI\left(w^{(2)} - \xi_1 l_c^2 w^{(4)}\right) - q\, l_c^2 \tag{55}$$

The three bondary conditions at $x = 0$ are:

$$\begin{cases} w(0) = 0 \\ w^{(1)}(0) = 0 \\ M(0) = EI\xi_1\, w^{(2)}(0) \end{cases} \tag{56}$$

The third one could be simplified by the help of Eq. (55) as the following:

$$EI\left[w^{(2)}(0) - \xi_1 l_c^2 w^{(4)}(0)\right] - q\, l_c^2 = EI\xi_1\, w^{(2)}(0) \tag{57}$$

Based on the relation $\xi_1 + \xi_2 = 1$, we have:

$$\xi_2 w^{(2)}(0) - \xi_1 l_c^2 w^{(4)}(0) = \frac{q\, l_c^2}{EI} \tag{58}$$

On the other hand, the three bondary conditions at $x = \mathrm{L}$ are:

$$\begin{cases} M(\mathrm{L}) = 0 \\ M^{(1)}(\mathrm{L}) = 0 \\ M(\mathrm{L}) = EI\xi_1\, w^{(2)}(\mathrm{L}) \end{cases} \tag{59}$$

These boundary conditions could be simplified, respectively, as the following:

$$M(\mathrm{L}) = EI\left[w^{(2)}(\mathrm{L}) - \xi_1 l_c^2 w^{(4)}(\mathrm{L})\right] - q\, l_c^2 = 0 \Rightarrow w^{(2)}(\mathrm{L}) - \xi_1 l_c^2 w^{(4)}(\mathrm{L}) = \frac{q\, l_c^2}{EI} \tag{60}$$

$$M^{(1)}(\mathrm{L}) = EI\left[w^{(3)}(\mathrm{L}) - \xi_1 l_c^2 w^{(5)}(\mathrm{L})\right] = 0 \Rightarrow w^{(3)}(\mathrm{L}) - \xi_1 l_c^2 w^{(5)}(\mathrm{L}) = 0 \tag{61}$$

$$EI\left[w^{(2)}(\mathrm{L}) - \xi_1 l_c^2 w^{(4)}(\mathrm{L})\right] - q\, l_c^2 = EI\xi_1\, w^{(2)}(\mathrm{L}) \Rightarrow \xi_2 w^{(2)}(\mathrm{L}) - \xi_1 l_c^2 w^{(4)}(\mathrm{L}) = \frac{q\, l_c^2}{EI} \tag{62}$$

By solving the first and the third equations simultaneously, we have:

$$\begin{cases} w^{(2)}(\mathrm{L}) = 0 \\ w^{(4)}(\mathrm{L}) = -\dfrac{q}{\xi_1 EI} \end{cases} \tag{63}$$

Therefore, the complete form of all boundary conditions for clamped-free beam under uniformly distributed loading becomes as the following:

$$\begin{cases} w(0) = 0 \\ w^{(1)}(0) = 0 \\ \xi_2 w^{(2)}(0) - \xi_1 l_c^2 w^{(4)}(0) = \dfrac{q\, l_c^2}{EI} \\ w^{(2)}(\mathrm{L}) = 0 \\ w^{(3)}(\mathrm{L}) - \xi_1 l_c^2 w^{(5)}(\mathrm{L}) = 0 \\ w^{(4)}(\mathrm{L}) = -\dfrac{q}{\xi_1 EI} \end{cases} \tag{64}$$

To solve the differential Eq. (54) by the help of Green's function, firstly, both sides of the differental equation are multiplied by the Green's function, which will be found in the next steps. Also, the independent variable is changed form x to ξ:

$$G(\xi; x)\left(w^{(4)}(\xi) - \xi_1 l_c^2 w^{(6)}(\xi)\right) = G(\xi; x)\left(-\frac{q}{EI}\right) \tag{65}$$

Assuming that the Green's function is known, the right-hand side of the above equation is known. For the left-hand side, using the "integration by parts" technique, we have:

$$\begin{cases} \int_0^L G\,w^{(4)}d\xi = \left[G\,w^{(3)} - G^{(1)}w^{(2)} + G^{(2)}w^{(1)} - G^{(3)}w\right]_0^L + \int_0^L w\,G^{(4)}d\xi \\ \int_0^L G\,w^{(6)}d\xi = \left[G\,w^{(5)} - G^{(1)}w^{(4)} + G^{(2)}w^{(3)} - G^{(3)}w^{(2)} + G^{(4)}w^{(1)} - G^{(5)}w\right]_0^L + \int_0^L w\,G^{(6)}d\xi \end{cases}$$
$$\Rightarrow \int_0^L G(\xi;x)\underbrace{\left(w^{(4)}(\xi) - \xi_1 l_c^2\,w^{(6)}(\xi)\right)}_{\left(-\frac{q}{EI}\right)}d\xi = [\ldots]_0^L + \int_0^L w(\xi)\underbrace{\left(G^{(4)} - \xi_1 l_c^2\,G^{(6)}\right)}_{\delta(\xi-x)}d\xi \tag{66}$$

with the following bracket:

$$\begin{aligned} [\ldots]_0^{\mathrm{L}} &= G(\mathrm{L};x)\left(w^{(3)}(\mathrm{L}) - \xi_1 l_c^2\,w^{(5)}(\mathrm{L})\right) - G^{(1)}(\mathrm{L};x)\left(w^{(2)}(\mathrm{L}) - \xi_1 l_c^2\,w^{(4)}(\mathrm{L})\right) \\ &+G^{(2)}(\mathrm{L};x)\left(w^{(1)}(\mathrm{L}) - \xi_1 l_c^2\,w^{(3)}(\mathrm{L})\right) - G^{(3)}(\mathrm{L};x)\left(w(\mathrm{L}) - \xi_1 l_c^2\,w^{(2)}(\mathrm{L})\right) \\ &-\xi_1 l_c^2\,G^{(4)}(\mathrm{L};x)\,w^{(1)}(\mathrm{L}) + \xi_1 l_c^2\,G^{(5)}(\mathrm{L};x)\,w(\mathrm{L}) \\ &-G(0;x)\left(w^{(3)}(0) - \xi_1 l_c^2\,w^{(5)}(0)\right) + G^{(1)}(0;x)\left(w^{(2)}(0) - \xi_1 l_c^2\,w^{(4)}(0)\right) \\ &-G^{(2)}(0;x)\left(w^{(1)}(0) - \xi_1 l_c^2\,w^{(3)}(0)\right) + G^{(3)}(0;x)\left(w(0) - \xi_1 l_c^2\,w^{(2)}(0)\right) \\ &+\xi_1 l_c^2\,G^{(4)}(0;x)\,w^{(1)}(0) - \xi_1 l_c^2\,G^{(5)}(0;x)\,w(0) \end{aligned} \tag{67}$$

In this step, we should apply the six boundary conditions listed in Eq. (64). Substituting these boundary conditions into bracket Eq. (67) yields to:

$$\begin{aligned} [\ldots]_0^{\mathrm{L}} = &-w^{(3)}(\mathrm{L})\left(\xi_1 l_c^2 G^{(2)}(\mathrm{L};x)\right) \\ &+ w^{(1)}(\mathrm{L})\left(G^{(2)}(\mathrm{L};x) - \xi_1 l_c^2\,G^{(4)}(\mathrm{L};x)\right) \\ &- w(\mathrm{L})\left(G^{(3)}(\mathrm{L};x) - \xi_1 l_c^2\,G^{(5)}(\mathrm{L};x)\right) \\ &+ w^{(5)}(0)\left(\xi_1 l_c^2 G(0;x)\right) \\ &- w^{(3)}(0)\left(G(0;x) - \xi_1 l_c^2 G^{(2)}(0;x)\right) \\ &+ w^{(2)}(0)\,\xi_1\left(G^{(1)}(0;x) - l_c^2 G^{(3)}(0;x)\right) \\ &+ G^{(1)}(0;x)\left(\frac{q\,l_c^2}{EI}\right) - G^{(1)}(\mathrm{L};x)\left(\frac{q\,l_c^2}{EI}\right) \end{aligned} \tag{68}$$

Since $w^{(3)}(\mathrm{L})$, $w^{(1)}(\mathrm{L})$, $w(\mathrm{L})$, $w^{(5)}(0)$, $w^{(3)}(0)$ and $w^{(2)}(0)$ are unknowns, we set their coefficients to zero in Eq. (68). Therefore, the six homogenous boundary conditions of Green's function are obtained as the following:

$$\begin{cases} G^{(2)}(\mathrm{L};x) = 0 \\ G^{(4)}(\mathrm{L};x) = 0 \\ G^{(3)}(\mathrm{L};x) - \xi_1 l_c^2\,G^{(5)}(\mathrm{L};x) = 0 \\ G(0;x) = 0 \\ G^{(2)}(0;x) = 0 \\ G^{(1)}(0;x) - l_c^2 G^{(3)}(0;x) = 0 \end{cases} \tag{69}$$

Then, bracket Eq. (67) becomes:

$$[\ldots]_0^{\mathrm{L}} = \left(G^{(1)}(0;x) - G^{(1)}(\mathrm{L};x)\right)\frac{q\,l_c^2}{EI} \tag{70}$$

By the help of the main property of the Dirac delta function (Eq. 10), and substituting Eq. (70) into Eq. (66), we can reach to the deflection function of simple-simple beam under uniformly distributed loading:

$$w(x) = \int_0^x G(\xi;x)\left(-\frac{q}{EI}\right)d\xi + \int_x^{\mathrm{L}} G(\xi;x)\left(-\frac{q}{EI}\right)d\xi + \left(G^{(1)}(\mathrm{L};x) - G^{(1)}(0;x)\right)\frac{q\,l_c^2}{EI} \tag{71}$$

Now, we should only find the Green's function. Eq. (69) shows the six boundary conditions of Green's function. Based on Eq. (66), its governing differential equation is:

$$\frac{d^4G(\xi;x)}{d\xi^4} - \xi_1 l_c^2\frac{d^6G(\xi;x)}{d\xi^6} = \delta(\xi - x) \tag{72}$$

Similar to the second-order DE, Eq. (72) has a complementary solution, named G_c, and a particular solution, named G_p, which $G =$

$G_c + G_p$. Obviously, G_c should satisfy the homogenous version of Eq. (72). It could be easily found as the below:

$$G_c = c_1(x)\sinh\left(\frac{\xi}{\sqrt{\xi_1 l_c}}\right) + c_2(x)\cosh\left(\frac{\xi}{\sqrt{\xi_1 l_c}}\right) + c_3(x)\xi^3 + c_4(x)\xi^2 + c_5(x)\xi + c_6(x) \tag{73}$$

The particular solution is assumed as the following form:

$$G_p = f(\xi)\,\widehat{H}(\xi - x) \tag{rep.20}$$

where $\widehat{H}$ is Heaviside function, and defined as:

$$\widehat{H}(\xi - x) = \begin{cases} 1 & \xi > x \\ 0 & \xi < x \end{cases} \tag{rep.21}$$

Similar to Section 3.1, this is easily proven that the complete boundary value problem (BVP) related to $f(\xi)$ becomes:

$$\begin{cases} \text{D.E. }: f^{(4)}(\xi) - \xi_1 l_c^2 f^{(6)}(\xi) = 0 \\ \text{B.C. }: \begin{cases} f(x) = 0 \\ f^{(1)}(x) = 0 \\ f^{(2)}(x) = 0 \\ f^{(3)}(x) = 0 \\ f^{(4)}(x) = 0 \\ f^{(5)}(x) = -\dfrac{1}{\xi_1 l_c^2} \end{cases} \end{cases} \tag{74}$$

The solution of Eq. (74) is:

$$f(\xi) = \xi_1^{\frac{3}{2}} l_c^3 \sinh\left(\frac{x-\xi}{\sqrt{\xi_1 l_c}}\right) - \frac{1}{6}(x-\xi)^3 - \xi_1 l_c^2 (x-\xi) \tag{75}$$

Based on Eqs. (73) and (75), the Green's function of deflection becomes as the following:

$$\begin{aligned} G(\xi;x) &= c_1(x)\sinh\left(\frac{\xi}{\sqrt{\xi_1 l_c}}\right) + c_2(x)\cosh\left(\frac{\xi}{\sqrt{\xi_1 l_c}}\right) \\ &+ c_3(x)\xi^3 + c_4(x)\xi^2 + c_5(x)\xi + c_6(x) \\ &+ \left[\xi_1^{\frac{3}{2}} l_c^3 \sinh\left(\frac{x-\xi}{\sqrt{\xi_1 l_c}}\right) - \frac{1}{6}(x-\xi)^3 - \xi_1 l_c^2 (x-\xi)\right]\widehat{H}(\xi - x) \end{aligned} \tag{76}$$

To find the remaining six unknown constants, it is sufficient to use the six boundary conditions (69). The final result will be as follows:

$$\begin{aligned} G(\xi;x) &= \frac{x\xi^2}{2} - \frac{\xi^3}{6} - l_c^2\xi + l_c^2\xi_1 x\left(1 - \cosh\left(\frac{\xi}{\sqrt{\xi_1 l_c}}\right)\right) \\ &+ \left(\frac{l_c x}{\sqrt{\xi_1}}\coth\left(\frac{\mathrm{L}}{\sqrt{\xi_1 l_c}}\right) + l_c^2\,\mathrm{csch}\left(\frac{\mathrm{L}}{\sqrt{\xi_1 l_c}}\right)\sinh\left(\frac{\mathrm{L}-x}{\sqrt{\xi_1 l_c}}\right)\right)\left(\xi_1^{\frac{3}{2}} l_c \sinh\left(\frac{\xi}{\sqrt{\xi_1 l_c}}\right) + \xi_2\xi\right) \\ &+ \left(\xi_1^{\frac{3}{2}} l_c^3 \sinh\left(\frac{x-\xi}{\sqrt{\xi_1 l_c}}\right) - \frac{1}{6}(x-\xi)^3 - \xi_1 l_c^2 (x-\xi)\right)\widehat{H}(\xi - x) \end{aligned} \tag{77}$$

By substituting the Green's function Eq. (77) and its first derivative into Eq. (71), we arrive at the following result for $w(x)$:

$$w(x) = -\frac{q}{24EI}\left(x^2\left(6\mathrm{L}^2 - 4\mathrm{L}x + x^2\right) - 12l_c^2\left(\mathrm{L}^2 + x^2 + 2\xi_1 l_c^2\right)\xi_2\right)$$
$$-\frac{q\,l_c\xi_2}{2EI\sqrt{\xi_1}}\left(\begin{array}{l} x\left(\mathrm{L}^2 + 2l_c^2\xi_1\right)\coth\left(\dfrac{\mathrm{L}}{\sqrt{\xi_1}l_c}\right) + \sqrt{\xi_1}l_c\,\mathrm{csch}\left(\dfrac{\mathrm{L}}{\sqrt{\xi_1}l_c}\right) \\ \times\left(-2\sqrt{\xi_1}\,l_c x + \left(\mathrm{L}^2 + 2l_c^2\xi_1\right)\sinh\left(\dfrac{\mathrm{L}-x}{\sqrt{\xi_1}l_c}\right) + 2l_c^2\xi_1\sinh\left(\dfrac{x}{\sqrt{\xi_1}l_c}\right)\right)\end{array}\right) \tag{78}$$

In previous sub-section, we found the "curvature" of clamped-free beam under uniformly distributed loading, i.e., the second derivative of $w(x)$, directly, by the help of another Green's function. For verification purpose, we found the second derivative of Eq. (78) as follows:

$$w^{(2)}(x) = \frac{q}{2\xi_1 EI}\Big[-\xi_1\left(\mathrm{L}^2 - 2\xi_2 l_c^2 - 2\mathrm{L}x + x^2\right) - \xi_2\Big(\left(\mathrm{L}^2 + 2\xi_1 l_c^2\right)\cosh\left(\frac{x}{\sqrt{\xi_1}l_c}\right)$$
$$-\left(\left(\mathrm{L}^2 + 2\xi_1 l_c^2\right)\coth\left(\frac{\mathrm{L}}{\sqrt{\xi_1}l_c}\right) - 2\xi_1 l_c^2\,\mathrm{csch}\left(\frac{\mathrm{L}}{\sqrt{\xi_1}l_c}\right)\right)\sinh\left(\frac{x}{\sqrt{\xi_1}l_c}\right)\Big)\Big] \tag{79}$$

Fortunately, the above-obtained functions is the same as Eq. (51).

3.4. General concentrated load (sixth-order DE)

As a next example, the general concentrated load is applied on the clamped-free beam, as shown in Fig. 3. In this case, we have to consider the sixth-order differential Eq. (2), due to imposing the six boundary conditions related to the location of the point load. In the following, all 12 boundary conditions of this example are expressed by the help of two deflection functions:

$w_L(x)$denotes the deflection function for Left segments of the point load, i.e., for,$x < a$, and

$w_R(x)$ denotes the deflection function for Right segments of the point load, i.e., for $x > a$.

Since there is no distributed load on the beam, based on Eq. (2), the governing differential equation for the both segments of the beam becomes:

$$w^{(4)}(x) - \xi_1 l_c^2 w^{(6)}(x) = 0 \tag{80}$$

The moment function of the beam could be expressed by Eq. (1). It should be mentioned that $M(x)$ is a linear function for this beam, and thus $M^{(2)}(x)$. Therefore, based on Eq. (1), we have:

$$M(x) = EI\left[w^{(2)}(x) - \xi_1 l_c^2 w^{(4)}(x)\right] \text{ with} \begin{cases} M(0) = EI\xi_1 w^{(2)}(0) \\ M(\mathrm{L}) = EI\xi_1 w^{(2)}(\mathrm{L}) \end{cases} \tag{rep.1}$$

By using the relation $\xi_1 + \xi_2 = 1$, it could be easily concluded that:

$$M(0) = EI\left[w_L^{(2)}(0) - \xi_1 l_c^2 w_L^{(4)}(0)\right] = EI\xi_1 w_L^{(2)}(0) \Rightarrow \xi_2 w_L^{(2)}(0) - \xi_1 l_c^2 w_L^{(4)}(0) = 0 \tag{81}$$

and:

$$M(\mathrm{L}) = EI\left[w_R^{(2)}(\mathrm{L}) - \xi_1 l_c^2 w_R^{(4)}(\mathrm{L})\right] = EI\xi_1 w_R^{(2)}(\mathrm{L}) \Rightarrow \xi_2 w_R^{(2)}(\mathrm{L}) - \xi_1 l_c^2 w_R^{(4)}(\mathrm{L}) = 0 \tag{82}$$

In addition to the two above-obtained constitutive boundary conditions, we have four classical boundary conditions at the both ends of the clamped-free beam under general point load. At $x = 0$, the clamped restraint dictates that:

$$\begin{cases} w_L(0) = 0 \\ w_L^{(1)}(0) = 0 \end{cases} \tag{83}$$

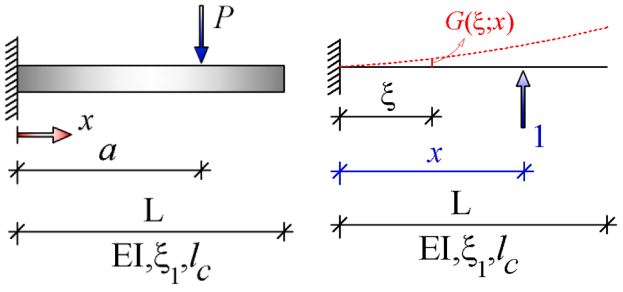

Fig. 3. Two-phase peridynamic clamped-free beam under general concentrated load.

Moreover, to obtain the two classical boundary conditions at free end, i.e., $x = \mathrm{L}$, we should use the moment function, and its first derivative, i.e., the shear force function. It means:

$$\begin{aligned} &M(x) = EI\left[w^{(2)}(x) - \xi_1 l_c^2 w^{(4)}(x)\right] \\ &M(\mathrm{L}) = 0 \Rightarrow w_R^{(2)}(\mathrm{L}) - \xi_1 l_c^2 w_R^{(4)}(\mathrm{L}) = 0 \end{aligned} \tag{84}$$

and:

$$\begin{aligned} &V(x) = M^{(1)}(x) = EI\left[w^{(3)}(x) - \xi_1 l_c^2 w^{(5)}(x)\right] \\ &V(\mathrm{L}) = 0 \Rightarrow w_R^{(3)}(\mathrm{L}) - \xi_1 l_c^2 w_R^{(5)}(\mathrm{L}) = 0 \end{aligned} \tag{85}$$

Therefore, up to now, the first half of 12 boundary conditions of the clamped-free beam becomes as the following:

$$\begin{cases} w_L(0) = 0 \\ w_L^{(1)}(0) = 0 \\ \xi_2 w_L^{(2)}(0) - \xi_1 l_c^2 w_L^{(4)}(0) = 0 \\ \left.\begin{aligned} &\xi_2 w_R^{(2)}(\mathrm{L}) - \xi_1 l_c^2 w_R^{(4)}(\mathrm{L}) = 0 \\ &w_R^{(2)}(\mathrm{L}) - \xi_1 l_c^2 w_R^{(4)}(\mathrm{L}) = 0 \end{aligned}\right\} \Rightarrow \begin{cases} w_R^{(2)}(\mathrm{L}) = 0 \\ w_R^{(4)}(\mathrm{L}) = 0 \end{cases} \\ w_R^{(3)}(\mathrm{L}) - \xi_1 l_c^2 w_R^{(5)}(\mathrm{L}) = 0 \end{cases} \tag{86}$$

For the concentrated load location, i.e., $x = a$, we have also six boundary conditions. At that point, the deflection, slope, and moment functions are assumed to be continuous; however, the shear force is discontinuous. These six boundary conditions could be expressed as the following:

$$\begin{cases} \Delta w(a) = 0 \\ \Delta w^{(1)}(a) = 0 \\ \Delta M(a) = 0 \\ \Delta M^{(1)}(a) = P \\ \Delta M(a) = EI\xi_1 \Delta w^{(2)}(a) \\ \Delta M^{(1)}(a) = EI\xi_1 \Delta w^{(3)}(a) \end{cases} \tag{87}$$

The two last higher-order continuity conditions can be expressed equivalently as:

$$\begin{cases} EI\xi_1 \Delta w^{(2)}(a) = 0 \\ EI\xi_1 \Delta w^{(3)}(a) = P \end{cases} \tag{88}$$

By using two functions $w_L(x)$ and $w_R(x)$ and with the help of Eqs. (84–85), the second half of 12 boundary conditions becomes:

$$\begin{cases} w_L(a) = w_R(a) \\ w_L^{(1)}(a) = w_R^{(1)}(a) \\ w_L^{(2)}(a) = w_R^{(2)}(a) \\ w_L^{(3)}(a) - w_R^{(3)}(a) = \dfrac{1}{\xi_1}\dfrac{P}{EI} \\ w_L^{(4)}(a) = w_R^{(4)}(a) \\ w_L^{(5)}(a) - w_R^{(5)}(a) = \dfrac{\xi_2}{\xi_1^2 l_c^2}\dfrac{P}{EI} \end{cases} \tag{89}$$

In the following, the new Green's function of clamped-free beam is obtained for the "deflection" function. It should be reminded that the Green's function utilized in two previous examples was obtained for the "curvature" function. Moreover, the curvarute function is continuous for the both end-tip load and uniform distributed loading; however, it is discontinuous in the current example, as it is clear from the forth equation of Eq. (89).

The governing differential equation of the Green's function corresponding to Eq. (80) is:

$$\frac{d^4 G(\xi; x)}{d\xi^4} - \xi_1 l_c^2 \frac{d^6 G(\xi; x)}{d\xi^6} = \delta(\xi - x) \tag{90}$$

If the right-hand side of the above differential equation assumed to be zero, its complementary solution is obtained as follows:

$$G_c(\xi; x) = c_1 \sinh\left(\frac{\xi}{\sqrt{\xi_1} l_c}\right) + c_2 \cosh\left(\frac{\xi}{\sqrt{\xi_1} l_c}\right) + c_3\xi^3 + c_4\xi^2 + c_5\xi + c_6 \tag{91}$$

The Dirac delta function on the right-hand side of Eq. (90) causes the Green's function to become discontinuous at $\xi = x$. Therefore, we assume the Green's function as the following:

$$G(\xi;x)=\begin{cases} c_1\sinh\left(\frac{\xi}{\sqrt{\xi_1}l_c}\right)+c_2\cosh\left(\frac{\xi}{\sqrt{\xi_1}l_c}\right)+c_3\xi^3+c_4\xi^2+c_5\xi+c_6 & 0<\xi<x \\ c_7\sinh\left(\frac{\xi}{\sqrt{\xi_1}l_c}\right)+c_8\cosh\left(\frac{\xi}{\sqrt{\xi_1}l_c}\right)+c_9\xi^3+c_{10}\xi^2+c_{11}\xi+c_{12} & x<\xi<\mathrm{L} \end{cases} \tag{92}$$

Based on the definition of the Green's function, $G(\xi;x)$ expresses the deflection of point ξ because of the unit point load at point x, as it is shown in Fig. (3a).

By the help of the new set of 12 boundary conditions expressed as Eqs. (86) and (89), the boundary conditions that must be considered for new Green's function are:

$$\begin{cases} G(0)=0 \\ G^{(1)}(0)=0 \\ \xi_2 G^{(2)}(0)-\xi_1 l_c^2 G^{(4)}(0)=0 \\ G^{(2)}(\mathrm{L})=0 \\ G^{(4)}(\mathrm{L})=0 \\ G^{(3)}(\mathrm{L})-\xi_1 l_c^2 G^{(5)}(\mathrm{L})=0 \end{cases} \qquad \begin{cases} G(x^-)=G(x^+) \\ G^{(1)}(x^-)=G^{(1)}(x^+) \\ G^{(2)}(x^-)=G^{(2)}(x^+) \\ G^{(3)}(x^-)-G^{(3)}(x^+)=-\frac{1}{\xi_1} \\ G^{(4)}(x^-)=G^{(4)}(x^+) \\ G^{(5)}(x^-)-G^{(5)}(x^+)=-\frac{\xi_2}{\xi_1^2 l_c^2} \end{cases} \tag{93}$$

Fortunately, the 10th and 12th boundary conidtions are consistent with the main differential Eq. (2). By integrating the both sides of this equation over x^- through x^+, we have:

$$\int_{x^-}^{x^+}\frac{d^4G(\xi;x)}{d\xi^4}d\xi-\xi_1 l_c^2\int_{x^-}^{x^+}\frac{d^6G(\xi;x)}{d\xi^6}d\xi=1 \tag{94}$$

Thus:

$$\left[G^{(3)}(x^+)-G^{(3)}(x^-)\right]-\xi_1 l_c^2\left[G^{(5)}(x^+)-G^{(5)}(x^-)\right]=\frac{1}{\xi_1}-\xi_1 l_c^2\frac{\xi_2}{\xi_1^2 l_c^2}=\frac{1-\xi_2}{\xi_1}=1 \quad \text{O.K.} \tag{95}$$

The 12 uknown constants of the Green's function (92) could be found by solving 12 Eq. (93) simultanously. After solving these equations, the Green's function of deflection for clamped- free beams is obtained as shown in Appendix B. Fig. 4 shows the dimensionless Green's function for some dimensionless values of ξ_1^* and l_c^*:

4. Simply supported two-phase peridynamic beam

In the next example, the static deflection of the two-phase simply supported peridynamic beam is studied. By this work, the classical

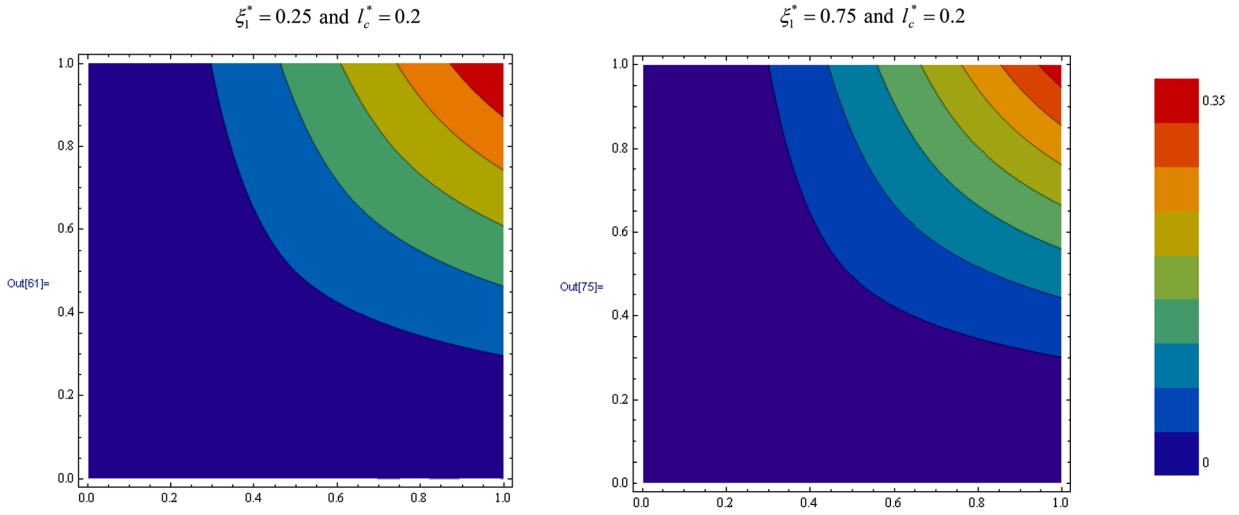

Fig. 4. Contours of Green's function for two-phase clamped-free beam.

boundary conditions are changed.

4.1. Uniformly distributed loading (second-order DE)

In this determinate beam, $M(x)$ is known, and it is as shown in Fig. 5:

$$M(x) = -\frac{1}{2}qx^2 + \frac{1}{2}q\,\mathrm{L}\,x \;\Rightarrow M^{(2)}(x) = -q \tag{96}$$

As it is clear, unlike the clamped-free cantilever beam with end point load, and similar to the clamped-free cantilever beam with distributed loading, the above-mentioned function has the non-zero second derivative. Therefore, the main Eq. (1) becomes:

$$\kappa(x) - \xi_1 l_c^2 \kappa^{(2)}(x) = \frac{1}{EI}\left(-\frac{1}{2}qx^2 + \frac{1}{2}q\,\mathrm{L}\,x + ql_c^2\right) \tag{97}$$

Moreover, two constitutive boundary conditions alter slightly, due to $M^{(2)}(0)$ and $M^{(2)}(\mathrm{L})$ are not equal to zero. Based on Eq. (19) in [22], we have:

$$\begin{cases} -q - EI\xi_1\kappa^{(2)}(0) + \dfrac{EI}{l_c^2}\xi_2\kappa(0) = 0 \\ -q - EI\xi_1\kappa^{(2)}(\mathrm{L}) + \dfrac{EI}{l_c^2}\xi_2\kappa(\mathrm{L}) = 0 \end{cases} \tag{98}$$

or:

$$\begin{cases} \xi_2\kappa(0) - \xi_1 l_c^2\kappa^{(2)}(0) = \dfrac{q\,l_c^2}{EI} \\ \xi_2\kappa(\mathrm{L}) - \xi_1 l_c^2\kappa^{(2)}(\mathrm{L}) = \dfrac{q\,l_c^2}{EI} \end{cases} \tag{99}$$

Similar to the previous examples, since in the Green's function method, the boundary conditions must have order less than the differential equation, we straightforwardly use the differential Eq. (97) twice: firstly at $x = 0$, and secondly at $x = \mathrm{L}$. Also, each time, a linear system of equations, including a boundary condition (rep.44) along with a new equation generated using the differential Eq. (99), is solved, as follows:

$$\begin{cases} \kappa(0) - \xi_1 l_c^2\kappa^{(2)}(0) = \dfrac{ql_c^2}{EI} \\ \xi_2\kappa(0) - \xi_1 l_c^2\kappa^{(2)}(0) = \dfrac{ql_c^2}{EI} \end{cases} \Rightarrow \kappa(0) = 0 \tag{100}$$

and, similarly:

$$\begin{cases} \kappa(\mathrm{L}) - \xi_1 l_c^2\kappa^{(2)}(\mathrm{L}) = \dfrac{ql_c^2}{EI} \\ \xi_2\kappa(\mathrm{L}) - \xi_1 l_c^2\kappa^{(2)}(\mathrm{L}) = \dfrac{ql_c^2}{EI} \end{cases} \Rightarrow \kappa(\mathrm{L}) = 0 \tag{101}$$

Interestingly again, both boundary conditions obtained above are consistent with the two constitutive boundary conditions coupled with Eq. (1). At the both ends of the simple-simple beam with $x = 0$ and$x = \mathrm{L}$, the moment is zero, and consequently, the curvature will also be zero.

Eqs. (100) and (101) are the new boundary conditions with order "zero" for simply supported beam under uniformly distributed loading.

Now, without any changes, except on the right-hand side of the differential equation due to the change in $M(x)$, we can use Eq. (46) in sub-Section 3.2. Herein, that equation becomes:

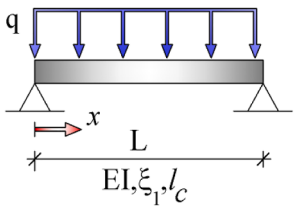

Fig. 5. Two-phase simply supported beam under uniformly distributed loading.

$$\kappa(x)=\int_0^{\mathrm{L}} G(\xi;x)\frac{1}{EI}\left(-\frac{1}{2}q\,\xi^2+\frac{1}{2}q\,\mathrm{L}\xi+ql_c^2\right)d\xi+\xi_1 l_c^2\left[G\frac{d\kappa}{d\xi}-\kappa\frac{dG}{d\xi}\right]_0^{\mathrm{L}} \tag{102}$$

The bracket is expanded as:

$$\left[G\frac{d\kappa}{d\xi}-\kappa\frac{dG}{d\xi}\right]_0^{\mathrm{L}}=G(\mathrm{L};x)\,\kappa^{(1)}(\mathrm{L})-G^{(1)}(\mathrm{L};x)\,\kappa(\mathrm{L}) -G(0;x)\,\kappa^{(1)}(0)+G^{(1)}(0;x)\,\kappa(0) \tag{rep.15}$$

By substituting Eqs. (100) and (101) into Eq. (rep.15), we have:

$$\left[G\frac{d\kappa}{d\xi}-\kappa\frac{dG}{d\xi}\right]_0^{\mathrm{L}}=G(\mathrm{L};x)\,\kappa^{(1)}(\mathrm{L})-G(0;x)\,\kappa^{(1)}(0) \tag{103}$$

Since $\kappa^{(1)}(0)$ and $\kappa^{(1)}(\mathrm{L})$ are unknowns, we set their coefficients to zero in Eq. (103). Thus:

$$\begin{cases} G(0;x)=0 \\ G(\mathrm{L};x)=0 \end{cases} \tag{rep.17}$$

Eq. (rep.17) shows the boundary conditions of the curvature Green's function which are exactly the same as the curvature Green's

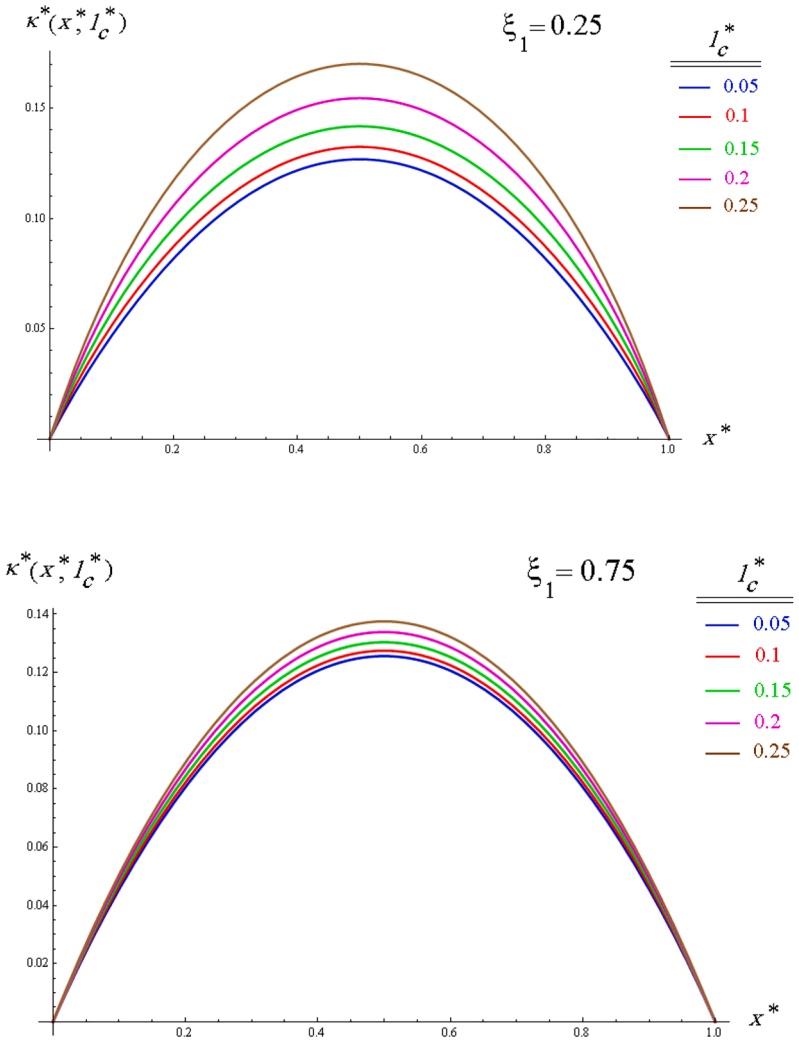

Fig. 6. The dimensionless curvature of SS two-phase peridynamic beam under uniformly distributed loading.

function of clamped-free beam. Therefore, the Green's function is the same as Eq. (38). By substituting the Green's function Eq. (38) into Eq. (102), and given that the bracket has been zeroed, we can find the unknown curvature function by the following equation:

$$\kappa(x) = \int_0^{\mathrm{L}} G(\xi;x)\frac{1}{EI}\left(-\frac{1}{2}q\,\xi^2 + \frac{1}{2}q\,\mathrm{L}\xi + q l_c^2\right)d\xi \tag{104}$$

By calculating the above integral over the both $[0,x]$ and $[x,\mathrm{L}]$ intervals, and then adding the results together, we arrive at the following result:

$$\kappa(x) = \frac{q}{2EI}\left[(\mathrm{L}-x)x + 2l_c^2\xi_2 - 2l_c^2\xi_2\,\mathrm{sech}\left(\frac{\mathrm{L}}{2l_c\sqrt{\xi_1}}\right)\cosh\left(\frac{\mathrm{L}-2x}{2l_c\sqrt{\xi_1}}\right)\right] \tag{105}$$

The above-obtained Green's function could be easily free dimensioned, by using the following dimensionless variables:

$$\kappa^* = \frac{EI\,\kappa}{q\,\mathrm{L}^2};\quad x^* = \frac{x}{\mathrm{L}};\quad l_c{}^* = \frac{l_c}{\mathrm{L}} \tag{106}$$

The dimensionless curvature can then be re-expressed by:

$$\kappa^*(x^*) = \frac{1}{2}(1-x^*)x^* + \xi_2\left(l_c^*\right)^2 - \xi_2\left(l_c^*\right)^2\mathrm{sech}\left(\frac{1}{2\sqrt{\xi_1}l_c^*}\right)\cosh\left(\frac{1-2x^*}{2\sqrt{\xi_1}l_c^*}\right) \tag{107}$$

Figs. 6 show this dimensionless curvature for some values of ξ_1^* and l_c^*.
It should be mentioned that Eq. (105) will be verified in sub-Section 4.3.

4.2. Sinusoidal distributed loading (second-order DE)

In the next example, the type of the distributed loading is changed as shown in Fig. 7. However, the two-phase peridynamic beam remains simply supported. Besides, the sinusoidal distributed loading is downward and therefore negative.
In this beam, $M(x)$ is as the below:

$$M(x) = \frac{q\,\mathrm{L}^2}{\pi^2}\sin\left(\frac{\pi x}{\mathrm{L}}\right) \Rightarrow M^{(2)}(x) = -q\sin\left(\frac{\pi x}{\mathrm{L}}\right) \tag{108}$$

Therefore, the main Eq. (1) becomes:

$$\kappa - \xi_1 l_c^2\kappa^{(2)} = \frac{1}{EI}\left[\frac{q\,\mathrm{L}^2}{\pi^2}\sin\left(\frac{\pi x}{\mathrm{L}}\right) + l_c^2 q\sin\left(\frac{\pi x}{\mathrm{L}}\right)\right] \tag{109}$$

or:

$$\kappa - \xi_1 l_c^2\kappa^{(2)} = \frac{q}{EI}\left(\frac{\mathrm{L}^2}{\pi^2} + l_c^2\right)\sin\left(\frac{\pi x}{\mathrm{L}}\right) \tag{110}$$

Moreover, two constitutive boundary conditions alter slightly in comparison to the previous example, due to $M^{(2)}(0)$ and $M^{(2)}(\mathrm{L})$ are equal to zero. Based on Eq. (19) in [22], we have:

$$\begin{cases} -EI\xi_1\kappa^{(2)}(0) + \dfrac{EI}{l_c^2}\xi_2\kappa(0) = 0 \\ -EI\xi_1\kappa^{(2)}(\mathrm{L}) + \dfrac{EI}{l_c^2}\xi_2\kappa(\mathrm{L}) = 0 \end{cases} \tag{111}$$

or:

$$\begin{cases} \xi_2\kappa(0) - \xi_1 l_c^2\kappa^{(2)}(0) = 0 \\ \xi_2\kappa(\mathrm{L}) - \xi_1 l_c^2\kappa^{(2)}(\mathrm{L}) = 0 \end{cases} \tag{112}$$

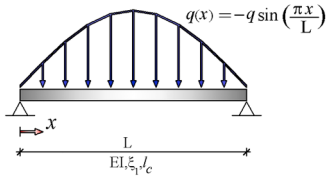

Fig. 7. Simply supported two-phase peridynamic beam under sinusoidal distributed loading.

Similar to the previous examples, since in the Green's function method, the boundary conditions must have order less than the differential equation, we should use the differential Eq. (110) twice: firstly at $x = 0$, and secondly at $x = \mathrm{L}$. Also, each time, a linear system of equations, including a boundary condition Eq. (112) along with a new equation generated using the differential Eq. (110), is solved, as follows:

$$\begin{cases} \kappa(0) - \xi_1 l_c^2 \kappa^{(2)}(0) = 0 \\ \xi_2 \kappa(0) - \xi_1 l_c^2 \kappa^{(2)}(0) = 0 \end{cases} \Rightarrow \kappa(0) = 0 \tag{113}$$

and, similarly:

$$\begin{cases} \kappa(\mathrm{L}) - \xi_1 l_c^2 \kappa^{(2)}(\mathrm{L}) = 0 \\ \xi_2 \kappa(\mathrm{L}) - \xi_1 l_c^2 \kappa^{(2)}(\mathrm{L}) = 0 \end{cases} \Rightarrow \kappa(\mathrm{L}) = 0 \tag{114}$$

Interestingly again, both boundary conditions obtained above are consistent with the two constitutive boundary conditions coupled with Eq. (1). At the both ends of the simple-simple beam with $x = 0$ and$x = \mathrm{L}$, the moment is zero, and consequently, the curvature will also be zero.

Exactly similar to the previous examples, the bracket in Eq. (11) becomes zero, and we can easily find the unknown curvature function by the following equation and the Green's function Eq. (38):

$$\kappa(x) = \int_0^{\mathrm{L}} G(\xi; x) \frac{q}{EI} \left(\frac{\mathrm{L}^2}{\pi^2} + l_c^2 \right) \sin\left(\frac{\pi \xi}{\mathrm{L}} \right) d\xi \tag{115}$$

By calculating the above integral over the both $[0, x]$ and $[x, \mathrm{L}]$ intervals, and then adding the results together, we arrive at the following result:

$$\kappa(x) = \frac{q\,\mathrm{L}^2}{EI\left(\mathrm{L}^2 + \xi_1 l_c^2 \pi^2\right)} \left(\frac{\mathrm{L}^2}{\pi^2} + l_c^2 \right) \sin\left(\frac{\pi x}{\mathrm{L}} \right) \tag{116}$$

In the next section, we will analyze the simply supported two-phase peridynamic Euler-Bernouli beam under uniformly distributed loading again, but this time by solving the sixth-order differential equation, for some verification purposes. It should be mentioned that to analyze the statically indeterminate beams (the main subject of Section 5 in this article) we have to solve this sixth-order differential equation, because the moment function is unknown.

4.3. *Uniformly distributed loading (sixth-order DE)*

This problem was previously solved partially by the help of the second-order differenial equation. Of course, the second-order DE gives the "curvature function", and the sixth-order DE gives the "deflection function". At the end, we will use the relation $\kappa = w^{(2)}$ for verification purpose.

Herein, we want to solve the six-order differential Eq. (2) which becomes as the following for this example:

$$w^{(4)}(x) - \xi_1 l_c^2 w^{(6)}(x) = \frac{1}{EI}\left(p - l_c^2 p''\right) = -\frac{q}{EI} \tag{117}$$

It should be mentioned that the uniformly distributed loading is downward and therefore negative. Also, its second derivative is equal to zero, because it is constant.

The differential Eq. (117) has six boundary conditions (four classical and the two constitutive boundary conditions). To obtain the two constitutive boundary conditions, we need to $M''(0)$ and $M''(\mathrm{L})$. We know $M''(x) = -q$. Therefore, Based on Eq. (19) in [22], we have:

$$\begin{cases} \xi_2 w^{(2)}(0) - \xi_1 l_c^2 w^{(4)}(0) = \dfrac{q\, l_c^2}{EI} \\ \xi_2 w^{(2)}(\mathrm{L}) - \xi_1 l_c^2 w^{(4)}(\mathrm{L}) = \dfrac{q\, l_c^2}{EI} \end{cases} \tag{rep.44}$$

The four classical boundary conditions for simple-clamped beam are as below:

$$\begin{cases} w(0) = 0 \\ w^{(2)}(0) = 0 \\ w(\mathrm{L}) = 0 \\ w^{(2)}(\mathrm{L}) = 0 \end{cases} \tag{118}$$

Substituting Eq. (118) into Eq.Eq. (rep.44), the complete form of all boundary conditions for simple-simple beam under uniformly distributed loading becomes as the following:

$$\begin{cases} w(0)=0 \\ w^{(2)}(0)=0 \\ w^{(4)}(0)=-\dfrac{q}{\xi_1 EI} \\ w(\mathrm{L})=0 \\ w^{(2)}(\mathrm{L})=0 \\ w^{(4)}(\mathrm{L})=-\dfrac{q}{\xi_1 EI} \end{cases} \tag{119}$$

To solve the differential Eq. (117) by the help of Green's function, firstly, both sides of the differental equation are multiplied by the Green's function, which will be found in the next steps. Also, the independent variable is changed form x to ξ:

$$G(\xi;x)\left(w^{(4)}(\xi)-\xi_1 l_c^2 w^{(6)}(\xi)\right)=G(\xi;x)\left(-\frac{q}{EI}\right) \tag{120}$$

Assuming that the Green's function is known, the right-hand side of the above equation is known. For the left-hand side, using the well-known "integration by parts" technique, we have:

$$\int_0^L G(\xi;x)\underbrace{\left(w^{(4)}(\xi)-\xi_1 l_c^2\, w^{(6)}(\xi)\right)}_{\left(-\frac{q}{EI}\right)}d\xi=[\ldots]_0^L+\int_0^L w(\xi)\underbrace{\left(G^{(4)}-\xi_1 l_c^2\, G^{(6)}\right)}_{\delta(\xi-x)}d\xi \tag{rep.66}$$

with the bracket introduced by Eq. (67). In this step, we should utilize the six boundary conditions exist in Eq. (119). Substituting these equations into bracket Eq. (67) yields to:

$$\begin{aligned} [\ldots]_0^{\mathrm{L}} &= G(\mathrm{L};x)\left(w^{(3)}(\mathrm{L})-\xi_1 l_c^2\, w^{(5)}(\mathrm{L})\right)-G^{(1)}(\mathrm{L};x)\left(\frac{q\,l_c^2}{EI}\right) \\ &+G^{(2)}(\mathrm{L};x)\left(w^{(1)}(\mathrm{L})-\xi_1 l_c^2\, w^{(3)}(\mathrm{L})\right)-\xi_1 l_c^2\, G^{(4)}(\mathrm{L};x)\, w^{(1)}(\mathrm{L}) \\ &-G(0;x)\left(w^{(3)}(0)-\xi_1 l_c^2\, w^{(5)}(0)\right)+G^{(1)}(0;x)\left(\frac{q\,l_c^2}{EI}\right) \\ &-G^{(2)}(0;x)\left(w^{(1)}(0)-\xi_1 l_c^2\, w^{(3)}(0)\right)+\xi_1 l_c^2\, G^{(4)}(0;x)\, w^{(1)}(0) \end{aligned} \tag{121}$$

By re-arranging Eq. (121), we approach to six boundary conditions of Green's function for simple-simple beam:

$$\begin{aligned} [\ldots]_0^{\mathrm{L}} = &-w^{(5)}(\mathrm{L})\left(\xi_1 l_c^2\, G(\mathrm{L};x)\right) \\ &+w^{(3)}(\mathrm{L})\left(G(\mathrm{L};x)-\xi_1 l_c^2\, G^{(2)}(\mathrm{L};x)\right) \\ &+w^{(1)}(\mathrm{L})\left(G^{(2)}(\mathrm{L};x)-\xi_1 l_c^2\, G^{(4)}(\mathrm{L};x)\right) \\ &+w^{(5)}(0)\left(\xi_1 l_c^2\, G(0;x)\right) \\ &-w^{(3)}(0)\left(G(0;x)-\xi_1 l_c^2\, G^{(2)}(0;x)\right) \\ &-w^{(1)}(0)\left(G^{(2)}(0;x)-\xi_1 l_c^2\, G^{(4)}(0;x)\right) \\ &+\left(G^{(1)}(0;x)-G^{(1)}(\mathrm{L};x)\right)\frac{q\,l_c^2}{EI} \end{aligned} \tag{122}$$

Since $w^{(5)}(\mathrm{L})$, $w^{(3)}(\mathrm{L})$, $w^{(1)}(\mathrm{L})$, $w^{(5)}(0)$, $w^{(3)}(0)$ and $w^{(1)}(0)$ are unknowns, we set their coefficients to zero in Eq. (122). Therefore, the six homogenous boundary conditions of Green's function are obtained as the following:

$$\begin{cases} G(0;x)=0 \\ G^{(2)}(0;x)=0 \\ G^{(4)}(0;x)=0 \\ G(\mathrm{L};x)=0 \\ G^{(2)}(\mathrm{L};x)=0 \\ G^{(4)}(\mathrm{L};x)=0 \end{cases} \tag{123}$$

Then, bracket (67) becomes:

$$[\ldots]_0^{\mathrm{L}}=\left(G^{(1)}(0;x)-G^{(1)}(\mathrm{L};x)\right)\frac{q\,l_c^2}{EI} \tag{124}$$

By the help of the main property of the Dirac delta function (Eq. 10), and substituting Eq. (124) into Eq. (rep.66), we can reach to the deflection function of simple-simple beam under uniformly distributed loading:

$$w(x)=\int_0^x G(\xi;x)\left(-\frac{q}{EI}\right)d\xi+\int_x^{\mathrm{L}} G(\xi;x)\left(-\frac{q}{EI}\right)d\xi+\left(G^{(1)}(\mathrm{L};x)-G^{(1)}(0;x)\right)\frac{q\,l_c^2}{EI} \tag{125}$$

Now, we should only find the Green's function. Eq. (123) shows the six boundary conditions of Green's function. Based on Eq. (rep.66), its governing differential equation is:

$$\frac{d^4G(\xi;x)}{d\xi^4}-\xi_1 l_c^2\frac{d^6G(\xi;x)}{d\xi^6}=\delta(\xi-x) \tag{126}$$

The solution of Eq. (126) together with boundary conditions Eq. (123) is:

$$\begin{aligned}G(\xi;x)=&\xi_1^{\frac{3}{2}}l_c^3\sinh\left(\frac{\mathrm{L}-x}{\sqrt{\xi_1}l_c}\right)\left(\frac{\sinh\left(\frac{\xi}{\sqrt{\xi_1}l_c}\right)}{\sinh\left(\frac{\mathrm{L}}{\sqrt{\xi_1}l_c}\right)}\right)-\frac{(\mathrm{L}-x)\,\xi}{6\mathrm{L}}\left(x^2-2\mathrm{L}x+\xi^2+6l_c^2\xi_1\right)\\&+\left(\xi_1^{\frac{3}{2}}l_c^3\sinh\left(\frac{x-\xi}{\sqrt{\xi_1}l_c}\right)-\frac{1}{6}(x-\xi)^3-\xi_1 l_c^2(x-\xi)\right)\widehat{H}(\xi-x)\end{aligned} \tag{127}$$

By substituting the Green's function Eq. (127) and its first derivative into Eq. (125), we arrive at the following result for $w(x)$:

$$\begin{aligned}w(x)=&-\xi_1\xi_2\frac{q\,l_c^4}{EI}\left(\frac{\cosh\left(\frac{\mathrm{L}-2x}{2\sqrt{\xi_1}l_c}\right)}{\cosh\left(\frac{\mathrm{L}}{2\sqrt{\xi_1}l_c}\right)}-1\right)\\&-\frac{q}{24EI}\left(x^4-2\mathrm{L}x^3-12\xi_2 l_c^2x^2+\left(\mathrm{L}^2+12\xi_2 l_c^2\right)\mathrm{L}x\right)\end{aligned} \tag{128}$$

In previous section, we found the "curvature" of simple-simple beam under uniformly distributed loading, i.e., the second derivative of $w(x)$, directly, by the help of another Green's function. For verification purpose, we find the second derivative of Eq. (128) and

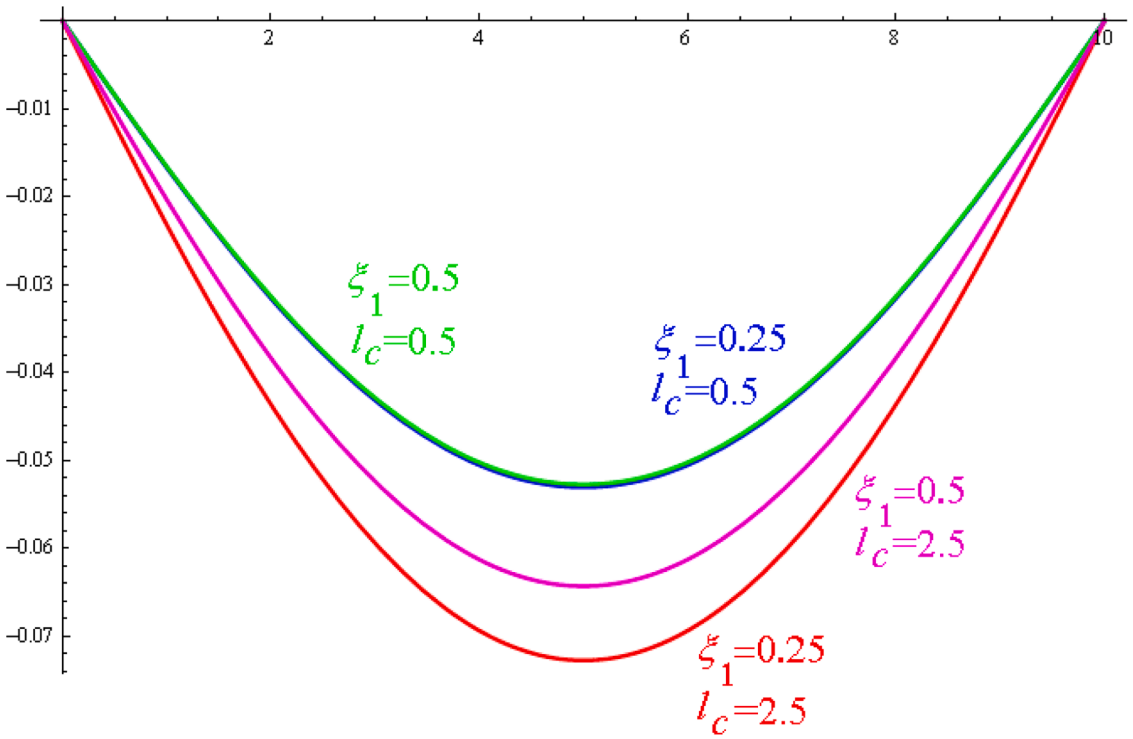

Fig. 8. Deflection of simply supported two-phase peridynamic beam under uniformly distributed loading.

compare it with Eq. (105). Fortunately, both functions are the same:

$$w^{(2)}(x)=\frac{q}{2EI}\left((\mathrm{L}-x)x+2l_c^2\xi_2-2l_c^2\xi_2\frac{\cosh\left(\frac{\mathrm{L}-2x}{2\sqrt{\xi_1}l_c}\right)}{\cosh\left(\frac{\mathrm{L}}{2\sqrt{\xi_1}l_c}\right)}\right) \tag{129}$$

For further verification, we will numerically find the deflection of simple-simple beam under uniformly distributed loading in Section 6, by the help of "series solution". In that section, Eq. (128) could be easily use for verification purpose.

Moreover, the numerical results extracted with the help of the closed-form solution Eq. (112) are as follows. The following graphs seem reasonable. They are plotted for the following input data. Besides, ξ_1 is dimensionless, and the unit of l_c is *nm*:

$$L=10nm,\ b=h=\frac{L}{10},\ E=30\times10^6\frac{nN}{nm^2},\ q=10^3\frac{nN}{nm^2} \tag{130}$$

Fig. 8 shows that the effect of ξ_1 is negligible for small l_c, of course, in simple-simple beam under uniformly distributed loading.

4.4. General concentrated load (sixth-order DE)

Alongside the distributed loading, we want to find the results for concentrated loads. Similar to Section 3.4, this problem is solved by using two different deflection functions (see Fig. 9)

$w_L(x)$denotes the deflection function for Left segments of the point load, i.e., for,$x<a$, and

$w_R(x)$ denotes the deflection function for Right segments of the point load, i.e., for $x>a$.

This problem has 12 boundary conditions as the following:

$$\begin{cases} w_L(0)=0 \\ w_L^{(2)}(0)=0 \\ w_L^{(4)}(0)=0 \\ w_R(\mathrm{L})=0 \\ w_R^{(2)}(\mathrm{L})=0 \\ w_R^{(4)}(\mathrm{L})=0 \end{cases} \quad \begin{cases} w_L(a)=w_R(a) \\ w_L^{(1)}(a)=w_R^{(1)}(a) \\ w_L^{(2)}(a)=w_R^{(2)}(a) \\ w_L^{(3)}(a)-w_R^{(3)}(a)=\frac{1}{\xi_1}\frac{P}{EI} \\ w_L^{(4)}(a)=w_R^{(4)}(a) \\ w_L^{(5)}(a)-w_R^{(5)}(a)=\frac{\xi_2}{\xi_1^2 l_c^2}\frac{P}{EI} \end{cases} \tag{131}$$

Based on the definition of the Green's function, $G(\xi;x)$ expresses the deflection of point ξ because of the unit point load at point x, as it is shown in Fig. 10.

Similar to Section 3.4, the Green's function could be expressed as:

$$G(\xi;x)=\begin{cases} c_1\sinh\left(\frac{\xi}{\sqrt{\xi_1}l_c}\right)+c_2\cosh\left(\frac{\xi}{\sqrt{\xi_1}l_c}\right)+c_3\xi^3+c_4\xi^2+c_5\xi+c_6 & 0<\xi<x \\ c_7\sinh\left(\frac{\xi}{\sqrt{\xi_1}l_c}\right)+c_8\cosh\left(\frac{\xi}{\sqrt{\xi_1}l_c}\right)+c_9\xi^3+c_{10}\xi^2+c_{11}\xi+c_{12} & x<\xi<\mathrm{L} \end{cases} \tag{132}$$

Based on the set of 12 boundary conditions Eq. (131), the bondary conditions that must be considered for deflection Green's function are:

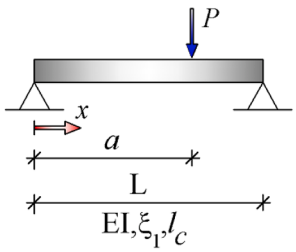

Fig. 9. Simply supported two-phase peridynamic beam under general concentrated load.

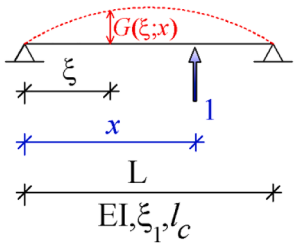

Fig. 10. Simply supported beam under general unit concentrated load.

$$\begin{cases} G(0)=0 \\ G^{(2)}(0)=0 \\ G^{(4)}(0)=0 \\ G(\mathrm{L})=0 \\ G^{(2)}(\mathrm{L})=0 \\ G^{(4)}(\mathrm{L})=0 \end{cases} \quad \begin{cases} G(x^-)=G(x^+) \\ G^{(1)}(x^-)=G^{(1)}(x^+) \\ G^{(2)}(x^-)=G^{(2)}(x^+) \\ G^{(3)}(x^-)-G^{(3)}(x^+)=-\dfrac{1}{\xi_1} \\ G^{(4)}(x^-)=G^{(4)}(x^+) \\ G^{(5)}(x^-)-G^{(5)}(x^+)=-\dfrac{\xi_2}{\xi_1^2 l_c^2} \end{cases} \tag{133}$$

The 12 uknown constants of the Green's function Eq. (132) could be found by solving 12 Eq. (133) simultanously. After solving these equations, the Green's function of deflection for two-phase simply supported beams is obtained as shown in Appendix C. Fig. 11 shows the dimensionless Green's function for some dimensionless values of ξ_1^* and l_c^*:

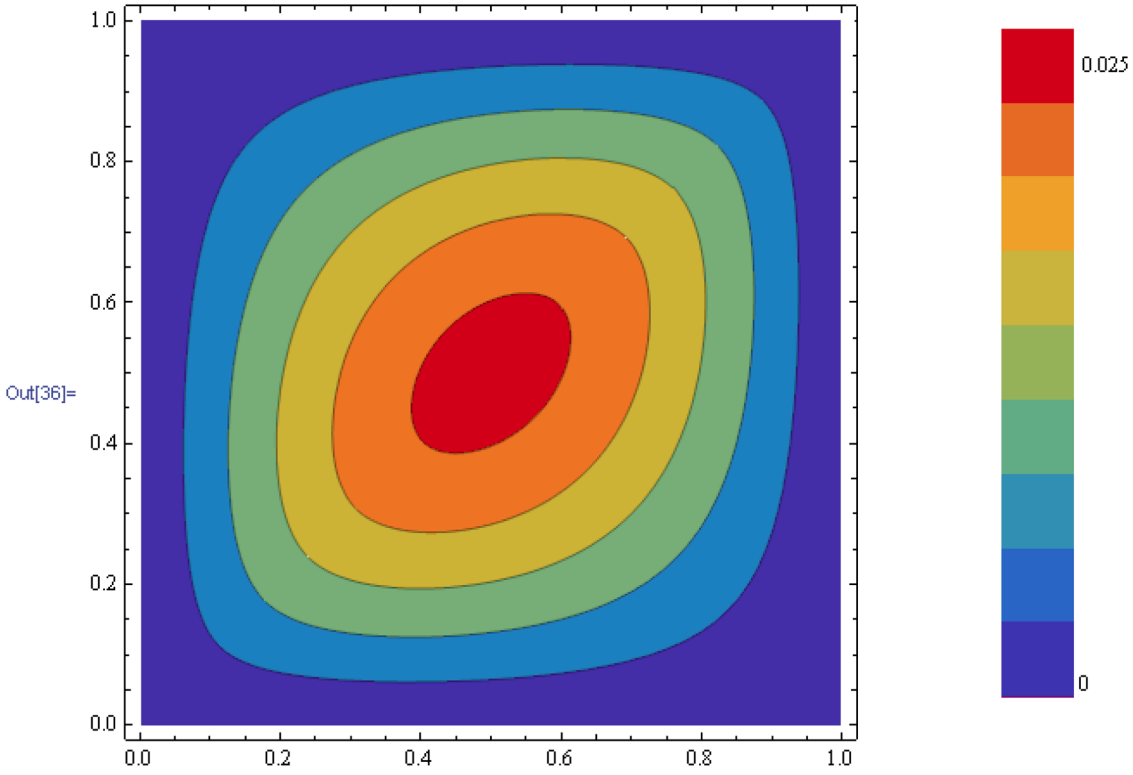

Fig. 11. Contours of green's function for simply supported two-phase peridynamic beam.

Besides, the dimensionless deflection function of the beam is:

$$w^*(x^*) = -G(x^*;a^*) \tag{134}$$

For example, by inserting $a^* = x^* = 1/2$ into Eq. (8), we obtain the following result, which fortunately coincides with the series solution which will be described in Section 6.

$$w^*\left(\frac{1}{2}\right) = \frac{1}{48} + \frac{1}{4}\xi_2 (l_c^*)^2 \left[1 - 2l_c^* \sqrt{\xi 1}\ \tanh\left(\frac{1}{2\sqrt{\xi 1} l_c^*}\right)\right] \tag{135}$$

5. Statically indeterminate beams (sixth-order DE)

In this kind of beams, the moment function is unknown. Therefore, we have to solve the six-order differential Eq. (2). This equation is as the following, for uniformly distributed loading:

$$w^{(4)}(x) - \xi_1 l_c^2 w^{(6)}(x) = \frac{1}{EI}\left(p - l_c^2 p''\right) = -\frac{q}{EI} \tag{136}$$

In the following, we will solve two different examples. It should be noted that the analysis of indeterminate two-phase peridynamic Euler-Bernoulli beams is performed for the first time in this article. It should be also mentioned that in the both examples, the first derivative of the curvature function is continuous, due to the absence of concentrated force. Therefore, we can easily use the general form of Green' function (73).

5.1. Simple-Clamped beam

The new example is as shown in Fig. 12. The slope at $x = \mathrm{L}$ is equal to zero in this beam.

Interestingly, although the moment function is unknown, its second derivative is known. In fact, $M''(x) = -q$. Therefore, based on Eq. (19) in [22], we have:

$$\begin{cases} \xi_2 w^{(2)}(0) - \xi_1 l_c^2 w^{(4)}(0) = \dfrac{q l_c^2}{EI} \\ \xi_2 w^{(2)}(\mathrm{L}) - \xi_1 l_c^2 w^{(4)}(\mathrm{L}) = \dfrac{q l_c^2}{EI} \end{cases} \tag{rep.44}$$

The four classical boundary conditions for simple-clamped beam are as below:

$$\begin{cases} w(0) = 0 \\ w^{(2)}(0) = 0 \\ w(\mathrm{L}) = 0 \\ w^{(1)}(\mathrm{L}) = 0 \end{cases} \tag{137}$$

To solve the differential Eq. (136) by the help of Green's function, firstly, both sides of the differental equation are multiplied by the Green's function, which will be found in the next steps. Similar to the previous example, we have:

$$\int_0^L G(\xi;x) \underbrace{\left(w^{(4)}(\xi) - \xi_1 l_c^2\, w^{(6)}(\xi)\right)}_{\left(-\frac{q}{EI}\right)} d\xi = [\ldots]_0^L + \int_0^L w(\xi) \underbrace{\left(G^{(4)} - \xi_1 l_c^2\, G^{(6)}\right)}_{\delta(\xi - x)} d\xi \tag{rep.66}$$

with the following bracket:

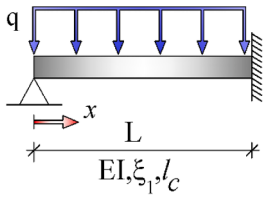

Fig. 12. Simple-clamped two-phase peridynamic beam under uniformly distributed loading.

$$
\begin{aligned}
&[\ldots]_0^{\mathrm{L}} = G(\mathrm{L};x)\left(w^{(3)}(\mathrm{L}) - \xi_1 l_c^2\, w^{(5)}(\mathrm{L})\right) - G^{(1)}(\mathrm{L};x)\left(w^{(2)}(\mathrm{L}) - \xi_1 l_c^2\, w^{(4)}(\mathrm{L})\right)\\
&+G^{(2)}(\mathrm{L};x)\left(w^{(1)}(\mathrm{L}) - \xi_1 l_c^2\, w^{(3)}(\mathrm{L})\right) - G^{(3)}(\mathrm{L};x)\left(w(\mathrm{L}) - \xi_1 l_c^2\, w^{(2)}(\mathrm{L})\right)\\
&-\xi_1 l_c^2\, G^{(4)}(\mathrm{L};x)\, w^{(1)}(\mathrm{L}) + \xi_1 l_c^2\, G^{(5)}(\mathrm{L};x)\, w(\mathrm{L})\\
&-G(0;x)\left(w^{(3)}(0) - \xi_1 l_c^2\, w^{(5)}(0)\right) + G^{(1)}(0;x)\left(w^{(2)}(0) - \xi_1 l_c^2\, w^{(4)}(0)\right)\\
&-G^{(2)}(0;x)\left(w^{(1)}(0) - \xi_1 l_c^2\, w^{(3)}(0)\right) + G^{(3)}(0;x)\left(w(0) - \xi_1 l_c^2\, w^{(2)}(0)\right)\\
&+\xi_1 l_c^2\, G^{(4)}(0;x)\, w^{(1)}(0) - \xi_1 l_c^2\, G^{(5)}(0;x)\, w(0)
\end{aligned}
\tag{rep.67}
$$

In this step, we should use the six boundary conditions exist in Eqs. Eqs. (rep.44) and (137). Substituting these boundary conditions into bracket Eq. (rep.84) yields to:

$$
\begin{aligned}
&[\ldots]_0^{\mathrm{L}} = G(\mathrm{L};x)\left(w^{(3)}(\mathrm{L}) - \xi_1 l_c^2\, w^{(5)}(\mathrm{L})\right) - G^{(1)}(\mathrm{L};x)\left(\xi_1\, w^{(2)}(\mathrm{L}) + \frac{q\, l_c^2}{EI}\right)\\
&-G^{(2)}(\mathrm{L};x)\left(\xi_1 l_c^2\, w^{(3)}(\mathrm{L})\right) + G^{(3)}(\mathrm{L};x)\left(\xi_1 l_c^2\, w^{(2)}(\mathrm{L})\right)\\
&-G(0;x)\left(w^{(3)}(0) - \xi_1 l_c^2\, w^{(5)}(0)\right) - G^{(1)}(0;x)\left(-\frac{q\, l_c^2}{EI}\right)\\
&-G^{(2)}(0;x)\left(w^{(1)}(0) - \xi_1 l_c^2\, w^{(3)}(0)\right) + \xi_1 l_c^2\, G^{(4)}(0;x)\, w^{(1)}(0)
\end{aligned}
\tag{138}
$$

By re-arranging Eq. (138), we approach to six boundary conditions of the Green's function:

$$
\begin{aligned}
[\ldots]_0^{\mathrm{L}} = &-w^{(5)}(\mathrm{L})\left(\xi_1 l_c^2\, G(\mathrm{L};x)\right)\\
&+ w^{(3)}(\mathrm{L})\left(G(\mathrm{L};x) - \xi_1 l_c^2\, G^{(2)}(\mathrm{L};x)\right)\\
&- w^{(2)}(\mathrm{L})\left(\xi_1\, G^{(1)}(\mathrm{L};x) - \xi_1 l_c^2\, G^{(3)}(\mathrm{L};x)\right)\\
&+ w^{(5)}(0)\left(\xi_1 l_c^2\, G(0;x)\right)\\
&- w^{(3)}(0)\left(G(0;x) - \xi_1 l_c^2\, G^{(2)}(0;x)\right)\\
&- w^{(1)}(0)\left(G^{(2)}(0;x) - \xi_1 l_c^2\, G^{(4)}(0;x)\right)\\
&+ \left(G^{(1)}(0;x) - G^{(1)}(\mathrm{L};x)\right)\frac{q\, l_c^2}{EI}
\end{aligned}
\tag{139}
$$

Since $w^{(5)}(\mathrm{L})$, $w^{(3)}(\mathrm{L})$, $w^{(2)}(\mathrm{L})$, $w^{(5)}(0)$, $w^{(3)}(0)$ and $w^{(1)}(0)$ are unknowns, we set their coefficients to zero in Eq. (139). Therefore, the six homogenous boundary conditions of the Green's function are obtained as the following:

$$
\begin{cases}
G(\mathrm{L};x) = 0\\
G^{(2)}(\mathrm{L};x) = 0\\
G^{(1)}(\mathrm{L};x) - l_c^2\, G^{(3)}(\mathrm{L};x) = 0\\
G(0;x) = 0\\
G^{(2)}(0;x) = 0\\
G^{(4)}(0;x) = 0
\end{cases}
\tag{140}
$$

Then, bracket (rep.67) becomes:

$$
[\ldots]_0^{\mathrm{L}} = \left(G^{(1)}(0;x) - G^{(1)}(\mathrm{L};x)\right)\frac{q\, l_c^2}{EI}
\tag{141}
$$

By the help of the main property of the Dirac delta function (Eq. 10), and substituting Eq. (141) into Eq. (rep.66), we can reach to the deflection function of simple-clamped beam under uniformly distributed loading:

$$
w(x) = \int_0^x G(\xi;x)\left(-\frac{q}{EI}\right)d\xi + \int_x^{\mathrm{L}} G(\xi;x)\left(-\frac{q}{EI}\right)d\xi + \left(G^{(1)}(\mathrm{L};x) - G^{(1)}(0;x)\right)\frac{q\, l_c^2}{EI}
\tag{142}
$$

Now, we should only find the Green's function. Eq. (140) shows the six boundary conditions of Green's function. Based on the right-hand side of Eq. (rep.66), its governing differential equation is:

$$
\frac{d^4 G(\xi;x)}{d\,\xi^4} - \xi_1 l_c^2 \frac{d^6 G(\xi;x)}{d\,\xi^6} = \delta(\xi - x)
\tag{rep.126}
$$

The solution of Eq. (rep.126) together with boundary conditions (140) is:

$$G(\xi;x)=\left(\xi_1^{\frac{3}{2}}l_c^3\sinh\left(\frac{x-\xi}{\sqrt{\xi_1}l_c}\right)-\frac{1}{6}(x-\xi)^3-\xi_1 l_c^2(x-\xi)\right)\widehat{H}(\xi-x)$$
$$+\frac{1}{A}\left(\begin{array}{l}6\mathrm{L}l_c\xi_2(\mathrm{L}-x)\xi\left(2\mathrm{L}x-x^2-\xi^2-6l_c^2\xi_1\right)\cosh\left(\frac{\mathrm{L}}{\sqrt{\xi_1}l_c}\right)+\\ \sqrt{\xi_1}\left(\begin{array}{l}-\xi\left(\begin{array}{l}-3\mathrm{L}^4x+x^3\left(6l_c^2+\xi^2\right)+2\mathrm{L}^3\left(3x^2+\xi^2+6l_c^2\xi_1\right)\\ -6\mathrm{L}l_c^2\xi_2\left(3x^2+\xi^2+6l_c^2\xi_1\right)-3\mathrm{L}^2x\left(x^2+6l_c^2(2\xi_1-1)+\xi^2\right)\end{array}\right)\sinh\left(\frac{\mathrm{L}}{\sqrt{\xi_1}l_c}\right)\\ +6\mathrm{L}l_c^2\left(\begin{array}{l}-\xi_2\xi\left(-\mathrm{L}^2+\xi^2+6l_c^2\xi_1\right)\sinh\left(\frac{x}{\sqrt{\xi_1}l_c}\right)\\ +\left(\begin{array}{l}\xi_1x\left(-\mathrm{L}^2+x^2-6l_c^2\xi_2\right)+6\mathrm{L}l_c^2\xi_1\xi_2\cosh\left(\frac{\mathrm{L}-x}{\sqrt{\xi_1}l_c}\right)\\ +2\xi_1l_c\left(\mathrm{L}^2-3l_c^2\xi_2\right)\sqrt{\xi_1}\sinh\left(\frac{\mathrm{L}-x}{\sqrt{\xi_1}l_c}\right)\end{array}\right)\sinh\left(\frac{\xi}{\sqrt{\xi_1}l_c}\right)\end{array}\right)\end{array}\right)\end{array}\right) \tag{143}$$

where:

$$A=12\mathrm{L}\left(3\mathrm{L}l_c\xi_2\cosh\left(\frac{\mathrm{L}}{l_c\sqrt{\xi_1}}\right)+\left(\mathrm{L}^2-3l_c^2\xi_2\right)\sqrt{\xi_1}\sinh\left(\frac{\mathrm{L}}{l_c\sqrt{\xi_1}}\right)\right) \tag{144}$$

and $\widehat{H}$ is Heaviside function, and defined as:

$$\widehat{H}(\xi-x)=\begin{cases}1 & \xi>x\\ 0 & \xi<x\end{cases} \tag{rep.21}$$

By substituting the Green's function (143) and its first derivative into Eq. (142), we arrive at the following result for $w(x)$:

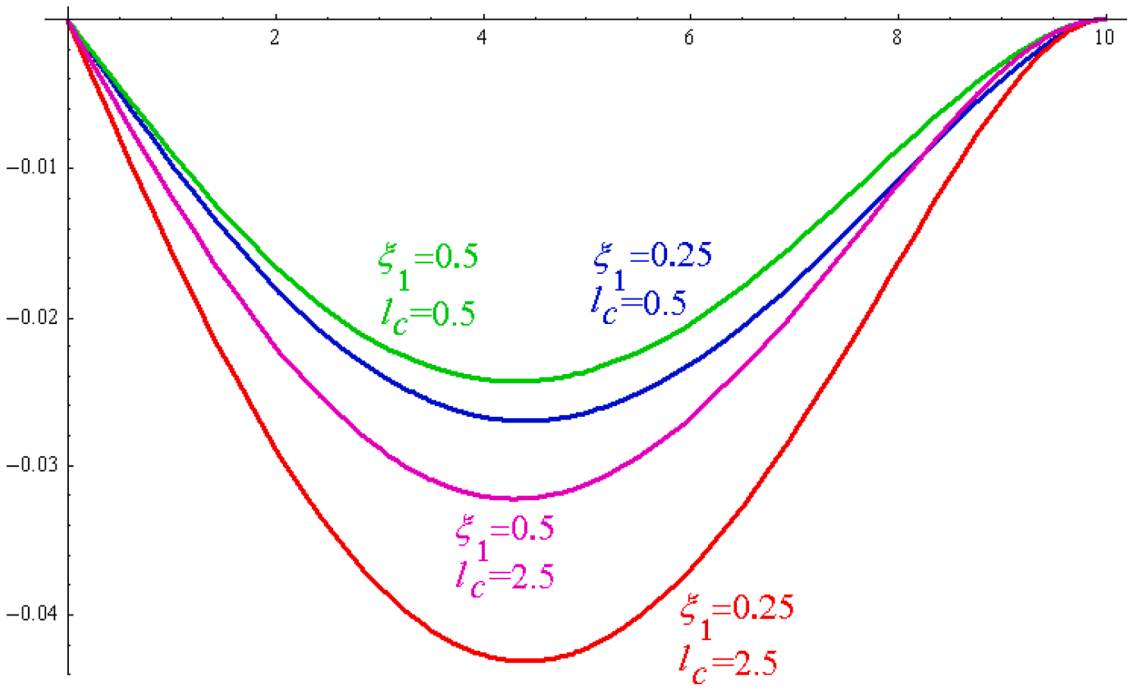

Fig. 13. Deflection function of simple-clamped two-phase peridynamic beam under uniformly distributed load.

$$w(x) = -\frac{q}{48EI}\frac{f(x)}{F};$$

$$f(x) = 6l_c(\mathrm{L}-x)\xi_2\left(\mathrm{L}^3x + \mathrm{L}^2x^2 + 4l_c^2\xi_1\left(x^2 - 6\xi_2 l_c^2\right) - \mathrm{L}x\left(4l_c^2(-3+2\xi_1) + x^2\right)\right)\cosh\left(\frac{\mathrm{L}}{l_c\sqrt{\xi_1}}\right)$$

$$+144\mathrm{L}l_c^5\xi_1{\xi_2}^2\cosh\left(\frac{\mathrm{L}-x}{l_c\sqrt{\xi_1}}\right)$$

$$-\sqrt{\xi_1}\begin{pmatrix}\mathrm{L}^5x - 3\mathrm{L}^3x^3 - 24\mathrm{L}l_c^2x\left(x^2 - 6l_c^2\xi_2\right)\xi_2 + 2\mathrm{L}^2\left(x^4 - 12l_c^2\xi_2x^2 - 24l_c^4\xi_1\xi_2\right)\\ -6l_c^2\xi_2\left(x^4 - 12l_c^2\xi_2x^2 - 24l_c^4\xi_1\xi_2\right)\end{pmatrix}\sinh\left(\frac{\mathrm{L}}{l_c\sqrt{\xi_1}}\right) \tag{145}$$

$$+6l_c^2\sqrt{\xi_1}\xi_2\begin{pmatrix}4l_cx\sqrt{\xi_1}\left(x^2 - \mathrm{L}^2 - 6l_c^2\xi_2\right) + 8l_c^2\left(\mathrm{L}^2 - 3l_c^2\xi_2\right)\xi_1\sinh\left(\frac{\mathrm{L}-x}{l_c\sqrt{\xi_1}}\right)\\ +\left(\mathrm{L}^4 - 4\mathrm{L}^2l_c^2(\xi_1 - 3) - 24l_c^4\xi_1\xi_2\right)\sinh\left(\frac{x}{l_c\sqrt{\xi_1}}\right)\end{pmatrix};$$

$$F = 3\mathrm{L}l_c\xi_2\cosh\left(\frac{\mathrm{L}}{2l_c\sqrt{\xi_1}}\right) + \left(\mathrm{L}^2 - 3l_c^2\xi_2\right)\sqrt{\xi_1}\sinh\left(\frac{\mathrm{L}}{2l_c\sqrt{\xi_1}}\right);$$

The numerical results extracted with the help of the above closed-form solution are illustrated in Fig. 13. The graph is plotted for the input data Eq. (130). It is noticeable that in all curves, the slope at x = L is equal to zero.

5.2. Clamped-clamped beam

The new example is as shown in Fig. 14, wherein, the slopes at $x = 0, \mathrm{L}$ are equal to zero.

Similar to the two previous examples, the six-order differential equation and the two constitutive boundary conditions are as the following:

$$w^{(4)}(x) - \xi_1 l_c^2 w^{(6)}(x) = \frac{1}{EI}\left(p - l_c^2 p''\right) = -\frac{q}{EI} \tag{rep.117}$$

$$\begin{cases}\xi_2 w^{(2)}(0) - \xi_1 l_c^2 w^{(4)}(0) = \dfrac{q\,l_c^2}{EI}\\ \xi_2 w^{(2)}(\mathrm{L}) - \xi_1 l_c^2 w^{(4)}(\mathrm{L}) = \dfrac{q\,l_c^2}{EI}\end{cases} \tag{rep.44}$$

The four classical boundary conditions for clamped-clamped beam are as below:

$$\begin{cases}w(0) = 0\\ w^{(1)}(0) = 0\\ w(\mathrm{L}) = 0\\ w^{(1)}(\mathrm{L}) = 0\end{cases} \tag{146}$$

The bracket is Eq. Eq. (rep.67) in the two previous examples. In this step, we should apply the six boundary conditions exist in Eqs. (rep.44) and (146). Substituting these boundary conditions into bracket (rep.48) yields to

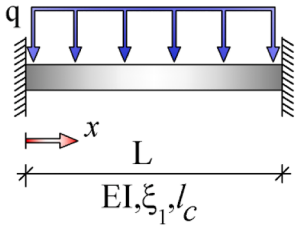

Fig. 14. Clamped-clamped two-phase peridynamic beam under uniformly distributed loading.

$$
\begin{aligned}
&[\ldots]_0^{\mathrm{L}} = G(\mathrm{L};x)\left(w^{(3)}(\mathrm{L}) - \xi_1 l_c^2 w^{(5)}(\mathrm{L})\right) - G^{(1)}(\mathrm{L};x)\left(\xi_1 w^{(2)}(\mathrm{L}) + \frac{q l_c^2}{EI}\right)\\
&-G^{(2)}(\mathrm{L};x)\left(\xi_1 l_c^2 w^{(3)}(\mathrm{L})\right) + G^{(3)}(\mathrm{L};x)\left(\xi_1 l_c^2 w^{(2)}(\mathrm{L})\right)\\
&-G(0;x)\left(w^{(3)}(0) - \xi_1 l_c^2 w^{(5)}(0)\right) + G^{(1)}(0;x)\left(\xi_1 w^{(2)}(0) + \frac{q l_c^2}{EI}\right)\\
&+G^{(2)}(0;x)\left(\xi_1 l_c^2 w^{(3)}(0)\right) - G^{(3)}(0;x)\left(\xi_1 l_c^2 w^{(2)}(0)\right)
\end{aligned}
\tag{147}
$$

By re-arranging Eq. (147), we approach to six boundary conditions of Green's function for simple beam:

$$
\begin{aligned}
[\ldots]_0^{\mathrm{L}} = &-w^{(5)}(\mathrm{L})\left(\xi_1 l_c^2 G(\mathrm{L};x)\right)\\
&+ w^{(3)}(\mathrm{L})\left(G(\mathrm{L};x) - \xi_1 l_c^2 G^{(2)}(\mathrm{L};x)\right)\\
&- w^{(2)}(\mathrm{L})\left(\xi_1 G^{(1)}(\mathrm{L};x) - \xi_1 l_c^2 G^{(3)}(\mathrm{L};x)\right)\\
&+ w^{(5)}(0)\left(\xi_1 l_c^2 G(0;x)\right)\\
&- w^{(3)}(0)\left(G(0;x) - \xi_1 l_c^2 G^{(2)}(0;x)\right)\\
&+ w^{(2)}(0)\left(\xi_1 G^{(1)}(0;x) - \xi_1 l_c^2 G^{(3)}(0;x)\right)\\
&+ \left(G^{(1)}(0;x) - G^{(1)}(\mathrm{L};x)\right)\frac{q l_c^2}{EI}
\end{aligned}
\tag{148}
$$

Since $w^{(5)}(\mathrm{L})$, $w^{(3)}(\mathrm{L})$, $w^{(2)}(\mathrm{L})$, $w^{(5)}(0)$, $w^{(3)}(0)$ and $w^{(2)}(0)$ are unknowns, we set their coefficients to zero in Eq. (148). Therefore, the six homogenous boundary conditions of Green's function are obtained as the following:

$$
\begin{cases}
G(\mathrm{L};x) = 0\\
G^{(2)}(\mathrm{L};x) = 0\\
G^{(1)}(\mathrm{L};x) - l_c^2 G^{(3)}(\mathrm{L};x) = 0\\
G(0;x) = 0\\
G^{(2)}(0;x) = 0\\
G^{(1)}(0;x) - l_c^2 G^{(3)}(0;x) = 0
\end{cases}
\tag{149}
$$

Then, bracket (rep.67) becomes:

$$
[\ldots]_0^{\mathrm{L}} = \left(G^{(1)}(0;x) - G^{(1)}(\mathrm{L};x)\right)\frac{q l_c^2}{EI}
\tag{150}
$$

Similar to the two previous examples, the deflection function of clamped-clamped beam under uniformly distributed loading become:

$$
w(x) = \int_0^x G(\xi;x)\left(-\frac{q}{EI}\right)d\xi + \int_x^{\mathrm{L}} G(\xi;x)\left(-\frac{q}{EI}\right)d\xi + \left(G^{(1)}(\mathrm{L};x) - G^{(1)}(0;x)\right)\frac{q l_c^2}{EI}
\tag{151}
$$

Now, it is sufficient to find the Green's function. Eq. (149) shows the six boundary conditions of Green's function. The governing differential equation for the Green's function is:

$$
\frac{d^4 G(\xi;x)}{d\xi^4} - \xi_1 l_c^2 \frac{d^6 G(\xi;x)}{d\xi^6} = \delta(\xi - x)
\tag{rep.126}
$$

The solution of Eq. (rep.126) together with boundary conditions (149) is so complicated. Herein, we have to represent the Green's function of clamped-clamped beam as follows:

$$
\begin{aligned}
G(\xi;x) = &\, c_1 \sinh\left(\frac{\xi}{\sqrt{\xi_1} l_c}\right) + c_2\left(\cosh\left(\frac{\xi}{\sqrt{\xi_1} l_c}\right) - 1\right) + c_3 \xi^3 - \frac{c_2}{2\xi_1 l_c^2}\xi^2\\
&+\left(6 l_c^2 c_3 + \frac{\xi_2}{\xi_1^{\frac{3}{2}} l_c} c_1\right)\xi + \left(\xi_1^{\frac{3}{2}} l_c^3 \sinh\left(\frac{x-\xi}{\sqrt{\xi_1} l_c}\right) - \frac{1}{6}(x-\xi)^3 - \xi_1 l_c^2 (x-\xi)\right)\widehat{H}(\xi - x)
\end{aligned}
\tag{152}
$$

which:

$$c_1 = \xi_1^{\frac{3}{2}} l_c^2 \frac{A}{B};$$

$$A = \sqrt{\xi_1}\left((\mathrm{L}-x)^2\left(\mathrm{L}x + 6\xi_2 l_c^2\right) - 2l_c^2\left(\mathrm{L}^2 + 6\xi_2 l_c^2\right)\xi_2\right)\cosh\left(\frac{\mathrm{L}}{l_c\sqrt{\xi_1}}\right)$$

$$+4l_c^2\left(\mathrm{L}^2 - 3\xi_2 l_c^2\right)\xi_2\sqrt{\xi_1}\cosh\left(\frac{\mathrm{L}-x}{l_c\sqrt{\xi_1}}\right) + 2l_c^2\left(\mathrm{L}^2 + 6\xi_2 l_c^2\right)\xi_2\sqrt{\xi_1}\cosh\left(\frac{x}{l_c\sqrt{\xi_1}}\right)$$

$$-2l_c(\mathrm{L}-x)\left(x(-2\mathrm{L}+x) - 6\xi_2 l_c^2\right)\xi_2\sinh\left(\frac{\mathrm{L}}{l_c\sqrt{\xi_1}}\right)$$

$$+\sqrt{\xi_1}\left(\mathrm{L}x^3 - 6\xi_2 l_c^2\left(x^2 - 2\xi_2 l_c^2\right) - \mathrm{L}^2\left(l_c^2(6\xi_1 + 4\xi_2 - 6) + x^2\right) + \mathrm{L}\,l_c\left(\mathrm{L}^2 - 12\xi_2 l_c^2\right)\sqrt{\xi_1}\sinh\left(\frac{\mathrm{L}-x}{l_c\sqrt{\xi_1}}\right)\right);$$

$$B = 4l_c\left(\mathrm{L}^2 + 6\xi_2 l_c^2\right)\xi_2\sqrt{\xi_1} + 8l_c\left(\mathrm{L}^2 - 3\xi_2 l_c^2\right)\xi_2\sqrt{\xi_1}\cosh\left(\frac{\mathrm{L}}{l_c\sqrt{\xi_1}}\right)$$

$$+\mathrm{L}\left(12\xi_2 l_c^2(\xi_2 - \xi_1) + \mathrm{L}^2\xi_1\right)\sinh\left(\frac{\mathrm{L}}{l_c\sqrt{\xi_1}}\right);$$

and:

$$c_2 = \xi_1^{\frac{3}{2}} l_c^2 \frac{C}{B};$$

$$C = 2l_c(\mathrm{L}-x)\left(x(-2\mathrm{L}+x) - 6l_c^2\xi_2\right)\xi_2\cosh\left(\frac{\mathrm{L}}{l_c\sqrt{\xi_1}}\right) + 12\mathrm{L}\,l_c^3\xi_2^2\cosh\left(\frac{\mathrm{L}-x}{l_c\sqrt{\xi_1}}\right)$$

$$+\sqrt{\xi_1}\left(-(\mathrm{L}-x)^2\left(\mathrm{L}x + 6\xi_2 l_c^2\right) + 2l_c^2\left(\mathrm{L}^2 + 6\xi_2 l_c^2\right)\xi_2\right)\sinh\left(\frac{x}{l_c\sqrt{\xi_1}}\right)$$

$$+2l_c\xi_2\left(-\mathrm{L}^2 x + x\left(x^2 - 6\xi_2 l_c^2\right) + l_c\sqrt{\xi_1}\left(2\left(\mathrm{L}^2 - 3\xi_2 l_c^2\right)\sinh\left(\frac{\mathrm{L}-x}{l_c\sqrt{\xi_1}}\right) - \left(\mathrm{L}^2 + 6\xi_2 l_c^2\right)\sinh\left(\frac{x}{l_c\sqrt{\xi_1}}\right)\right)\right)$$

and:

$$c_3 = \frac{1}{6\mathrm{L}}\frac{D}{E};$$

$$D = 2l_c\sqrt{\xi_1}\xi_2\left(2x^3 - 3\mathrm{L}x^2 + 3\mathrm{L}^2 x - 2\mathrm{L}^3 - 6\mathrm{L}l_c^2\xi_2\right)$$

$$+2l_c\sqrt{\xi_1}\xi_2\left(2x^3 - 3\mathrm{L}x^2 - 3\mathrm{L}^2 x + 4\mathrm{L}^3 - 6\mathrm{L}l_c^2\xi_2\right)\cosh\left(\frac{\mathrm{L}}{l_c\sqrt{\xi_1}}\right) + 12\mathrm{L}l_c^3\sqrt{\xi_1}\xi_2^2\cosh\left(\frac{\mathrm{L}-x}{l_c\sqrt{\xi_1}}\right)$$

$$-\mathrm{L}\left(\xi_1(\mathrm{L}-x)^2(\mathrm{L}+2x) - 6\mathrm{L}l_c^2\xi_1\xi_2 + 12l_c^2(\mathrm{L}-x)\xi_2^2\right)\sinh\left(\frac{\mathrm{L}}{l_c\sqrt{\xi_1}}\right)$$

$$-6\mathrm{L}l_c^2\sqrt{\xi_1}\xi_2\cosh\left(\frac{x}{l_c\sqrt{\xi_1}}\right)\left(2l_c\xi_2 - \mathrm{L}\sqrt{\xi_1}\sinh\left(\frac{\mathrm{L}}{l_c\sqrt{\xi_1}}\right)\right)$$

$$-6\mathrm{L}^2 l_c^2\xi_1\left(1 - \xi_1 + \xi_2\cosh\left(\frac{\mathrm{L}}{l_c\sqrt{\xi_1}}\right)\right)\sinh\left(\frac{x}{l_c\sqrt{\xi_1}}\right);$$

$$E = 4l_c\left(\mathrm{L}^2 + 6\xi_2 l_c^2\right)\xi_2\sqrt{\xi_1} + 8l_c\left(\mathrm{L}^2 - 3\xi_2 l_c^2\right)\xi_2\sqrt{\xi_1}\cosh\left(\frac{\mathrm{L}}{l_c\sqrt{\xi_1}}\right)$$

$$-\mathrm{L}\left(12\xi_2 l_c^2(\xi_1 - \xi_2) - \mathrm{L}^2\xi_1\right)\sinh\left(\frac{\mathrm{L}}{l_c\sqrt{\xi_1}}\right);$$

By substituting the above-mentioned Green's function and its first derivative into Eq. (151), we arrive at the following result for $w(x)$:

$$w(x) = -\frac{q}{24EI}\frac{f(x)}{F};$$

$$F = \mathrm{L}\xi_1\cosh\left(\frac{\mathrm{L}}{2l_c\sqrt{\xi_1}}\right) + 2l_c\sqrt{\xi_1}\xi_2\sinh\left(\frac{\mathrm{L}}{2l_c\sqrt{\xi_1}}\right);$$

$$f(x) = \mathrm{L}\left(-24l_c^4\xi_1\xi_2 - 2\mathrm{L}x^3\xi_1 + \xi_1x^4 + \mathrm{L}^2\left(x^2 - \left(x^2 + 2l_c^2\xi_1\right)\xi_2\right)\right)\cosh\left(\frac{\mathrm{L}}{2l_c\sqrt{\xi_1}}\right)$$

$$+2\mathrm{L}l_c^2\xi_1\xi_2\left(\mathrm{L}^2 + 12l_c^2\right)\cosh\left(\frac{\mathrm{L}-2x}{2l_c\sqrt{\xi_1}}\right) \tag{153}$$

$$+2l_c(\mathrm{L}-x)x\sqrt{\xi_1}\xi_2\left(12l_c^2 + \mathrm{L}^2 + \mathrm{L}x - x^2\right)\sinh\left(\frac{\mathrm{L}}{2l_c\sqrt{\xi_1}}\right);$$

The numerical results extracted with the help of the above closed-form solution are shown in Fig. 15, where the deflection function is plotted for the input data Eq. (130). It is noticeable that in all curves, the slope at x = L is equal to zero.

6. Series solution

In this section, we exemplarily calculate the deflection function of two previously solved examples by the help of "Navier-type series solution" for some verification purposes. For this reason, the sixth-order differential Eq. (2) is considered, and then numerically solve for simple-simple beam under two different loading: uniformly distributed loading and mid-span concentrated load. Based on the "Navier-type series solution", we assumed the both loading and deflection functions as the following:

$$q(x) = \sum_m Q_m \sin\left(\frac{m\pi x}{\mathrm{L}}\right) \tag{154}$$

$$w(x) = \sum_m W_m \sin\left(\frac{m\pi x}{\mathrm{L}}\right) \tag{155}$$

Based on these two series, the second derivative of $q(x)$, and the forth and sixth derivative of the deflection function becomes:

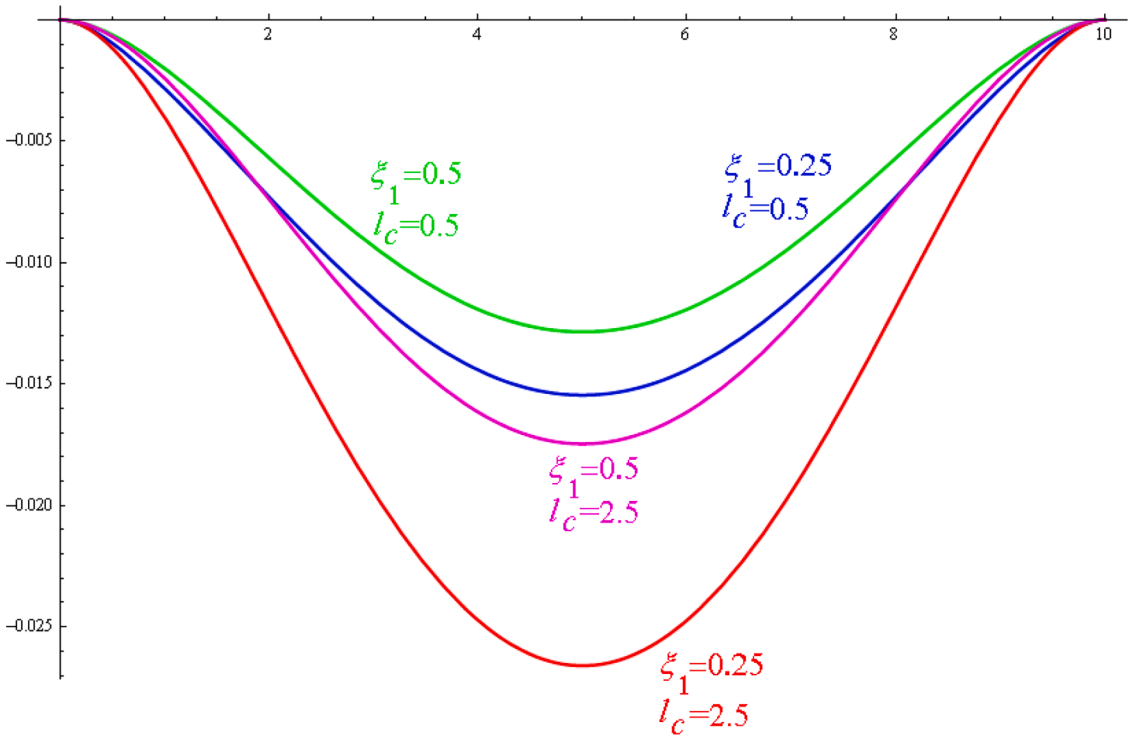

Fig. 15. Deflection function of clamped-clamped two-phase peridynamic beam under uniformly distributed load.

$$q^{(2)}(x) = \sum_m -Q_m \left(\frac{m\pi}{\mathrm{L}}\right)^2 \sin\left(\frac{m\pi x}{\mathrm{L}}\right) \tag{156}$$

$$w^{(4)}(x) = \sum_m W_m \left(\frac{m\pi}{\mathrm{L}}\right)^4 \sin\left(\frac{m\pi x}{\mathrm{L}}\right) \tag{157}$$

$$w^{(6)}(x) = \sum_m -W_m \left(\frac{m\pi}{\mathrm{L}}\right)^6 \sin\left(\frac{m\pi x}{\mathrm{L}}\right) \tag{158}$$

By substituting Eqs. (156), (157) and (158) into Eq. (2), we have:

$$EI\left[w^{(4)}(x) - \xi_1 l_c^2 w^{(6)}(x)\right] = p - l_c^2 p^{(2)} \tag{rep.2}$$

$$\Rightarrow EI\left[\sum_m W_m \left(\frac{m\pi}{\mathrm{L}}\right)^4 \left[1 + \xi_1 l_c^2 \left(\frac{m\pi}{\mathrm{L}}\right)^2\right] \sin\left(\frac{m\pi x}{\mathrm{L}}\right)\right] = \sum_m Q_m \left[1 + l_c^2 \left(\frac{m\pi}{\mathrm{L}}\right)^2\right] \sin\left(\frac{m\pi x}{\mathrm{L}}\right)$$

$$\Rightarrow W_m = \frac{Q_m}{EI} \frac{1 + \left(\frac{m\pi l_c}{\mathrm{L}}\right)^2}{\left(\frac{m\pi}{\mathrm{L}}\right)^4 \left[1 + \xi_1 \left(\frac{m\pi l_c}{\mathrm{L}}\right)^2\right]} \tag{159}$$

For uniformly distributed loading, we have $q(x) = q_0$ and then:

$$q_0 = \sum_m Q_m \sin\left(\frac{m\pi x}{\mathrm{L}}\right) \Rightarrow Q_m = \frac{2q_0}{\mathrm{L}} \int_0^{\mathrm{L}} \sin\left(\frac{m\pi x}{\mathrm{L}}\right) dx \tag{160}$$

Therefore:

$$Q_m = \frac{2q_0}{m\pi}\left[1 - (-1)^m\right] = \frac{4q_0}{m\pi} \quad : \text{for } m \text{ odd} \tag{161}$$

By substituting Eq. (161) into Eq. (159), we have:

$$W_m = \frac{4q_0}{m\pi EI}\left(\frac{\mathrm{L}}{m\pi}\right)^4 \left[\frac{1 + \left(\frac{m\pi l_c}{\mathrm{L}}\right)^2}{1 + \xi_1 \left(\frac{m\pi l_c}{\mathrm{L}}\right)^2}\right] \quad : \text{for } m \text{ odd} \tag{162}$$

Thus, the deflection function of simple-simple beam under uniform loading q_0 becomes:

$$w(x) = \frac{4q_0}{EI} \sum_{m,odd} \frac{\mathrm{L}^4}{(m\pi)^5} \left[\frac{1 + \left(\frac{m\pi l_c}{\mathrm{L}}\right)^2}{1 + \xi_1 \left(\frac{m\pi l_c}{\mathrm{L}}\right)^2}\right] \sin\left(\frac{m\pi x}{\mathrm{L}}\right) \tag{163}$$

The maximum deflection of the beam is occurred at $x = \mathrm{L}/2$. For this point, we have:

$$\Delta_{\max} = w\left(\frac{\mathrm{L}}{2}\right) = \frac{q_0 \mathrm{L}^4}{EI} \sum_{m,odd} \frac{4}{(m\pi)^5} \left[\frac{1 + \left(\frac{m\pi l_c}{\mathrm{L}}\right)^2}{1 + \xi_1 \left(\frac{m\pi l_c}{\mathrm{L}}\right)^2}\right] (-1)^{\frac{m-1}{2}} \tag{164}$$

Based on Eq. (29) in [22], the following dimensionless variables can be introduced:

$$\Delta_{\max}^* = \frac{EI\,\Delta_{\max}}{q_0 \mathrm{L}^4}; \quad l_c^* = \frac{l_c}{\mathrm{L}}; \tag{165}$$

Therefore:

$$\Delta_{\max}^* = \sum_{m,odd} \frac{4}{(m\pi)^5} \left[\frac{1 + (m\pi l_c^*)^2}{1 + \xi_1 (m\pi l_c^*)^2}\right] (-1)^{\frac{m-1}{2}} \tag{166}$$

The maximum deflection of the beam at $x = \mathrm{L}/2$ could be also found by the help of the closed-form solution which was obtained in sub-Section 4.3. This value is:

$$\Delta_{\max}^{\text{closed-form}} = \frac{5q_0\mathrm{L}^4}{384EI} + \xi_2\frac{q_0 l_c^2}{8EI}\left[\mathrm{L}^2 - 8l_c^2\xi_1 + 8l_c^2\xi_1\,\mathrm{sech}\left(\frac{\mathrm{L}}{2l_c\sqrt{\xi 1}}\right)\right] \tag{167}$$

The closed-form solution also becomes similarly dimensionless as the following:

$$\Delta_{\max}^{\text{closed-form}^*} = \frac{5}{384} + \xi_2\frac{\left(l_c^*\right)^2}{8}\left[1 - 8\left(l_c^*\right)^2\xi_1 + 8\left(l_c^*\right)^2\xi_1\,\mathrm{sech}\left(\frac{1}{2l_c^*\sqrt{\xi 1}}\right)\right] \tag{168}$$

Interestingly, by setting $\xi_1 = 1$, ξ_2 becomes zero, and we reach to the well-known value 5/384 which is the maximum dimensionless deflection of SS beam under uniform distributed load.

Table 1 shows the numerical dimensionless results for some values of dimensionless parameters ${l_c}^*$ and ξ_1. The series is calculated for only 20 first non-zero terms. Fortunately, the results coincide with the closed-form solution until ten digits after point.

Moreover, Fig. 16 shows the dimensionless deflection function of SS beam under uniform distributed loading. In this figure, "M" denotes the number of non-zero terms in series solution (163). As it is clear in Fig. 16, as the number of series terms increases, the approximate solution converges to the closed-form one, although in the case of the SS beam under uniform distributed loading, a suitable responce can be achieved even with a very small number of terms.

Furthermore, the logarithm of absolute error (the difference between the exact solution and the series response) for the dimensionless deflection of mid-span point is plotted as Fig. 17, with respect to the number of series' terms. As expected, the error decreases dramatically as the number of terms increases.

Moreover, the series solution is also presented for the two-phase simply supported beam under mid-span point load. In this case, we have:

$$q(x) = P\,\delta\left(x - \frac{\mathrm{L}}{2}\right) \tag{169}$$

$$\Rightarrow Q_m = \frac{2P}{\mathrm{L}}\int_0^{\mathrm{L}}\delta\left(x - \frac{\mathrm{L}}{2}\right)\sin\left(\frac{m\pi x}{\mathrm{L}}\right)dx = \frac{2P}{\mathrm{L}}\sin\left(\frac{m\pi}{2}\right) \tag{170}$$

By substituting Eq. (170) into Eq. (159), we have:

$$W_m = \frac{2P}{EI\,\mathrm{L}}\frac{1 + \left(\frac{m\pi l_c}{\mathrm{L}}\right)^2}{\left(\frac{m\pi}{\mathrm{L}}\right)^4\left[1 + \xi_1\left(\frac{m\pi l_c}{\mathrm{L}}\right)^2\right]}\sin\left(\frac{m\pi}{2}\right) \tag{171}$$

Thus, the deflection function for this case becomes:

$$w(x) = \frac{2P\mathrm{L}^3}{EI}\sum_m\left(\frac{1}{m\pi}\right)^4\left[\frac{1 + \left(\frac{m\pi l_c}{\mathrm{L}}\right)^2}{1 + \xi_1\left(\frac{m\pi l_c}{\mathrm{L}}\right)^2}\right]\sin\left(\frac{m\pi}{2}\right)\sin\left(\frac{m\pi x}{\mathrm{L}}\right) \tag{172}$$

The maximum deflection of the beam is occurred at $x = \mathrm{L}/2$. For this point, we have:

$$\Delta_{\max} = w\left(\frac{\mathrm{L}}{2}\right) = \frac{2P\mathrm{L}^3}{EI}\sum_m\left(\frac{1}{m\pi}\right)^4\left[\frac{1 + \left(\frac{m\pi l_c}{\mathrm{L}}\right)^2}{1 + \xi_1\left(\frac{m\pi l_c}{\mathrm{L}}\right)^2}\right]\sin^2\left(\frac{m\pi}{2}\right) \tag{173}$$

If m is even, the series' term is equal to zero. Also, for odd m, we have:

$$\sin^2\left(\frac{m\pi}{2}\right) = 1 \quad : \text{for } m \text{ odd} \tag{174}$$

Table 1
Dimensionless deflection of mid-span for SS two-phase peridynamic beam under uniform distributed load.

$\Delta_{\max}^*$	$\xi_1 = 0.25$	$\xi_1 = 0.50$	$\xi_1 = 0.75$
$l_c^* = 0.05$	0.013254036	0.013175521	0.013097786
$l_c^* = 0.10$	0.013939585	0.013620876	0.013314700
$l_c^* = 0.15$	0.015035528	0.014302791	0.013633078
$l_c^* = 0.20$	0.016474876	0.015144128	0.014004184
$l_c^* = 0.25$	0.018174607	0.01606556	0.014385605

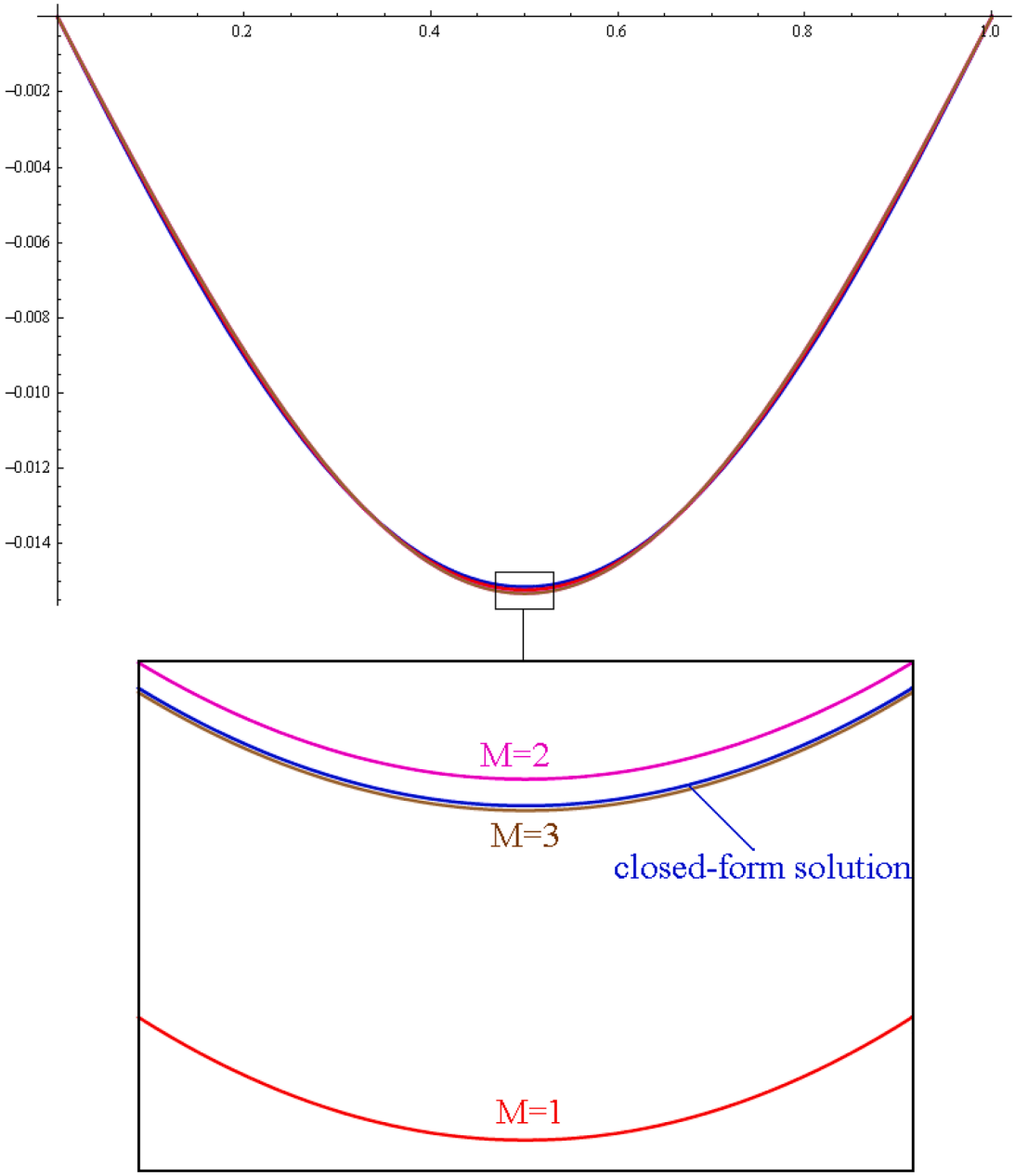

Fig. 16. Dimensionless deflection function of SS two-phase peridynamic beam under uniform distributed load.
("M" denotes the number of non-zero terms in series solution).

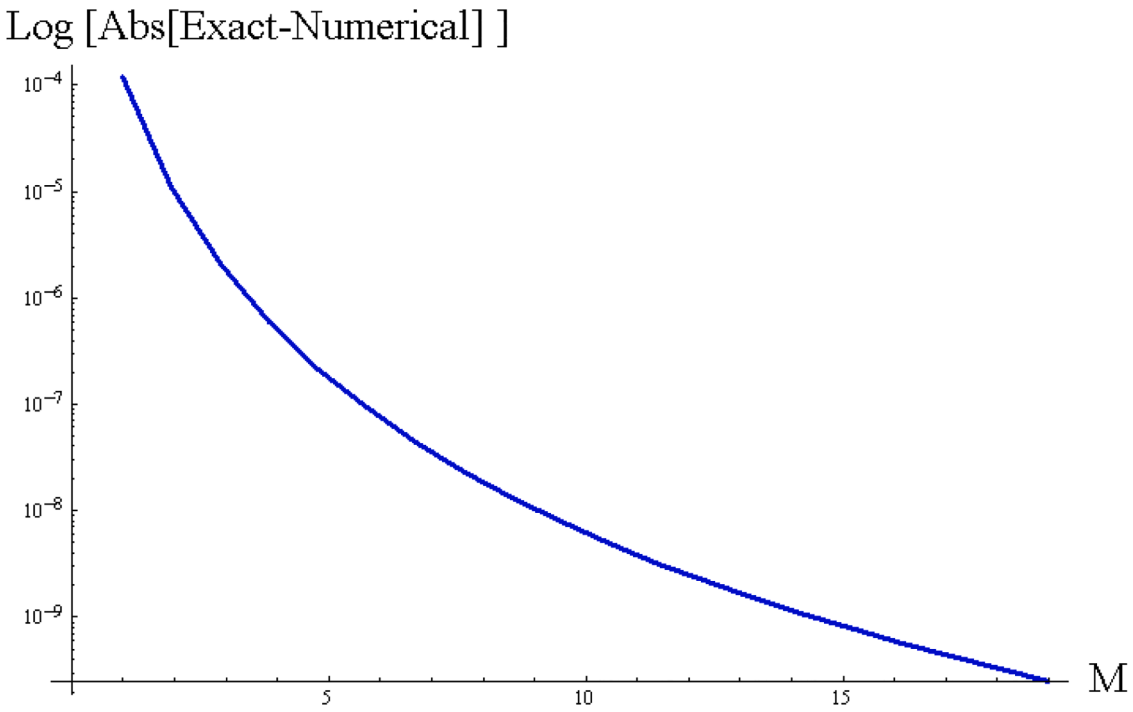

Fig. 17. The Log-error-chart of dimensionless deflection of mid-span point for SS two-phase peridynamic beam under uniform distributed load vs. number of series' terms.

$$\Rightarrow \Delta_{\max} = \frac{2PL^3}{EI}\sum_{m,odd}\left(\frac{1}{m\pi}\right)^4\left[\frac{1+\left(\frac{m\pi l_c}{L}\right)^2}{1+\xi_1\left(\frac{m\pi l_c}{L}\right)^2}\right] \tag{175}$$

Similar to the previous sample, the following dimensionless variables can be introduced:

$$\Delta^*_{\max} = \frac{EI\,\Delta_{\max}}{PL^3};\quad l_c{}^* = \frac{l_c}{L}; \tag{176}$$

Thus:

$$\Delta^*_{\max} = \sum_{m,odd}\frac{2}{(m\pi)^4}\left[\frac{1+(m\pi l_c{}^*)^2}{1+\xi_1(m\pi l_c{}^*)^2}\right] \tag{177}$$

The maximum deflection of the beam at $x = L/2$ could be also found by the help of the closed-form solution which was obtained in section sub-Section 4.4. The dimensionless value of the maximum deflection of this beam is as the following:

$$\Delta^{\text{closed-form}^*}_{\max} = \frac{1}{48}+\frac{1}{4}\xi_2\left(l_c^*\right)^2\left[1-2l_c^*\sqrt{\xi 1}\,\tanh\left(\frac{1}{2\sqrt{\xi 1}l_c^*}\right)\right] \tag{178}$$

Interestingly, by setting $\xi_1 = 1$, ξ_2 becomes zero, and we reach to the well-known value 1/48 which is the maximum dimensionless deflection of SS beam under central concentrated load.

Table 2 tabulates the numerical dimensionless results for some values of dimensionless parameters $l_c{}^*$ and ξ_1. The series is

Table 2
Dimensionless deflection of mid-span for SS beam under concentrated load.

$\Delta^*_{\max}$	$\xi_1 = 0.25$	$\xi_1 = 0.50$	$\xi_1 = 0.75$
$l_c^* = 0.05$	0.0212786	0.0211237	0.0209761
$l_c^* = 0.10$	0.0225208	0.0219066	0.0213501
$l_c^* = 0.15$	0.0244193	0.0230493	0.0218746
$l_c^* = 0.20$	0.0268335	0.0244215	0.0224727
$l_c^* = 0.25$	0.0296244	0.0259029	0.0230812

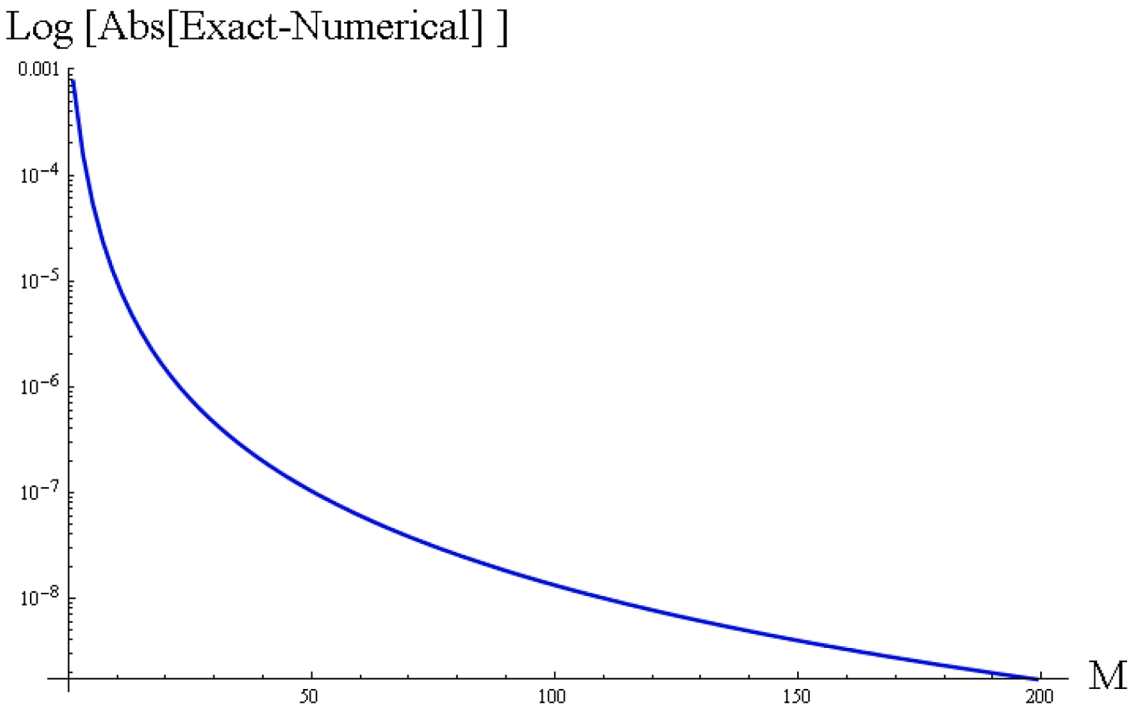

Fig. 18. The Log-error-chart of dimensionless deflection of mid-span point for SS two-phase peridynamic beam under concentrated load vs. number of series' terms.

calculated for only 40 first non-zero terms. Fortunately, the results coincide with the closed-form solution until seven digits after point. In comparison with the uniformly distributed loading, the convergence rate is slightly slower. This fact is also confirmed by comparing two Figs. 17 and 18. As it is clear, the absolute error becomes lower than 10^{-9} by using only 17 terms for uniformly distributed loading. However, this happens for a concentrated load of about 200 terms.

In the following, the deflection function of two-phase simply supported beam under sinusoidal loading is also obtained. For this reason:

$$q(x) = -q\sin\left(\frac{\pi x}{\mathrm{L}}\right) \Rightarrow \begin{cases} Q_1 = -q \\ Q_m = 0 \end{cases} : \text{for } m \geq 2 \tag{179}$$

By substituting Eq. (180) into Eq. (159), we have:

$$W_1 = \frac{-q\mathrm{L}^4}{\pi^4 EI}\left[\frac{1+\left(\frac{\pi l_c}{\mathrm{L}}\right)^2}{1+\xi_1\left(\frac{\pi l_c}{\mathrm{L}}\right)^2}\right] \quad \text{and} \quad W_m = 0 \quad : \text{for } m \geq 2 \tag{180}$$

Therefore:

$$w(x) = \frac{-q\mathrm{L}^4}{\pi^4 EI}\left[\frac{1+\left(\frac{\pi l_c}{\mathrm{L}}\right)^2}{1+\xi_1\left(\frac{\pi l_c}{\mathrm{L}}\right)^2}\right]\sin\left(\frac{\pi x}{\mathrm{L}}\right) = \frac{-q\mathrm{L}^4}{\pi^4 EI}\left[\frac{\mathrm{L}^2+(\pi l_c)^2}{\mathrm{L}^2+\xi_1(\pi l_c)^2}\right]\sin\left(\frac{\pi x}{\mathrm{L}}\right) \tag{181}$$

The second derivative of Eq. (181) is the curvature:

$$w^{(2)}(x) = \frac{q\mathrm{L}^2}{\pi^2 EI}\left[\frac{\mathrm{L}^2+(\pi l_c)^2}{\mathrm{L}^2+\xi_1(\pi l_c)^2}\right]\sin\left(\frac{\pi x}{\mathrm{L}}\right) \tag{182}$$

which is exactly the same as Eq. (rep.116).

$$\kappa(x) = \frac{q\mathrm{L}^2}{EI\left(\mathrm{L}^2+\xi_1 l_c^2\pi^2\right)}\left(\frac{\mathrm{L}^2}{\pi^2}+l_c^2\right)\sin\left(\frac{\pi x}{\mathrm{L}}\right) \tag{rep.116}$$

7. Finite difference solution

In this section, for further verification of the analytical results obtained by the Green's functions, all four beams examined in the paper, i.e., SS, CS, CC and CF beams, are also analyzed using the finite difference method (FDM). It should be noted that this numerical method is applied to the integro-differential equation (A.9) and not to the higher-order differential Eq. (2), which itself can be considered as a factor in increasing the quality of verification. In the following, the FDM methodology will be briefly explained, and the, the numerical results which are compared with the analytical results will be thoroughly presented.

The discretized form of the total potential energy (A.1) could be expressed as [22]:

$$U = \sum_{j=1}^{m-1} \frac{1}{2} \frac{C^l}{(\Delta x)^2} \left(w_{j+1} - 2w_j + w_{j-1}\right)^2 + \sum_{j=1}^{m-1} \sum_{h=j+1}^{m} \frac{1}{2} \frac{C^{nl}_{j-1/2,h-1/2}}{(\Delta x)^2} \left(w_h - w_{h-1} - w_j + w_{j-1}\right)^2 - \sum_{j=1}^{m-1} q_j w_j \Delta x \tag{183}$$

where "m" is the number of equilength segment, $\Delta x = \mathrm{L}/m$, and:

$$C^l = \frac{EI\,\xi_1}{\Delta x} \text{ and } C^{nl}_{j-1/2,h-1/2} = EI\,\xi_2 (\Delta x)^2 H\left(x_{j-1/2}, x_{h-1/2}\right) \tag{184}$$

It is worth to mentioning that the upper bound of the summation over j is equal to m for CF beam. The general component of stiffness matrix could be found as:

$$\mathbf{K}_{jk} = \frac{\partial^2 \Pi}{\partial w_j \partial w_k} \tag{185}$$

Based on Eq. (183), this stiffness matrix includes two local and non-local parts. By substituting Eq. (183) into (185), we have:

$$\mathbf{K}^l_{jk} = \beta \frac{C^l}{(\Delta x)^2} \text{ and } \mathbf{K}^{nl}_{jk} = \frac{1}{(\Delta x)^2} \left(C^{nl}_{j,k+1} - C^{nl}_{j,k} - C^{nl}_{j+1,k+1} + C^{nl}_{j+1,k} + \gamma\right) \tag{186}$$

where $\beta = 6$ for $k = j$, $\beta = 1$ for $k = j \pm 2$ and $\beta = -4$ for $k = j \pm 1$. Moreover:

$$\gamma = \begin{cases} -\sum_{\substack{h=1 \\ h \neq j}}^{m} C^{nl}_{j,h} & : \text{if } k = j-1 \\ \sum_{\substack{h=1 \\ h \neq j}}^{m} C^{nl}_{j,h} + \sum_{\substack{h=1 \\ h \neq j+1}}^{m} C^{nl}_{j+1,h} & : \text{if } k = j \\ -\sum_{\substack{h=1 \\ h \neq j+1}}^{m} C^{nl}_{j+1,h} & : \text{if } k = j+1 \end{cases} \tag{187}$$

In the following, some small but very important changes that must be made in some components of the stiffness matrix due to the boundary conditions of the beams will be explained for SS, CS, CC and CF beams, respectively.

Since the both supports at the beginning and end of the SS beam are simple, and the second derivative of the deflection function is zero at them, the first and last two rows of the stiffness matrix will be different from the other rows. The following relations explain this fact:

Fig. 19

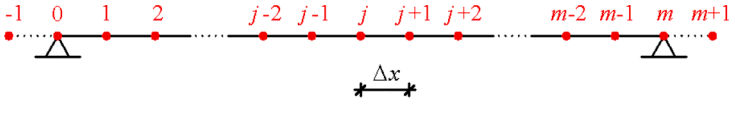

Fig. 19. FD mesh of SS beam with two virtual nodes.

$$w''_j = \frac{w_{j+1} - 2w_j + w_{j-1}}{(\Delta x)^2} \Rightarrow \begin{cases} w''_0 = \dfrac{w_1 - 2w_0 + w_{-1}}{(\Delta x)^2} = 0 \xrightarrow{w_0 = 0} w_{-1} = -w_1 \\ w''_m = \dfrac{w_{m+1} - 2w_m + w_{m-1}}{(\Delta x)^2} = 0 \xrightarrow{w_m = 0} w_{m+1} = -w_{m-1} \end{cases} \tag{188}$$

The local part in Eq. (183) has the following general form, from which the local stiffness matrix is extracted (the nonlocal part is named as B, and will be obtained for CF beam):

$$A = w_{j+2} - 4w_{j+1} + 6w_j - 4w_{j-1} + w_{j-2} \tag{189}$$

For $j = 1$ and $j = m - 1$, we have:

$$\begin{cases} j = 1 & \Rightarrow A = w_3 - 4w_2 + 6w_1 - 4w_0 + w_{-1} = 5w_1 - 4w_2 + w_3 \\ j = m-1 & \Rightarrow A = w_{m+1} - 4w_m + 6w_{m-1} - 4w_{m-2} + w_{m-3} = 5w_{m-1} - 4w_{m-2} + w_{m-3} \end{cases} \tag{190}$$

Also, for $j = 2$ and $j = m - 2$, we have:

$$\begin{cases} j = 2 & \Rightarrow A = w_4 - 4w_3 + 6w_2 - 4w_1 + w_0 = -4w_1 + 6w_2 - 4w_3 + w_4 \\ j = m-2 & \Rightarrow A = -4w_{m-1} + 6w_{m-2} - 4w_{m-3} + w_{m-4} \end{cases} \tag{191}$$

Similar changes must be made to the non-local stiffness matrix, which are not mentioned here for the sake of brevity. In the following, the necessary changes of the stiffness matrices of CS, CC and CF beam are also presented only for the local part, again for the sake of brevity.

In CS beam, the derivative of the deflection function is zero at $x = 0$. Therefore:

Fig. 20

$$w'_0 = \frac{1}{\Delta x}\left(\frac{1}{2}w_1 - \frac{1}{2}w_{-1}\right) = 0 \Rightarrow w_{-1} = w_1 \tag{192}$$

Based on Eq. (192), the general Eq. (189) becomes for $j = 1$ as the following:

$$A = w_3 - 4w_2 + 6w_1 - 4w_0 + w_{-1} = 7w_1 - 4w_2 + w_3 \tag{193}$$

The other relations for $j = 2, j = m - 1$ and $j = m - 2$ are exactly similar to SS beam. In CC beam, Eq. (189) also holds for the end of the beam:

Fig. 21

$$w'_m = \frac{1}{\Delta x}\left(\frac{1}{2}w_{m+1} - \frac{1}{2}w_{m-1}\right) = 0 \Rightarrow w_{m-1} = w_{m+1} \tag{194}$$

Thus, the general Eq. (189) becomes for $j = m - 1$ as the following:

$$A = w_{m+1} - 4w_m + 6w_{m-1} - 4w_{m-2} + w_{m-3} = 7w_{m-1} - 4w_{m-2} + w_{m-3} \tag{195}$$

The other relations for $j = 2$ and $j = m - 2$ are exactly similar to SS and CS beams.

Among the four beams under studied, imposing the boundary conditions to CF beam in the finite difference model is perhaps the most interesting. In this beam, the changes in both local and nonlocal parts of the stiffness matrices are thoroughly described below.

Fig. 22

The second derivative of the deflection function is zero at the free end. It means:

$$w''_m = \frac{w_{m+1} - 2w_m + w_{m-1}}{(\Delta x)^2} = 0 \Rightarrow w_{m+1} = 2w_m - w_{m-1} \tag{196}$$

Therefore, the genearl relation (189) for $j = m - 1$ becomes:

$$A = w_{m+1} - 4w_m + 6w_{m-1} - 4w_{m-2} + w_{m-3} = -2w_m + 5w_{m-1} - 4w_{m-2} + w_{m-3} \tag{197}$$

In the following, the changes that should be imposed in nonlocal part of the stiffness matrix of CF beam is described. For $j = m$, Eq. (187) becomes:

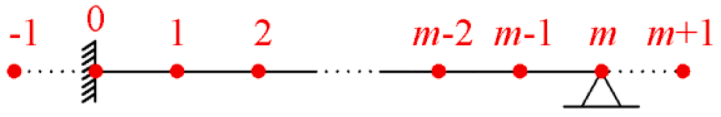

Fig. 20. FD mesh of CS beam with two virtual nodes.

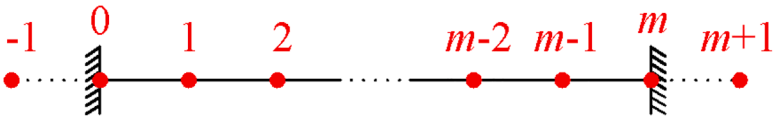

Fig. 21. FD mesh of CS beam with two virtual nodes.

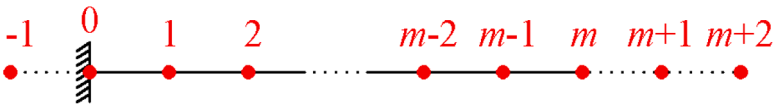

Fig. 22. FD mesh of CF beam with three virtual nodes.

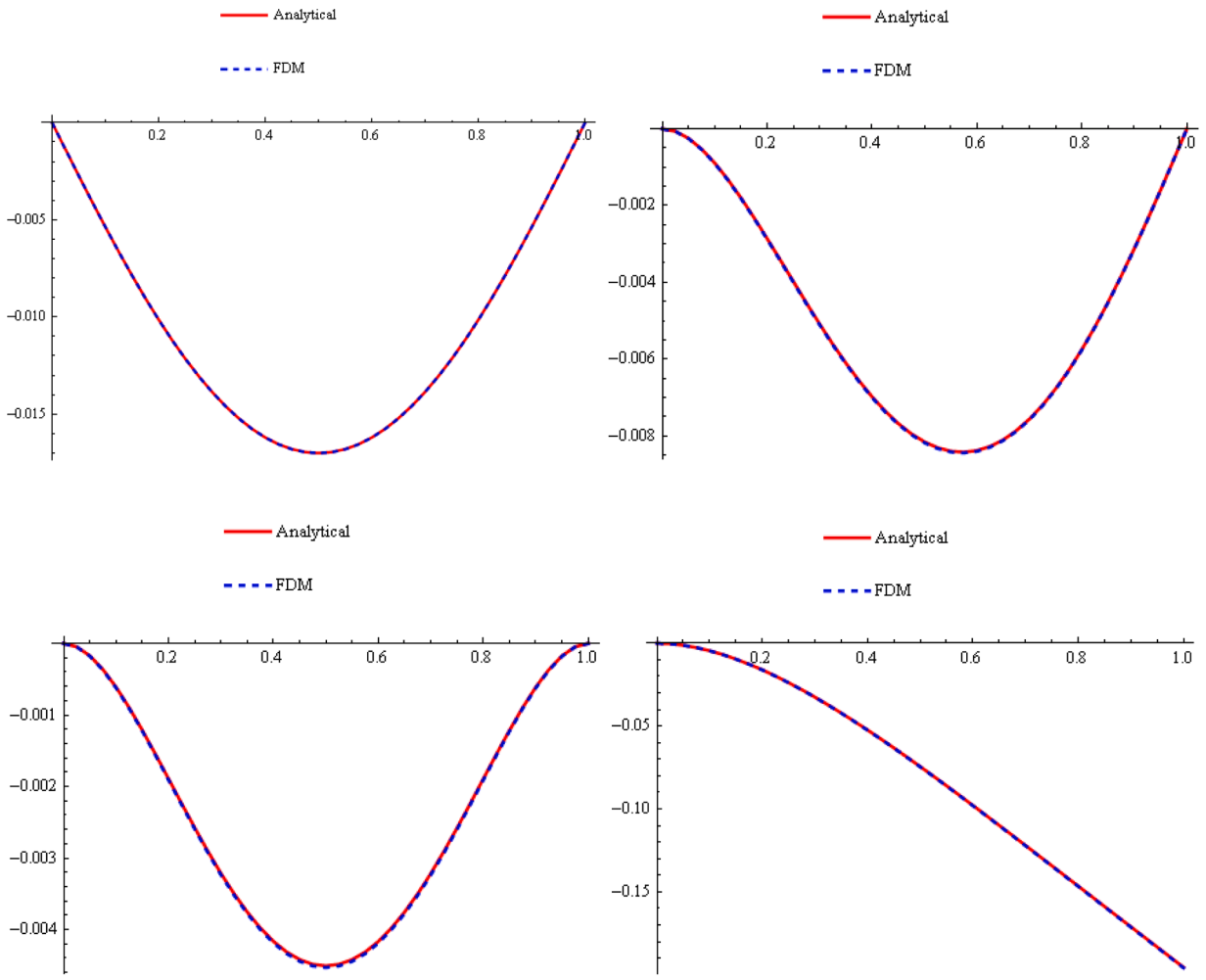

Fig. 23. The deflection function of TPPEB beams obtained by both methods.

$$\mathbf{K}^{nl}_{mk} = \left(C^{nl}_{m,k+1} - C^{nl}_{m,k} - C^{nl}_{m+1,k+1} + C^{nl}_{m+1,k} + \gamma\right);\ \ \gamma = \begin{cases} -\sum\limits_{\substack{h=1\\h\neq m}}^{m} C^{nl}_{m,h} & : \text{if } k = m-1 \\ \sum\limits_{\substack{h=1\\h\neq m}}^{m} C^{nl}_{m,h} + \sum\limits_{\substack{h=1\\h\neq m+1}}^{m} C^{nl}_{m+1,h} & : \text{if } k = m \\ -\sum\limits_{\substack{h=1\\h\neq m+1}}^{m} C^{nl}_{m+1,h} & : \text{if } k = m+1 \end{cases} \tag{198}$$

In front of the real point "m", we have two virtual (non-material) points: "$m+1$" and "$m+2$". For these points, $C^{nl}_{m+1,h}$ is not defined. We assume that C^{nl} at the points "$m+1$" and "$m+2$" is equal to zero:

$$C^{nl}_{m+1,h} = C^{nl}_{m+2,h} = C^{nl}_{j,m+1} = C^{nl}_{j,m+2} = 0 \tag{199}$$

By using these assumptions, the non-local terms of the last equation become:

$$\begin{aligned} B = {} & \left(C^{nl}_{m,2} - C^{nl}_{m,1} - C^{nl}_{m+1,2} + C^{nl}_{m+1,1}\right) w_1 + \left(C^{nl}_{m,3} - C^{nl}_{m,2} - C^{nl}_{m+1,3} + C^{nl}_{m+1,2}\right) w_2 + \cdots \\ & + \left(- C^{nl}_{m,m-1} - \underbrace{C^{nl}_{m+1,m}}_{0} + \underbrace{C^{nl}_{m+1,m-1}}_{0} - \sum_{h=1}^{m-1} C^{nl}_{m,h} \right) w_{m-1} \\ & + \left(\underbrace{C^{nl}_{m,m+1}}_{0} + \underbrace{C^{nl}_{m+1,m}}_{0} + \sum_{h=1}^{m-1} C^{nl}_{m,h} + \sum_{h=1}^{m} \underbrace{C^{nl}_{m+1,h}}_{0} \right) w_m \\ & + \left(\underbrace{C^{nl}_{m,m+2}}_{0} - \underbrace{C^{nl}_{m,m+1}}_{0} - \underbrace{C^{nl}_{m+1,m+2}}_{0} - \sum_{h=1}^{m} \underbrace{C^{nl}_{m+1,h}}_{0} \right) w_{m+1} \end{aligned} \tag{200}$$

The nonlocal terms for the last row of matrix equation are simplified as:

$$B = \left(C^{nl}_{m,2} - C^{nl}_{m,1} - C^{nl}_{m+1,2} + C^{nl}_{m+1,1}\right) w_1 + \cdots + \left(- C^{nl}_{m,m-1} - \sum_{h=1}^{m-1} C^{nl}_{m,h} \right) w_{m-1} + \left(\sum_{h=1}^{m-1} C^{nl}_{m,h} \right) w_m \tag{201}$$

Based on the above-described FDM, the deflection functions of all four beams studied in the previous sections, i.e., SS, CS, CC and CF beams, are numerically obtained. These numerical results are compared with the closed-form results attained earlier by the Green's functions. Fortunanately, an adequate agreement is observed between the both analytical and numerical results. Finally, the case of a simply supported two-phase peridynamic Euler-Bernoulli beam under pure bending moment ($M(x) = M_0$, where M_0 is applied at both extremities) is also investigated. This case could be interesting as well to show the ill-posedness of the pure peridynamic problem.

Table 3
The experimental order of convergence for FDM.

SS beam				CC beam			
m	Value*	Abs. Error	Order	m	Value	Abs. Error	Order
8	−0.0171366507	0.0001356844	N.D.	8	−0.0051429557	0.0006377897	N.D.
16	−0.0170348221	0.0000338557	**2.00**	16	−0.0046606264	0.0001554604	**2.04**
32	−0.0170094264	0.0000084601	**2.00**	32	−0.0045430761	0.0000379100	**2.04**
64	−0.0170030811	0.0000021148	**2.00**	64	−0.0045144922	9.326171483×10^−6	**2.02**
128	-0.0170014950	0.0000005287	**2.00**	128	-0.0045074765	2.310472122*10^-6	**2.01**
Exact	−0.0170009663			Exact	−0.0045051660		
CS beam				CF beam			
m	Value	Abs. Error	Order	m	Value	Abs. Error	Order
8	−0.0086985534	0.0005402893	N.D.	8	−0.2020285965	0.0065692762	N.D.
16	−0.0082960077	0.0001377436	**1.97**	16	−0.1971147999	0.0016554796	**1.99**
32	−0.0081928735	0.0000346094	**1.99**	32	−0.1958740357	0.0004147154	**2.00**
64	−0.0081669274	0.0000086633	**2.00**	64	−0.1955630524	0.0001037321	**2.00**
128	−0.0081604306	0.0000021665	**2.00**	128	−0.1954852569	0.0000259367	**2.00**
Exact	−0.0081582641			Exact	−0.1954593203		

* "Value" is the mid-span displacement for SS, CC and CS beams, and the end displacement for CF Beam.

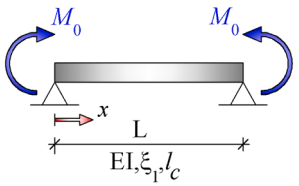

Fig. 24. Simply supported two-phase peridynamic Euler-Bernoulli beam under pure bending moment.

Fig. 23 shows the dimensionless deflection functions of the two-phase peridynamic beams under uniformly distributed loading, for $\xi_1 = 0.5$ and $l_c = 0.3\,\mathrm{L}$, by using $m = 40$. As it is clear, two curves are hardly distinguishable. This agreement reaffirms the correctness of the results obtained from the Green's function method.

Besides, the order of convergence is computed utilizing the absolute errors of two different discretization sizes as the following:

$$\left.\begin{aligned} e_m &= |R_m - R_{exact}| = C\,(\Delta x)^p \\ e_{2m} &= |R_{2m} - R_{exact}| = C\left(\frac{\Delta x}{2}\right)^p \end{aligned}\right\} \Rightarrow \frac{e_m}{e_{2m}} = 2^p \Rightarrow p = \log_2\left(\frac{e_m}{e_{2m}}\right) \tag{202}$$

Table 3 shows that the experimental order of convergence for static analyses by FDM is almost 2 for all boundary conditions (SS, CS, CC and CF). Herein, we assume $\xi_1 = 0.5$ and $l_c = 0.3\,\mathrm{L}$.

As the last case, a simply supported two-phase peridynamic Euler-Bernoulli beam is considered under pure bending moment ($M(x) = M_0$, where M_0 is applied at both extremities). Fig. 24 shows this case.

The second derivative of the moment function is equal to zero. Therefore, Eq. (1) becomes:

$$\kappa(x) - \xi_1 l_c^2 \frac{d^2\kappa}{dx^2} = \frac{M_0}{EI} \tag{203}$$

By using Eq. (11) we have:

$$\kappa(x) = \int_0^{\mathrm{L}} G(\xi;x)\frac{M_0}{EI}\,d\xi + \xi_1 l_c^2\left[G\frac{d\kappa}{d\xi} - \kappa\frac{dG}{d\xi}\right]_0^{\mathrm{L}} \tag{204}$$

The bracket becomes (we know from Eq. (17) that $G(0;x) = 0$ and $G(\mathrm{L};x) = 0$):

$$\left[G\frac{d\kappa}{d\xi} - \kappa\frac{dG}{d\xi}\right]_0^{\mathrm{L}} = G^{(1)}(0;x)\,\kappa(0) - G^{(1)}(\mathrm{L};x)\,\kappa(\mathrm{L}) \tag{205}$$

To find $\kappa(0)$ and $\kappa(L)$ we should use the constitutive boundary conditions (7):

$$\left\{\begin{aligned} &\xi_2\kappa(0) - \xi_1 l_c^2\kappa^{(2)}(0) = 0 \\ &\xi_2\kappa(\mathrm{L}) - \xi_1 l_c^2\kappa^{(2)}(\mathrm{L}) = 0 \end{aligned}\right. \tag{rep.7}$$

To find $\kappa(0)$ and $\kappa(\mathrm{L})$, we straightforwardly use the differential Eq. (203) twice: firstly at $x = 0$, and secondly at $x = \mathrm{L}$. Also, each time, we solve a linear system of equations, including a boundary condition along with a new equation generated using the differential equation, as follows:

$$\left\{\begin{aligned} &\kappa(0) - \xi_1 l_c^2\kappa^{(2)}(0) = \frac{M_0}{EI} \\ &\xi_2\kappa(0) - \xi_1 l_c^2\kappa^{(2)}(0) = 0 \end{aligned}\right. \Rightarrow \kappa(0) = \frac{M_0}{\xi_1 EI} \tag{206}$$

and

$$\left\{\begin{aligned} &\kappa(\mathrm{L}) - \xi_1 l_c^2\kappa^{(2)}(\mathrm{L}) = \frac{M_0}{EI} \\ &\xi_2\kappa(\mathrm{L}) - \xi_1 l_c^2\kappa^{(2)}(\mathrm{L}) = 0 \end{aligned}\right. \Rightarrow \kappa(\mathrm{L}) = \frac{M_0}{\xi_1 EI} \tag{207}$$

Eqs. (206) and (207) contradict the common sense derived from Fig. 24 that declares $\kappa(0) = \kappa(\mathrm{L}) = M_0/EI$. Of course, these equations are consistent in pure local case, i.e., $\xi_1 = 1$. By substituting Eqs. (206) and (207) into Eq. (205), we have:

$$\left[G\frac{d\kappa}{d\xi} - \kappa\frac{dG}{d\xi}\right]_0^{\mathrm{L}} = \left[G^{(1)}(0;x) - G^{(1)}(\mathrm{L};x)\right]\frac{M_0}{\xi_1 EI} \tag{208}$$

Therefore, Eq. (204) becomes after calculating the integral as:

$$\kappa(x) = \frac{M_0}{EI}\left(1 + \frac{\xi_2}{\xi_1}\left[\cosh\left(\frac{x}{l_c\sqrt{\xi_1}}\right) - \sinh\left(\frac{x}{l_c\sqrt{\xi_1}}\right)\tanh\left(\frac{\mathrm{L}}{2l_c\sqrt{\xi_1}}\right)\right]\right) \tag{209}$$

In pure local case, $\xi_1 = 1$ and $\xi_2 = 0$ and Eq. (209) gives $\kappa(x) = M_0/EI$ which agrees with $\kappa(0) = \kappa(\mathrm{L}) = M_0/EI$. However, in two-phase peridynamic case with non-zero ξ_1 and ξ_2, we are faced with varying curvature as Eq. (209), although the pure bending moment is applied to the beam. Morover, in pure peridynamic case with $\xi_2 = 1$ and $\xi_1 = 0$ Eq. (209) becomes ill-posed, because of the presence of ξ_1 in the denominator of the fractions. The ill-posedness of the pure peridynamic beam ($\xi_2 = 1$) is due to a conflict between the peridynamic constitutive boundary conditions and the natural boundary conditions, when $\xi_1 = 0$. The same ill-posedness arises in the pure peridynamic rod problem in pure tension, as already commented by Challamel and Zingales (2025) [14]. We note that this phenomenon is analogous to the ill-posedness of the pure curvature-driven nonlocal beam model, as shown by Challamel and Wang (2008) [26]. Challamel and Wang (2008) [26] have also obtained a well-posed curvature-driven nonlocal beam model, using a two-phase curvature-driven nonlocal approach. In both integral approaches, the two-phase peridynamic beam model or the two-phase curvature-driven nonlocal beam model, the phase parameter plays a physical role but also a regularizing role, which avoids the ill-posedness of the pure peridynamic or curvature-driven nonlocal beam models.

8. Conclusion

A comprehensive study of static analysis of two-phase peridynamic Euler-Bernoulli beams under general loading and boundary conditions was presented in this paper, by the help of Green's function method. Depending on whether or not the two-phase peridynamic beam is determinate, and according to the absence or presence of concentrated external load, three different kinds of Green's functions were introduced, and applied to two determinate beams (clamped-free and simple-simple), and two indeterminate beams (simple-clamped and clamped-clamped). As a first example, the clamped-free two-phase peridynamic beam under end tip load was analyzed by using the first kind of Green's function, and the curvature function was obtained as a closed-form expression. After that, the curvature function of the same beam, of course under the uniformly distributed loading, is attained by the same Green's function. The second kind of Green's function was introduced in the third example, when the deflection function of the same beam under the same loading was desirable. It should be mentioned that the first and the second kinds of Green's function were obtained by solving the second- and the sixth-order differential equation together with the two and six boundary conditions, respectively. However, the third kind of Green's function introduced in the forth example (i.e., clamped-free beam under general point load) was extracted by the help of twelve boundary conditions derived when the concentrated load was applied. These three kinds of Green's function were utilized in simply supported two-phase peridynamic beams under three different loading: uniformly and sinusoidal distributed loading and general point load. It is noticeable that the results of simply supported beam under three above-mentioned loading were verified by the help of series solution. Additionally, for further verification, all four two-phase peridynamic beams examined in the paper, i.e., SS, CS, CC and CF beams, were also numerically analyzed using FDM. The experimental order of convergence for the proposed FDM scheme has been shown to be equal to 2, for all the considered boundary conditions. The details of FD solution applied to the statics of two-phase peridynamic beams were presented in the article.

For all the considered boundary conditions, it is observed that the two-phase peridynamic beam theory tends to soften the static response, as compared to the classical Euler-Bernoulli beam, a phenomenon controlled by the peridynamic phase ξ_1 and length scale l_c parameters. This softening phenomenon of the small length scale effects is consistent with that obtained from another integral nonlocal model, the two-phase strain-driven nonlocal model or the two-phase curvature-driven nonlocal beam model (Challamel and Wang, 2008 [26]; Zhang et al., 2010 [27]; Challamel et al., 2025 [28]). In other words, the deflection of the two-phase peridynamic Euler-Bernoulli beam model is larger than the one of the local beam. The nonlocal contributions are more significant for larger values of the l_c parameter. Furthermore, it is shown that the two-phase peridynamic Euler-Bernoulli beam model avoids the possible ill-posedness of the pure peridynamic Euler-Bernoulli (no local elastic phase), as studied from the paradigmatic structural problem of a beam in pure bending.

A possible extension of this work could be to investigate dynamics and stability of the two-phase peridynamic Euler-Bernoulli beams, and even, the more complex kinematics, including two-phase peridynamic Timoshenko beams or two-phase peridynamic higher-order shear beams. It can be also considered extending the main idea presented in this article to plates and shells, by finding the explicit form of the Green's function, or its' series representation.

CRediT authorship contribution statement

Ahmad Aftabi-Sani: Writing – review & editing, Writing – original draft, Visualization, Validation, Methodology, Investigation, Formal analysis. **Noël Challamel:** Writing – review & editing, Writing – original draft, Visualization, Validation, Supervision, Methodology, Investigation, Formal analysis, Conceptualization.

Declaration of competing interest

The authors declare that they have no known competing financial interests or personal relationships that could have appeared to influence the work reported in this paper.

Appendix A: Two-phase peridynamic Euler-Bernoulli beam with exponential kernels

The total potential energy $U[w]$ of the two-phase peridynamic Euler-Bernoulli beam of length L, is assumed in the following form, using the simple and the double integration operator, as considered by di Paola et al. [21]:

$$U[w] = \int_0^L \frac{1}{2} EI\xi_1 \left(\frac{\partial \theta}{\partial x}\right)^2 dx + \int_0^L \int_0^L \frac{1}{4} EI\xi_2 H(x,y)[\theta(y) - \theta(x)]^2 dxdy - \int_0^L pwdx \tag{A.1}$$

with $\xi_1 \in [0;1]$ and $\xi_2 \in [0;1]$ are two (positive) weighting coefficients such that $\xi_1 + \xi_2 = 1$. E is the Young modulus, I the moment of inertia and EI the elastic bending rigidity. $w(x)$ is the deflection displacement field, and $\theta(x) = \partial w/\partial x$ is the rotation. $p(x)$ is the transversal distributed load. The symmetric peridynamic kernel $H(x,y)$ is chosen in exponential form, as proposed by Challamel and Zingales (2025) [22] given by Eq. (A.2).

$$\begin{cases} H(x,y) = \dfrac{1}{l_c^3} \dfrac{\cosh\left(\dfrac{L-y}{l_c}\right)}{\sinh\left(\dfrac{L}{l_c}\right)} \cosh\left(\dfrac{x}{l_c}\right) & if \quad x \le y \\ \\ H(x,y) = \dfrac{1}{l_c^3} \dfrac{\cosh\left(\dfrac{L-x}{l_c}\right)}{\sinh\left(\dfrac{L}{l_c}\right)} \cosh\left(\dfrac{y}{l_c}\right) & if \quad x \ge y \end{cases} \tag{A.2}$$

which verifies the symmetry of the peridynamic operator $H(x,y) = H(y,x)$.

The stationary of the total potential energy $\delta U = 0$ implies, after two integration by parts:

$$\begin{aligned} \delta U = & \int_0^L EI\xi_1 w^{(4)} \delta w \, dx + \int_0^L \frac{\partial}{\partial x} \left\{ \int_0^L EI\xi_2 H(x,y) \left[\frac{\partial w}{\partial y}(y) - \frac{\partial w}{\partial x}(x)\right] dy \right\} \delta w dx \\ & + [EI\xi_1 w'' \delta w']_0^L - [EI\xi_1 w''' \delta w]_0^L - \left[\left\{ \int_0^L EI\xi_2 H(x,y) \left[\frac{\partial w}{\partial y}(y) - \frac{\partial w}{\partial x}(x)\right] dy \right\} \delta w \right]_0^L \\ & - \int_0^L p\delta w \, dx = 0 \end{aligned} \tag{A.3}$$

The static behaviour of the uniform beam of length L under distributed lateral load p may be equivalently expressed from the principle of virtual work:

$$\int_0^L [M\delta w'' - p\delta w] dx = 0 \tag{A.4}$$

After two integration by parts, the principle of virtual work is rewritten:

$$\int_0^L [M'' - p]\delta w dx + [M\delta w']_0^L - [M'\delta w]_0^L = 0 \qquad \Rightarrow \qquad M'' = p \tag{A.5}$$

By comparing Eq. (A.3) and Eq. (A.5), we identify the two-phase peridynamic beam constitutive equations:

$$\frac{\partial^2 M}{\partial x^2} = EI\xi_1 \frac{\partial^4 w}{\partial x^4} + EI\xi_2 \frac{\partial}{\partial x} \int_0^L H(x,y) \left[\frac{\partial w}{\partial y}(y) - \frac{\partial w}{\partial x}(x)\right] dy \tag{A.6}$$

The constitutive boundary conditions of the peridynamic model are issued of the variational principle and formulated in the local sense for the bending terms:

$$M(0) = EI\xi_1 \frac{\partial^2 w}{\partial x^2}(0) \text{ and } M(L) = EI\xi_1 \frac{\partial^2 w}{\partial x^2}(L) \tag{A.7}$$

Eq. (A.7) express the locality principle of the peridynamic model at its boundaries, as consistently introduced by di Paola et al. (2014) [21] for two-phase peridynamic Euler-Bernoulli beams.

For the shear boundary conditions, we have:

$$\begin{aligned} V(0) &= EI\xi_1 w'''(0) + \int_0^L EI\xi_2 H(0,y) \left[\frac{\partial w}{\partial y}(y) - \frac{\partial w}{\partial x}(0)\right] dy \text{ and} \\ V(L) &= EI\xi_1 w'''(L) + \int_0^L EI\xi_2 H(L,y) \left[\frac{\partial w}{\partial y}(y) - \frac{\partial w}{\partial x}(L)\right] dy \end{aligned} \tag{A.8}$$

The integro-differential equation to be solved for the two-phase peristatic Euler-Bernoulli beam is finally written, as obtained by di Paola et al. (2014):

$$EI\xi_1\frac{\partial^4 w}{\partial x^4}+EI\xi_2\frac{\partial}{\partial x}\int_0^L H(x,y)[\theta(y)-\theta(x)]dy=p \text{ with } \xi_1+\xi_2=1 \tag{A.9}$$

The nonlocal peristatic equation Eq. (A.6) can be integrated one time to give:

$$\frac{\partial M}{\partial x}=EI\xi_1\frac{\partial^2\theta}{\partial x^2}+EI\xi_2\int_0^L H(x,y)[\theta(y)-\theta(x)]dy \tag{A.10}$$

where the integration constant is assumed to vanish, due to the shear force boundary conditions. We finally obtain for the considered normalized kernel:

$$\frac{\partial M}{\partial x}-EI\xi_1\frac{\partial^2\theta}{\partial x^2}+\frac{EI\xi_2}{l_c^2}\theta=EI\xi_2\int_0^L H(x,y)\theta(y)dy \tag{A.11}$$

Challamel and Zingales (2025) [22] have shown that this integro-differential constitutive law (two-phase peridynamic Euler-Bernoulli beam) can be reformulated as a pure differential problem:

$$M-l_c^2\frac{\partial^2 M}{\partial x^2}=EI\left(\frac{\partial^2 w}{\partial x^2}-\xi_1 l_c^2\frac{\partial^4 w}{\partial x^4}\right) \tag{A.12}$$

coupled to the two constitutive boundary conditions Eq. (A.7).

By coupling Eq. (A.12) with Eq. (A.5), the two-phase peridynamic Euler-Bernoulli beam problem is governed by a linear sixth-order differential equation for the displacement:

$$EI\left[w^{(4)}-\xi_1 l_c^2 w^{(6)}\right]=p-l_c^2 p^{(2)} \tag{A.13}$$

coupled to the classical natural and essential boundary conditions, in addition to the two "local" constitutive boundary conditions (six boundary conditions).

Appendix B: Green's function of CF beam for deflection under P

As it was shown in Section 3.4, the Green's function of deflection for clamped-free beam could be obtained as the following

$$G(\xi;x)=\begin{cases}
-\frac{\xi^3}{6}+\frac{x\xi^2}{2}-\xi_2 l_c^2 x+\frac{\xi_2}{\sqrt{\xi_1}}l_c x\xi\coth\left(\frac{\mathrm{L}}{\sqrt{\xi_1}l_c}\right)\\
\quad+\xi_2 l_c^2\left[\xi\cosh\left(\frac{x}{\sqrt{\xi_1}l_c}\right)+x\cosh\left(\frac{\xi}{\sqrt{\xi_1}l_c}\right)\right]\\
\quad-\xi_2\sqrt{\xi_1}l_c^3\operatorname{csch}\left(\frac{\mathrm{L}}{\sqrt{\xi_1}l_c}\right)\sinh\left(\frac{\mathrm{L}-x}{\sqrt{\xi_1}l_c}\right)\sinh\left(\frac{\xi}{\sqrt{\xi_1}l_c}\right)\\
\quad-\xi_2 l_c^2\coth\left(\frac{\mathrm{L}}{\sqrt{\xi_1}l_c}\right)\left[\xi\sinh\left(\frac{x}{\sqrt{\xi_1}l_c}\right)+x\sinh\left(\frac{\xi}{\sqrt{\xi_1}l_c}\right)\right] \qquad 0<\xi<x\\
-\frac{x^3}{6}+\frac{x^2\xi}{2}-\xi_2 l_c^2\xi+\frac{\xi_2}{\sqrt{\xi_1}}l_c x\xi\coth\left(\frac{\mathrm{L}}{\sqrt{\xi_1}l_c}\right)\\
\quad+\xi_2 l_c^2\left[\xi\cosh\left(\frac{x}{\sqrt{\xi_1}l_c}\right)+x\cosh\left(\frac{\xi}{\sqrt{\xi_1}l_c}\right)\right]\\
\quad-\xi_2\sqrt{\xi_1}l_c^3\operatorname{csch}\left(\frac{\mathrm{L}}{\sqrt{\xi_1}l_c}\right)\sinh\left(\frac{\mathrm{L}-\xi}{\sqrt{\xi_1}l_c}\right)\sinh\left(\frac{x}{\sqrt{\xi_1}l_c}\right)\\
\quad-\xi_2 l_c^2\coth\left(\frac{\mathrm{L}}{\sqrt{\xi_1}l_c}\right)\left[\xi\sinh\left(\frac{x}{\sqrt{\xi_1}l_c}\right)+x\sinh\left(\frac{\xi}{\sqrt{\xi_1}l_c}\right)\right] \qquad x<\xi<\mathrm{L}
\end{cases} \tag{B.1}$$

Since the differential operator of Eq. (2) is "self-adjoint", the above Green's function is symmetric: By changing $x$to ξ and vice versa, the two above functions are converted into each other (similar to the kernel presented in Appnedix A, as Eq.A.2). This fact could be considered as a verification fact.

The above-obtained Green's function could be easily free dimensioned, by using:

$$G^*=\frac{G}{\mathrm{L}^3};\quad x^*=\frac{x}{\mathrm{L}};\quad \xi^*=\frac{\xi}{\mathrm{L}};\quad {l_c}^*=\frac{l_c}{\mathrm{L}} \tag{B.2}$$

The dimensionless Green's function can then be re-expressed by:

$$G(\xi^*;x^*)=\begin{cases}-\dfrac{(\xi^*)^3}{6}+\dfrac{x^*(\xi^*)^2}{2}-\xi_2(l_c^*)^2x^*+\dfrac{\xi_2}{\sqrt{\xi_1}}l_c^*x^*\xi^*\coth\left(\dfrac{1}{\sqrt{\xi_1}l_c^*}\right)\\ \quad+\xi_2(l_c^*)^2\left[\xi^*\cosh\left(\dfrac{x^*}{\sqrt{\xi_1}l_c^*}\right)+x^*\cosh\left(\dfrac{\xi^*}{\sqrt{\xi_1}l_c^*}\right)\right]\\ \quad-\xi_2\sqrt{\xi_1}(l_c^*)^3\operatorname{csch}\left(\dfrac{1}{\sqrt{\xi_1}l_c^*}\right)\sinh\left(\dfrac{1-x^*}{\sqrt{\xi_1}l_c^*}\right)\sinh\left(\dfrac{\xi^*}{\sqrt{\xi_1}l_c^*}\right)\\ \quad-\xi_2(l_c^*)^2\coth\left(\dfrac{1}{\sqrt{\xi_1}l_c^*}\right)\left[\xi^*\sinh\left(\dfrac{x^*}{\sqrt{\xi_1}l_c^*}\right)+x^*\sinh\left(\dfrac{\xi^*}{\sqrt{\xi_1}l_c^*}\right)\right] & 0<\xi^*<x^*\\ -\dfrac{(x^*)^3}{6}+\dfrac{(x^*)^2\xi^*}{2}-\xi_2(l_c^*)^2\xi^*+\dfrac{\xi_2}{\sqrt{\xi_1}}l_c^*x^*\xi^*\coth\left(\dfrac{1}{\sqrt{\xi_1}l_c^*}\right)\\ \quad+\xi_2(l_c^*)^2\left[\xi^*\cosh\left(\dfrac{x^*}{\sqrt{\xi_1}l_c^*}\right)+x^*\cosh\left(\dfrac{\xi^*}{\sqrt{\xi_1}l_c^*}\right)\right]\\ \quad-\xi_2\sqrt{\xi_1}(l_c^*)^3\operatorname{csch}\left(\dfrac{1}{\sqrt{\xi_1}l_c^*}\right)\sinh\left(\dfrac{1-\xi^*}{\sqrt{\xi_1}l_c^*}\right)\sinh\left(\dfrac{x^*}{\sqrt{\xi_1}l_c^*}\right)\\ \quad-\xi_2(l_c^*)^2\coth\left(\dfrac{1}{\sqrt{\xi_1}l_c^*}\right)\left[\xi^*\sinh\left(\dfrac{x^*}{\sqrt{\xi_1}l_c^*}\right)+x^*\sinh\left(\dfrac{\xi^*}{\sqrt{\xi_1}l_c^*}\right)\right] & x^*<\xi^*<1\end{cases}\tag{B.3}$$

Appendix C: Green's function of SS beam for deflection under P

As it was shown in Section 4.4, the Green's function of deflection for simple-simple beam could be obtained as the following

$$G(\xi;x)=\begin{cases}\xi_2\sqrt{\xi_1}l_c^3\sinh\left(\dfrac{\xi}{\sqrt{\xi_1}l_c}\right)\sinh\left(\dfrac{L-x}{\sqrt{\xi_1}l_c}\right)\operatorname{csch}\left(\dfrac{L}{\sqrt{\xi_1}l_c}\right)\\ \quad-\dfrac{1}{6L\xi_1}\xi(L-x)\left[\xi_1\left(x^2+\xi^2-2Lx\right)-6\xi_1\xi_2l_c^2\right] & 0<\xi<x\\ \xi_2\sqrt{\xi_1}l_c^3\sinh\left(\dfrac{x}{\sqrt{\xi_1}l_c}\right)\sinh\left(\dfrac{L-\xi}{\sqrt{\xi_1}l_c}\right)\operatorname{csch}\left(\dfrac{L}{\sqrt{\xi_1}l_c}\right)\\ \quad-\dfrac{1}{6L\xi_1}x(L-\xi)\left[\xi_1\left(x^2+\xi^2-2L\xi\right)-6\xi_1\xi_2l_c^2\right] & x<\xi<L\end{cases}\tag{C.1}$$

Since the differential operator of Eq. (2) is "self-adjoint", the above Green's function is symmetric: By changing $x$to ξ and vice versa, the two above functions are converted into each other. We can consider this fact as a verification.

The above-obtained Green's function could be easily free dimensioned, by using the following dimensionless variables:

$$G^*=\frac{G}{L^3};\quad x^*=\frac{x}{L};\quad \xi^*=\frac{\xi}{L};\quad l_c{}^*=\frac{l_c}{L}\tag{rep.96}$$

The dimensionless curvature can then be re-expressed by:

$$G(\xi^*;x^*)=\begin{cases}\xi_2\sqrt{\xi_1}(l_c^*)^3\sinh\left(\dfrac{\xi^*}{\sqrt{\xi_1}l_c^*}\right)\sinh\left(\dfrac{1-x^*}{\sqrt{\xi_1}l_c^*}\right)\operatorname{csch}\left(\dfrac{1}{\sqrt{\xi_1}l_c^*}\right)\\ \quad-\dfrac{1}{6\xi_1}\xi^*(1-x^*)\left[\xi_1\left[(x^*)^2+(\xi^*)^2-2x^*\right]-6\xi_1\xi_2(l_c^*)^2\right] & 0<\xi^*<x^*\\ \xi_2\sqrt{\xi_1}(l_c^*)^3\sinh\left(\dfrac{x^*}{\sqrt{\xi_1}l_c^*}\right)\sinh\left(\dfrac{1-\xi^*}{\sqrt{\xi_1}l_c^*}\right)\operatorname{csch}\left(\dfrac{1}{\sqrt{\xi_1}l_c^*}\right)\\ \quad-\dfrac{1}{6\xi_1}x^*(1-\xi^*)\left[\xi_1\left[(x^*)^2+(\xi^*)^2-2\xi^*\right]-6\xi_1\xi_2(l_c^*)^2\right] & x^*<\xi^*<1\end{cases}\tag{C.2}$$

Appendix D: Table of three types of Green's function of SS beam

In the next page, three types of static Green's function for simply supported beam are tabulated, along with associated governing equations and boundary conditions. They are respectively suitable for analyzing the SS beam under distributed (types I and II) and concentrated loads (type III), to find the curvature (type I) and deflection (types II and III).

Type	Governing differential equation	Boundary conditions	Green's function
I	$G(\xi;x)-\xi_1 l_c^2\frac{d^2G(\xi;x)}{d\xi^2}=\delta(\xi-x)$	$\begin{cases} G(0;x)=0 \\ G(\mathrm{L};x)=0 \end{cases}$	$G(\xi;x)=\frac{1}{\sqrt{\xi_1}l_c}\operatorname{csch}\left(\frac{\mathrm{L}}{\sqrt{\xi_1}l_c}\right)\sinh\left(\frac{\mathrm{L}-x}{\sqrt{\xi_1}l_c}\right)\sinh\left(\frac{\xi}{\sqrt{\xi_1}l_c}\right)+\frac{1}{\sqrt{\xi_1}l_c}\sinh\left(\frac{x-\xi}{\sqrt{\xi_1}l_c}\right)\widehat{H}(\xi-x)$
II	$\frac{d^4G(\xi;x)}{d\xi^4}-\xi_1 l_c^2\frac{d^6G(\xi;x)}{d\xi^6}=\delta(\xi-x)$	$\begin{cases} G(0;x)=0 \\ G^{(2)}(0;x)=0 \\ G^{(4)}(0;x)=0 \\ G(\mathrm{L};x)=0 \\ G^{(2)}(\mathrm{L};x)=0 \\ G^{(4)}(\mathrm{L};x)=0 \end{cases}$	$G(\xi;x)=\xi_1^{\frac{3}{2}}l_c^3\sinh\left(\frac{\mathrm{L}-x}{\sqrt{\xi_1}l_c}\right)\left(\frac{\sinh\left(\frac{\xi}{\sqrt{\xi_1}l_c}\right)}{\sinh\left(\frac{\mathrm{L}}{\sqrt{\xi_1}l_c}\right)}\right)-\frac{(\mathrm{L}-x)\,\xi}{6\mathrm{L}}\left(x^2-2\mathrm{L}x+\xi^2+6l_c^2\xi_1\right)+\left(\xi_1^{\frac{3}{2}}l_c^3\sinh\left(\frac{x-\xi}{\sqrt{\xi_1}l_c}\right)-\frac{1}{6}(x-\xi)^3-\xi_1 l_c^2(x-\xi)\right)\times\widehat{H}(\xi-x)$
III	$\frac{d^4G(\xi;x)}{d\xi^4}-\xi_1 l_c^2\frac{d^6G(\xi;x)}{d\xi^6}=\delta(\xi-x)$	$\begin{cases} G(0)=0 \\ G^{(2)}(0)=0 \\ G^{(4)}(0)=0 \\ G(\mathrm{L})=0 \\ G^{(2)}(\mathrm{L})=0 \\ G^{(4)}(\mathrm{L})=0 \end{cases}$ and $\begin{cases} G(x^-)=G(x^+) \\ G^{(1)}(x^-)=G^{(1)}(x^+) \\ G^{(2)}(x^-)=G^{(2)}(x^+) \\ G^{(3)}(x^-)-G^{(3)}(x^+)=-\frac{1}{\xi_1} \\ G^{(4)}(x^-)=G^{(4)}(x^+) \\ G^{(5)}(x^-)-G^{(5)}(x^+)=-\frac{\xi_2}{\xi_1^2 l_c^2} \end{cases}$	$G(\xi;x)=\begin{cases} \xi_2\sqrt{\xi_1}l_c^3\sinh\left(\frac{\xi}{\sqrt{\xi_1}l_c}\right)\sinh\left(\frac{\mathrm{L}-x}{\sqrt{\xi_1}l_c}\right)\times\operatorname{csch}\left(\frac{\mathrm{L}}{\sqrt{\xi_1}l_c}\right)-\frac{1}{6\mathrm{L}\xi_1}\xi(\mathrm{L}-x)\times\left[\xi_1\left(x^2+\xi^2-2\mathrm{L}x\right)-6\xi_1\xi_2 l_c^2\right] & :\ 0<\xi<x \\ \xi_2\sqrt{\xi_1}l_c^3\sinh\left(\frac{x}{\sqrt{\xi_1}l_c}\right)\sinh\left(\frac{\mathrm{L}-\xi}{\sqrt{\xi_1}l_c}\right)\times\operatorname{csch}\left(\frac{\mathrm{L}}{\sqrt{\xi_1}l_c}\right)-\frac{1}{6\mathrm{L}\xi_1}x(\mathrm{L}-\xi)\times\left[\xi_1\left(x^2+\xi^2-2\mathrm{L}\xi\right)-6\xi_1\xi_2 l_c^2\right] & :\ x<\xi<\mathrm{L} \end{cases}$

Data availability

No data was used for the research described in the article.

References

[1] S.A. Silling, Reformulation of elasticity theory for discontinuities and long-range forces, J. Mech. Phys. Solids. 48 (1) (2000) 175–209.
[2] F. Bobaru, J T Foster, P H Geubelle, S A Silling (Eds.), Handbook of Peridynamic Modeling, CRC press, 2016.
[3] F. Bobaru, M. Yang, L.F. Alves, S.A. Silling, E. Askari, J. Xu, Convergence, adaptive refinement, and scaling in 1D peridynamics, Int. J. Numer. Methods Eng. 77 (6) (2009) 852–877.
[4] M.R. Tupek, R. Radovitzky, An extended constitutive correspondence formulation of peridynamics based on nonlinear bond-strain measures, J. Mech. Phys. Solids. 65 (2014) 82–92.
[5] E. Madenci, A. Barut, M. Futch, Peridynamic differential operator and its applications, Comput. Methods Appl. Mech. Eng. 304 (2016) 408–451.
[6] B. Kilic, E. Madenci, An adaptive dynamic relaxation method for quasi-static simulations using the peridynamic theory, Theor. Appl. Fract. Mech. 53 (3) (2010) 194–204.
[7] C. Diyaroglu, E. Oterkus, S. Oterkus, F. Madenci, Peridynamics for bending of beams and plates with transverse shear deformation, Int. J. Solids. Struct. 69 (2015) 152–168.
[8] C. Diyaroglu, E. Oterkus, S. Oterkus, An Euler–Bernoulli beam formulation in an ordinary state-based peridynamic framework, Math. Mech. Solids. 24 (2) (2019) 361–376.
[9] J. O'Grady, J. Foster, Peridynamic beams: a non-ordinary, state-based model, Int. J. Solids. Struct. 51 (18) (2014) 3177–3183.

[10] Z. Yang, E. Oterkus, S. Oterkus, Peridynamic higher-order beam formulation, J. Peridynamics. Nonlocal. Model. 3 (1) (2021) 67–83.
[11] Z. Yang, E. Oterkus, C.T. Nguyen, S. Oterkus, Implementation of peridynamic beam and plate formulations in finite element framework, Contin. Mech. Thermodyn. 31 (1) (2019) 301–315.
[12] Z. Yang, K. Naumenko, H. Altenbach, C.C. Ma, E. Oterkus, S. Oterkus, Some analytical solutions to peridynamic beam equations, ZAMM J. Appl. Math. Mech. Zeitschrift für Angewandte Mathematik und Mechanik 102 (10) (2022) e202200132.
[13] Z. Yang, K. Naumenko, H. Altenbach, C.C. Ma, E. Oterkus, S. Oterkus, Beam buckling analysis in peridynamic framework, Arch. Appl. Mech. 92 (12) (2022) 3503–3514.
[14] N. Challamel, M. Zingales, Two-phase peridynamic elasticity with exponential kernels. I: statics and vibrations of axial rods, J. Eng. Mech. 151 (5) (2025) 04025013.
[15] J. Altenbach, H. Altenbach, V.A. Eremeyev, On generalized Cosserat-type theories of plates and shells: a short review and bibliography, Arch. Appl. Mech. 80 (1) (2010) 73–92.
[16] M. Marin, M.M. Bhatti, O.M. Hapenciuc, S.A. Pirlog, Spatial decay estimates for a thermoelastic Cosserat body without energy dissipation, J. Comput. Appl. Mech. 56 (3) (2025) 611–626.
[17] M.M. Bhatti, O.A. Bég, C.M. Khalique, T.A. Bég, C. Kuharat, Computation of manganese ferrite/nickel ferrite ethylene glycol hybrid ferro-magnetic nanofluid stretching flow with radiative flux: applications in solar nano-coatings. the European physical, J. Spec. Top. 26 (2025) 1–25.
[18] M. Di Paola, G. Failla, M. Zingales, Physically-based approach to the mechanics of strong non-local linear elasticity theory, J. Elast. 97 (2009) 103–130.
[19] M. Di Paola, G. Failla, A. Sofi, M. Zingales, A mechanically based approach to non-local beam theories, Int. J. Mech. Sci. 53 (9) (2011) 676–687.
[20] M. Di Paola, G. Failla, A. Sofi, M. Zingales, On the vibrations of a mechanically based non-local beam model, Comput. Mater. Sci. 64 (2012) 278–282.
[21] M. Di Paola, G. Failla, M. Zingales, Mechanically based nonlocal Euler-Bernoulli beam model, J. Nanomechanics Micromech. 4 (1) (2014) A4013002.
[22] N. Challamel, M. Zingales, Two-phase peridynamic elasticity with exponential kernels. II: bending, buckling, and vibration of beams, J. Eng. Mech. 151 (5) (2025) 04025014.
[23] S.M. Hozhabrossadati, N. Challamel, M. Rezaiee-Pajand, A. Aftabi Sani, Application of Green's function method to bending of stress gradient nano-beams, Int. J. Solids. Struct. 143 (2018) 209–217.
[24] M.S. Behnam-Rasouli, N. Challamel, A. Karamodin, A. Aftabi Sani, Application of the Green's function method for static analysis of nonlocal stress-driven and strain gradient elastic nanobeams, Int. J. Solids. Struct. 295 (2024), 112794-11281.
[25] N. Challamel, A. Aftabi Sani, Green's functions of size-dependent Timoshenko beams: gradient elasticity versus stress-driven nonlocal theories, Int. J. Solids. Struct. 314 (2025) 113308.
[26] N. Challamel, C.M. Wang, The small length scale effect for a non-local cantilever beam: a paradox solved, Nanotechnology 19 (2008) 345703.
[27] Y.Y. Zhang, C.M. Wang, N. Challamel, Bending, buckling and vibration of hybrid nonlocal beams, J. Eng. Mech. 136 (5) (2010) 562–574.
[28] N. Challamel, C.M. Wang, J.N. Reddy, S.A. Faghidian, Equivalence between micromorphic, nonlocal gradient and two-phase nonlocal beam theories, Acta Mech. 236 (2025) 871–902.